ADDIS ABABA UNIVERSITY
SCHOOL OF EARTH SCIENCES

GEOLOGY AND GENESIS OF GOLD MINERALIZATION IN BURIKARO AND EJERSA AREAS, GUJI ZONE, OROMIA NATIONAL REGIONAL STATE, SOUTHERN ETHIOPIA.

By

Munir Ridwan Kedir

A thesis submitted to the School of Graduate Studies of Addis Ababa University in partial fulfillment of the requirements for the degree of masters in Earth Sciences (Mineral Exploration)

Addis Ababa University

Addis Ababa, Ethiopia

May 30, 2014

Advisor: Dr.Worash Getaneh

ADDIS ABABA UNIVERSITY

SCHOOL OF EARTH SCIENCES

GEOLOGY AND GENESIS OF GOLD MINERALIZATION IN BURIKARO AND EJERSA AREAS, GUJI ZONE, OROMIA NATIONAL REGIONAL STATE, SOUTHERN ETHIOPIA

BY

MUNIR RIDWAN KEDIR

APPROVED BY EXAMINING BOARD	**SIGNATURE**
Dr.Tesfaye Kidane ---------------------- Chair person	------------------------
Dr. Worash Getaneh ------------------------ Advisor	-----------------------
Examiners	
Prof. Solomon Tadesse --------------------------	---------------------
Dr. Mulugeta Alene -------------------------	--------------------

ABSTRACT

This study deals about geology and genesis of gold mineralization in Burikaro and Ejersa areas, which are located in the Neoproterozoic Adola gold field of southern Ethiopia. The area is not well explored and almost no research work has been done so far. Detailed review of the geodynamic evolution and mineralization history of the region, field description and geological mapping, rock and ore petrography, and surface sample chemical analysis were conducted. Secondary data from trench sample chemical analysis were also utilized in the study.

The area comprises highly weathered and variably deformed upper greenschist to epidote-amphibolite facies metamorphic rocks like amphibolite, talc-tremolite-actinolite schist, graphite-quartz-mica schist, meta-conglomerate, and meta-sandstone. Intermediate to mafic meta-plutons such as meta-dolerite and meta-gabbro are also present intruding the amphibolite rock. A major N-S and two minor NW-SE and E-W trending shear zones; early- and late-tectonic quartz (± calcite) veins; and hydrothermal alterations like silicification, carbonatiztion, tourmalinization, and chloritization were observed.

Besides its occurrence as a free gold, the gold mineralization of the study area is mainly associated with the hydrothermally altered major N-S trending shear zones containing late-tectonic quartz (± calcite) veins with associated sulfides and present mainly in the graphite-quartz-mica schist and meta-conglomerate/meta-sandstone. The ore minerals associated with gold are dominantly pyrite, magnetite, and ilmenite; minor amounts of hematite and chalcopyrite, and accessory mounts of sphalerite, covellite, and limonite chiefly occurring as open-space filling and replacement type mineralization. Based on texture, mineral association, and alteration a paragenetic sequence is suggested.

The presence of not mineralized higher grade mafic metamorphic rocks at the base, the association of the gold mineralization with the lower grade meta-sediments, and the negative correlation between gold and metals like cobalt and nickel suggest that the possible source rocks of the gold are the underlying mafic rocks and metamorphic dehydration is the probable source for the hydrothermal fluids and leaching of gold from the mafic rocks. The association of gold mineralization with sulfides suggest that HS^--or H_2S-complexes were responsible for gold transport in the area.

Acknowledgements

Undertaking such a research work is a difficult task and usually needs the supports of many individuals and agents besides my effort. Many individuals and agents have supported me otherwise the research work would not have been accomplished without their unlimited supports. Consequently; there are many individuals and agents to be acknowledged.

First of all, I want to present my warmest thank to my advisor Dr.Worash Getaneh for spending his valuable time and effort on continuous and patient encouragement, guidance, support, motivation and invaluable comments from the beginning up to the final stage of this research work. Really you did a lot that cannot be expressed with words and once again thank you for all!

My gratitude also goes to the School of Earth Sciences of Addis Ababa University, National Mining Corporation, Geological Survey of Ethiopia, and Sebaboru Worada Administrative Office of Oromia National Regional State for funding and offering field equipments; offering secondary data and allowing me work on their licensed area; offering secondary data and laboratory facilities, and for arranging some logistics, respectively.

I am also thankful to Shiferaw Demissie, Solomon Geda, Gashaw Dibabie, Dr. Seifu Kebede, Nazimu Gibril, Mudin Gibril, Gelchu Tumukessa, Workeleul Gebreyesus, and Girma Kasssa for their invaluable support.

My special thanks also go to my classmate Abebe Bedassa for his unforgettable support and suggestions from the start to the beginning of this research work.

Finally yet importantly, my sincere thanks go to my family and all my classmates who directly or indirectly involved on supporting me and your supports was so vital in accomplishing this research work.

Table of Contents

List of figures

List of tables

Abbreviations

Act = actinolite

BE = a general prefix code given for all samples used throughout this paper (e.g., BE01denotes sample number 01, BE30 denotes sample number 30 and so on). Individual samples used for chemical analysis, polished section study, and thin section study are labeled by adding the upper case English letters A, P, and T respectively to the general code BE, that is, BEA, BEP, and BET and attaching their respective numbers.

Bt = biotite

Cal = calcite

Chl= chlorite

Covt = covellite

Cpx = clinopyroxene

Cpy = chalcopyrite

EIGS = Ethiopian Institute of Geological Surveys

Ep = epidote

E-W= East –West

GPS = geographical positioning system

Grp = graphitic material

GSE = Geological Survey of Ethiopia

Hbl = hornblende

Hemt = hematite

Ilm = ilmanite

Limt = limonite

NMiC = National Mining Corporation

N-S= North-south

NNE-SSW= North North East- South South West

NNW-SSE= North North West- South South East

NW-SE= North West-South East

Magt = magnetite

MoM = Ministry of Mines

MoME = Ministry of Mines and Energy

Ms = muscovite

Ol = olivine

Opq = opaque

Pl = plagioclase feldspar

PPL = plane polarized light

Ppm = parts per million

Py = pyrite

Qtz = quartz

Ser = sericite

Sph = sphalerite

Tal = talc

Tr = Tremolite

XPL = Cross polarized light

CHAPTER ONE

1 INTRODUCTION

1.1 General

Understanding the nature, origin, and distribution of the worlds mineral deposits remains a strategic topic to respond to the increased demand for and production of natural resources due to the unprecedented growth of human population over the past century (Robb,2005). Mineral deposits are nothing but the anomalous concentrations of elements of a certain commodity in a certain restricted and geologically and structurally suitable settings of the earth's crust. Evidently, understanding the geologic and structural setting of a given area is unquestionably a key point to have knowledge on the distribution and potential of mineral occurrences. In addition to these, the development of mineral deposits is also dependent upon sound geological, geochemical, geophysical, and remote sensing exploration techniques. Political and economic factors and labor conditions must also be considered (Jensen and Bateman, 1981).

Ethiopia hosts a wide diversity of earth resources ranging from metallic mineral deposits such us gold, platinum, tantalum, molybdenum, etc.; non-metallic mineral deposits which include industrial minerals like bentonite, diatomite, potash, soda ash, limestone and quartz, to building materials, gemstones, and energy resources. According to Solomon (2009) current mining activities in Ethiopia include the pilot scale production of tantalite and soda ash, the primary gold from Lega Dembi, placer gold mining mainly from Adola, and mining of industrials such as kaolin, dolomite, magnesite, and dimension stones (limestone, marble, granite, basalt, and sand) as well as small scale artisanal mining of precious metals, gemstones, and salt. In addition to the aforementioned examples, the recent discoveries of gold in Okote area by National Mining Corporation, skarn-type gold deposit by Midroc Gold Mine in Benshangul Regional State and epithermal gold in Afar indicates the country's further mineral potential and invite for additional extensive mineral exploration works which may lead to the discovery of economic deposits. As pointed out in Mogessie et al.(2002); Solomon (2009) the Precambrian basement rocks are hosts for most of the known mined metallic and industrial commodities of the country including, among others, gold, copper, nickel, platinum, chromium, iron, asbestos, feldspar, and marble.

Even though geo-scientific works for academic and mineral prospecting purposes dates back to the end of 18^{th} century, modern and systematic mineral exploration in Ethiopia started in 1968 with the establishment of the Ethiopian Geological Survey as a department within the Ministry of Mines and Energy (Solomon, 2009; Hundie, 2010). After the establishment of the Geological Survey, many geological mapping and mineral exploration works have been carried out in different parts of the country. The most outstanding ones include the Adola Gold Exploration project led by the Soviet Union (1979-1981), United Nations Development program training for mineral exploration (1967-1971), Ethio-Canadian Omo River project (1976-1978), Ethio-Soviet Bulbul-Ageremariam-Moyale Exploration project, Asosa-Kurmuk Mineral Exploration Project, Ethio-Norwegian Mineral Exploration Project, and Western Tigray Mineral Exploration Project (MoM, 2003 and 2010; Hundie, 2010). Such systematic mineral exploration work in the country led to the discovery of many metallic and industrial mineral deposits such as the discovery of the Lega Dembi primary gold deposit, platinum, tantalum, potash, diatomite, and graphite (Gebremichael**,** 2006; Lingeswara et al., 2012).

1.2 Description of the study area

1.2.1 Location and accessibility

The study area is one of the sites within the Dawa-Digati Gold Exploration Project prospect area which is in the Hageremariam, Oddo Shakiso, and Derme Dama woredas of Guji and Borena Zones (locally known as the Adola area) of the Oromia National Regional state, Ethiopia. It is geographically bounded approximately between latitude 5^{o}22'19" N - 5^{o}22'34" N and longitude 34^{o}48'37" E - 38^{o}50'20" E. More specifically it is located between 593665mN - 600000mN latitude and 478850mE - 482100mE longitude covering about 20 square kilometers (Fig.1.1). It is accessible through the 562 km partly asphalted and partly all-weather gravel Addis Ababa-Awassa-Shakiso- Dawa Digati route.

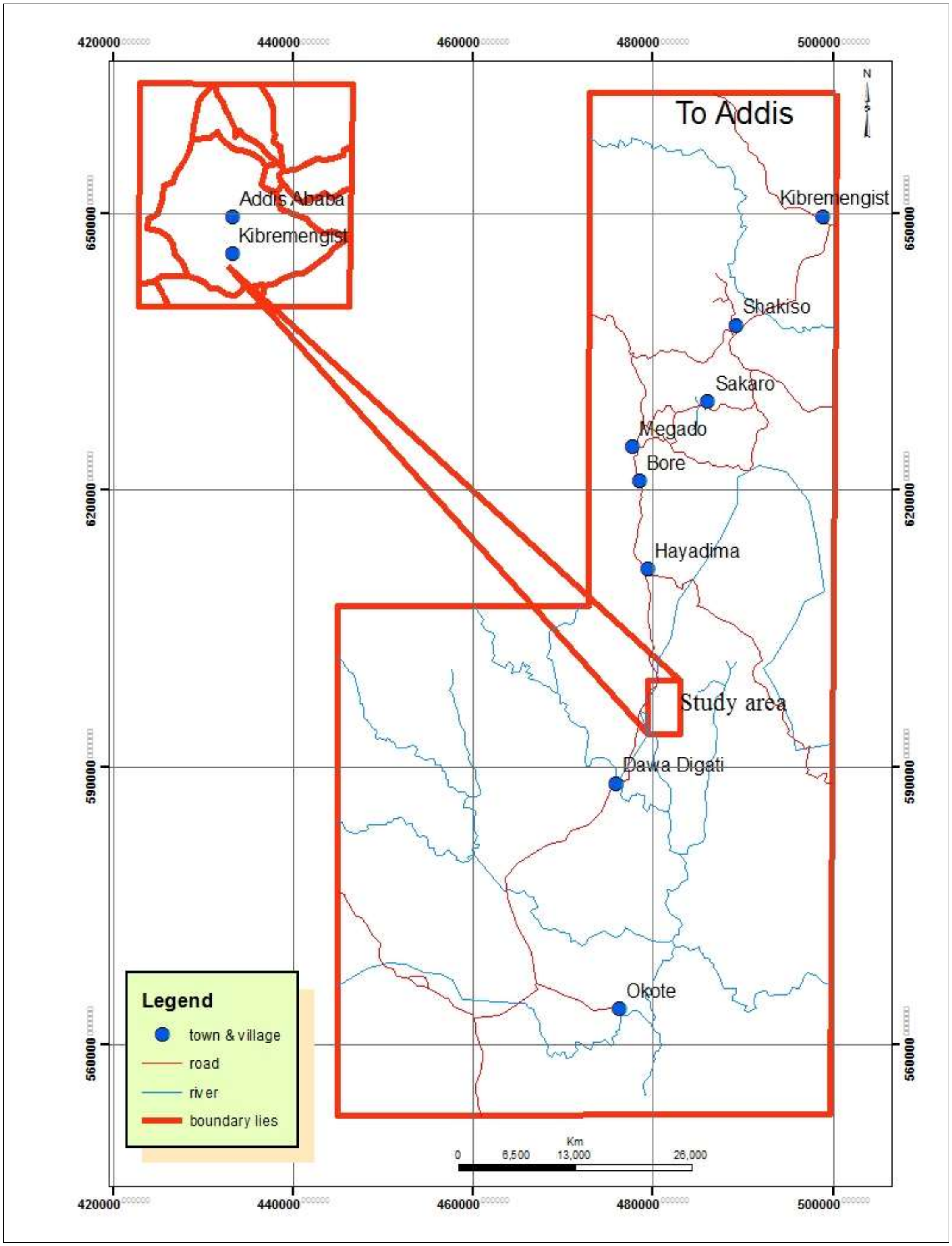

Figure 1.1 Location map of the study area

An alternative path to access the study area is the Addis Ababa-Awassa-Agremariam-Dawa Digati-Shakiso route. Moreover, there are many mainly dry-weather foot paths connecting the different segments of the study area.

1.2.2 Land use

The study area is very sparsely populated dominantly by the Guji people of Oromia National Regional State; the majority of who are pastoralists with some engaged in gold mining and very limited small scale agro-pastoral activities. The permanent settlement is mainly restricted to the relatively plain areas of mostly in Burikaro- and some parts of Ejersa-sub-areas. The people also temporarily settle by arranging moveable tents in places where free gold is suspected to occur and where there is shallow level stream water. The rest of the land is covered by bushes, acacia, and small sized trees that are locally used for feeding animals, making houses and fencing purposes.

1.2.3 Physiography and climate

The study area is characterized by both plain areas, that are typical for Burikaro sub-area, and ridges which are found in Ejersa and between Burikaro and Ejersa sub-areas. The area is dissected by smaller and dry streams majority of them flowing southwards. The drainage pattern is a direct reflection of the currently existing discontinuities in the bed rocks. The streams flow following structurally weak zones, such as fault scarps, and marked by gullies or stream valleys. The minimum and maximum elevations in the study area are respectively about 1420 and 1760 meters above sea level. March-May and October-November are generally the two inconsistent rainy seasons in the study area (NMiC, 2004). The rest of the time is exclusively dry condition.

1.3 Statement of the problem

The Adola Gold belt or Goldfield of southern Ethiopia has undergone exploration for an extended period of time. While a known deposit is undergoing active exploitation (Lega Dembi Gold Mine), several previous workers have inferred that the remainder of the Adola belt of southern Ethiopia remains prospective for Au and even base metals (e.g. Worku, 1996, as cited in Basson, 2006).The area is by far the most important gold producer in Ethiopia. A number of researchers studied the Adola belt either for scientific interest or economic considerations. It has been the subject of study since the classical placer gold investigation in the Bedakessa valley in the late 1930s (EIGS, 1995). However,according to the Ethiopian Institute of Geological Survey report (EIGS, 1993) more attention was focused on Lega Dembi, where an open pit mine is operating, and at Sakaro, where opencast stripping and washing of highly weathered gold bearing schists is being carried out. Besides the Lega Dembi primary and Sakaro gold deposits, currently attractive results are also obtained by National Mining Corporation from Okote area, which is located at the southern limit of the Megado belt.

The Burikaro and Ejersa areas, the targets of this paper, are among the mineral prospect areas in the Megado belt. As discussed above, most of the detail gold exploration works of the region have been focussed to the Lega Dembi primary gold area, Sakaro, and currently in the Okote ares. The Burikaro and Ejersa areas are less explored except those few works summarized in the section dealing about prevous works in the study area. This is mainly because most of the exploration works so far conducted are grade oriented and priority is,therefore, given to the aforementioned areas. All the exploration works so far conducted showed gold positive results in the Burikaro and Ejersa areas. Therefore; it is worthto thinkthat since the study area is within Megado belt,where almost all of the gold resources of southern greenstone belt are associated with, further exploration work will locate economic concentration of gold. Moreover, almost no academic work has been done so far in the study area. Therefore; conducting such an academic work fills the gap and also adds alot to the scintific concept of the gold mineralization of the area in partiular and the region as a whole. To summarize, besides being very important for academic interest, the study area is related with the Adola belt mineralization and it may contain economic concentration of gold deposit. All the mentioned discoveries suggest the need to undertake mineralization related studies.

1.4 Objectives of the study

1.4.1 General objective

The main objective of this research work is studying the occurrence and genesis of gold mineralization in Burikaro and Ejersa areas.

1.4.2 Specific objectives

- To describe the processes of ore formation and the various types of hydrothermal alterations associated with gold mineralization

- ❖ To describe the mineral paragenesis
- ❖ To indicate the type of rocks and structures that control gold mineralization
- ❖ To identify and describe the different rock types and prepare a geological map of the study area at a scale of 1: 25,000
- ❖ To review the regional geo-dynamics and show its influence on mineralization events of the study area.

1.5 Literature review

1.5.1 Introduction

Mineral deposits have supplied important material for human consumption long before they become subjects of scientific curiosity or commercial exploitation. The history of mineral usage indicates that the livelihood of our society greatly depends on earth resources. Mining began by prehistoric societies who wanted to improve their living such as mining of copper by native Americans from about 7, 500 to 3000 years before the present, the use of super glue (which is made of red hematite and acacia gum) over 70,000 years ago by people living in the present day South Africa, and the use of soapstone by early humans are worth to mention (Morton, 2009). The collecting of flints or obsidian for hunting purpose, salt for nutrition, and building materials in many countries are other examples of early mineral usages by human beings. Gemstones and native copper, gold, and silver were highly valued as ornaments and as materials for making simple implements (Park and MacDiarmid, 1975; Guilbert and Park, 2007). However, essentially nothing was understood about the origin of minerals in ancient times except some hypotheses about ore genesis postulated by philosophers of early Greek and Roman civilizations none of whom had knowledge of ores in the ground (Guilbert and Park, 2007). The increase in human population, the related great demand for resources and the advancement in technology made the usage of mineral resources diversified, sophisticated their prospecting and processing, and brought a more tight relationship between mineral resources and development.

Mineral resource deposits are unevenly distributed through igneous, sedimentary, and metamorphic rocks. They form in many different ways, some well understood (such as the formation of salts from sea and ocean water, formation of placer deposits, and the separation of minerals by fractionation in cooling magmas), some are poorly understood such as the formation of hydrothermal mineral deposits which are formed in a complex and complicated ways (Barnes, 1997). However, only in exceptional cases those both metallic and nonmetallic minerals concentrate in ore bodies in amount that permits economic recovery although they are widely distributed in the rocks of the earth's crust (Guilbert and Park, 2007). Significance progress has been made in the past on the understanding the origin, distribution, genesis, and mining of mineral deposits by the combined application of geology, geochemistry, geophysics, remote sensing, drilling, and complex computer modeling.

1.5.2 General geochemistry and properties of gold

Gold has a chemical symbol of Au and it is located in the subgroup IB of the Periodic table. Gold's atomic number is 79 and its atomic weight is 196.967 and has specific gravity of19.3 grams per cubic centimeter in pure state; while it is 16 to 18 grams per cubic centimeter in an impure state. The melting point of gold is about 1064^{0}c and has almost negligible volatility. The principal oxidation states of gold are +1 (aurous) and +3 (auric) and since gold mainly occur in complexes of the type $[Au(CN)2]^{-}$, $[AuCl2]^{-}$, $[Au(OH)4]^{-}$, $[AuCl4]^{-}$, and $[AuS]^{-}$, these states are unknown as aquo-ions in solutions (Boyle, 1987). As discussed in Robb (2005) a variety of different ligands (electron donors or electropositive ions with lone pairs of valance electrons) will affect the solubility of metals in solution, the common ones include Cl^{-}, HS^{-}, H_2S, SO_3, NH_3, CN^{-}, SCN^{-}, organic ligands, etc. and based on the Lewis acid /base concept, ligands can be grouped in to soft, intermediate, and hard ligands that shows preferences of forming complexes with soft, intermediate, and hard metals respectively. However, which complex or complexes will be the most important for a given metal depends on the properties of the metal, composition of the solution, temperature and pressure (Krauskopf and Bird, 1995). Gold, for example, is the softest of all metals and prefers forming complex compounds with soft ligands such as the bisulphate ion, rather than chloride. Gold typically occurs in a monovalent state (Au^{+}) in aqueous solutions and will form the complex AuHS at low pH and $Au(HS)^{2-}$ under weakly acidic to basic solutions. The bisulfide complexes predominate in most hydrothermal fluids and are stable over a wide range of temperature, whilst under very oxidizing, saline, and acidic conditions, it is possible to form both Au^{+}- and Au^{3+}-chloride complexes in the form of $Au(Cl)^{2-}$ and $Au(Cl)^{4-}$ respectively (Robb, 2005).

Only one stable isotope ^{197}Au is known for gold in nature and gold isotopes, which can be artificially produced, with mass number 177 to 183 are alpha-emitting, with half-life of less than one minute (Debele, 2000; Nekrasov, 2009). The electronegativity of gold atoms, a quantitative feature of their ability (in molecules) to attract electrons, is relatively high. According to Nekrasov (2009) a comparison of the energy values of Cu, Ag, and Au shows that a favorable combination of their optimal values for gold makes for its high chemical inertness; this is supported by a comparison of the oxidation potential values of gold Au^{+} or Au^{3+}. They also point to the ease with which gold compounds are readily reduced to native gold.

Gold is the most noble of metals and its geochemistry is principally controlled by this fact. Under temperature and oxygen fugacity conditions of the earth's surface, gold is stable metal because it is not noticeably attacked by air or moist acids (Krauskopf and Bird, 1995; Misra, 2000). Its chemical inertness and very high density made gold to be concentrated in placer deposits even though it is not very resistance to mechanical attrition by hard minerals and it is therefore breakdown in to fine dust during transport. In nature, gold occurs predominantly in the native state or as a major constituent of various alloys containing mainly silver, copper, or platinum group metals (Boyle, 1987). Gold also occurs as an isolated grains and veinlets in many sulfides, especially pyrite, chalcopyrite, and arsenopyrite and it is recognized by its "golden" color and very high reflectance (Craig and Vaughan, 1994). In addition to these, several gold and gold-silver tellurides are known, of which the most common are sylvanite, calaverite, petzite, krennerite, and nagyagite (Boyle, 1987). The most outstanding geochemical feature of gold is that it can be concentrated in ores of extremely divergent genesis, ranging from typical magmatogene to low temperature (epithermal) hydrothermal and from chemogenic sedimentary to metamorphic. In many types of ores gold is in small quantities compared to the minerals of other metals and constitutes a negligible proportion of mineral assemblies (Nekrasov, 2009). Even though the common gangue mineral of gold is quartz, carbonates, tourmaline, fluorspar, and a few other non-metals may also present (Jensen and Bateman, 1981). The most universal associates of gold are silver and copper; whilst halogens, sulfur, oxygen, and carbon are among the most prominent elements forming soluble compounds with gold and thus determine its mobility under natural conditions (Boyle, 1987).

1.5.3 Types of auriferous deposits and proposed models

Gold deposits can form in many different types of geological environments, tectonic settings, and in almost all geologic epochs from Archean to Cenozoic. As clearly pointed out in Tatsch (1975) these deposits have developed at different stages in the evolution of mobile belts, platforms, and stabilized structures of the earth. Plate tectonics is, therefore, the most important mechanism which is responsible for the formation of the world wide giant gold deposits on the earth and also other mineral deposits in general. The deposits are found in all parts of the world in a variety of host rocks, but there are some noticeable clusters in the distribution pattern, the most conspicuous of these being the green stone belts of Archean Cratons and the Circum Pacific belt (Misra, 2000). According to Nekrasov (2009) most gold deposits are complex, along with gold in economic concentrations they often contain silver, copper, lead, zinc, bismuth, antimony, molybdenum, tin and other metals whose total value is comparable to that of the gold recovered. In such complex ores gold may have been deposited simultaneous with minerals of the above secondary metals such galena, sphalerite, chalcopyrite, etc., and their crystallization proceeded together with quartz or have been completed along with carbonates. Except trace amount of gold obtained as a byproduct from Ni-Cu sulphide ores associated with mafic and ultramafic rocks, volcanic massive sulphide ores, and copper ores of porphyry Cu deposits, the rest ores come from deposits mined primarily for their gold.

Historically most gold deposit types were classified according to their depth and temperature of formation, structural style, age, host rock type, or geographic area; while in more recent times, with advances in analytical capabilities, there is an increased emphasis on associations with genetic models or fluid sources, thus labeling a deposit as a metamorphogenic, meteoric, evolved meteoric, or magmatic type of gold deposits (Hart and Goldfarb, 2007). In general, the complicated natures of gold deposits pushed many writers to propose equally different types of gold deposit classification schemes.

Following the several classification schemes proposed for the different gold deposit types, there has been a need for conceptual models that describe the essential characteristics of groups of similar deposits thereby reducing the lists of gold deposit types by combining many of them in to clans sharing certain commonalities. As discussed in Cox and Singer (1987) there are three main types of models in mineral deposits: empirical, genetic, and grade-tonnage models. Accordingly, the empirical model is based on deposit description and has two parts: the first is, the geological environment, which describes the environment in which the deposits are found and the second part is the deposit description, which provides the identifying characteristics of the deposits themselves with particular emphasis on aspects by which the deposits might be recognized through their geochemical and geophysical anomalies. The genetic model explains deposits in terms of causative geological processes and it is necessarily more subjective but can be more powerful, as it can predict deposits not contained in the descriptive database (Moon et al., 2006). The grade-tonnage model, on the other hand, is extremely useful for preliminary economic evaluations and accumulates grade and tonnage data for known deposits and from this it is possible to estimate the size and grade of an average or large deposit (Moon et al., 2006).

Auriferous deposits have been classified in a number of ways and equally important models have been proposed in the last decade. Noteworthy among these are the classification schemes and proposed models by Tatsch (1975); Jensen and Bateman (1981); Boyle (1987); Groves et al., (1997); Robert et al., (1997, 2007); Misra (2000); Dubé and Gosselin (2007); Nekrasov (2009) and many others. Lithological associations, metal associations and tectonic settings of host rocks are the important parameters employed by most of the proposed classifications. However, a classification proposed by Robert et al.(2007) has been preferred for this discussion and the proposed classification is briefly presented below. Accordingly, three main clans of deposits which effectively correspond to the main clans of gold models are now broadly defined by Robert et al.(2007), each including a range of specific deposit types with common characteristics and tectonic settings. These are the orogenic, reduced-intrusion related, and oxidized-intrusion related models (Fig. 1.2). Other important deposit types are dealt separately.

1.5.3.1 The orogenic model

The term orogenic has been originally introduced by Groves et al.(1998) in recognition of the fact that quartz vein deposits in greenstone and slate belts, including those in banded iron formation, have similar characteristics and have formed by similar processes. As further stated in Robert et al.(2007) the orogenic model was originally applied strictly to syn-tectonic vein-type deposits formed at mid crustal levels in compressional or transpressional settings, i.e., syn-orogenic deposits. However, the term has been progressively broadened to include deposits that are post-orogenic relative to processes at their crustal depth of formation. This has led to significant ambiguity in the definition of the boundary between the orogenic and reduced intrusion-related (which will be discussed below) deposit models. The confusion is that greenstone belts also contain gold deposit types that do not fit the orgenic model as defined by Robert et al.(2005)and Groves et al.(2003). Therefore, to avoid such confusion the orogenic model is defined here to only include the syn-tectonic quartz-carbonate vein-type deposits and their equivalents, formed at mid-crustal levels. Specific deposit types in this clan include the turbidite-hosted and greenstone hosted vein deposits, as well as the BIF-hosted veins and sulfidic replacement deposits. According to Groves et al.(1998) most ores of this model are post-orgenic with respect to tectonism of their immediate host rocks, but are simultaneously syn-genetic with respect to ongoing deep-crustal, subduction-related thermal processes and the prefix orogenic satisfies both these conditions.

1.5.3.2 The reduced intrusion-related model

The reduced intrusion-related model was mainly developed in response to observations, explorations, discoveries, and research on gold systems across central Alaska and Yukon where they are part of the Tintina Gold Province and includes well studied examples such as Fort Knox, Dublin Gulch, Clear Creek, and Scheelite Dome (Hart, 2005). According to Thompson et al.(1999) the reduced intrusion-related gold mineralization is related with regions lacking copper, but known for W and Sn deposits. Deposits of this model are distinguished by an Au-Bi-Te-As metal associations and a close spatial and temporal association with moderately-reduced equigranular granitic intrusions (Thomson and Nexberry, 2000).

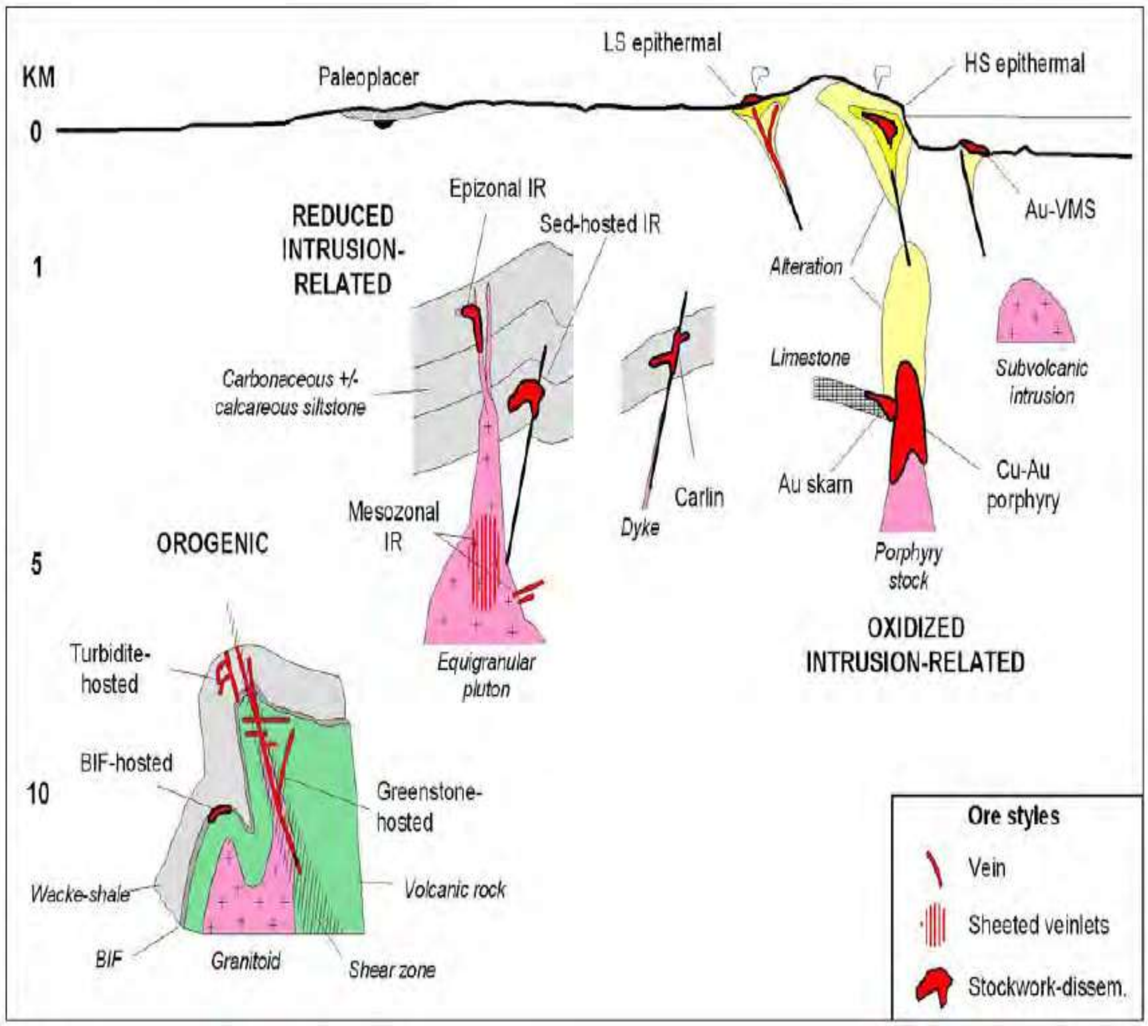

Figure 1.2 Schematic cross section showing the key geologic elements of the main gold systems and their crustal depths of emplacement (given in logarithmic depth scale). [Source: Robert et al.(2007)]

These deposits occur in reduced siliciclastic sedimentary sequences and a range of styles and depths of formation has been documented for intrusion-related deposits, including intrusion hosted deposits of mesozonal to epizonal character, and more distal, sediment-hosted mesozonal equivalents (Groves et al., 1998). According to Hart and Goldfarb (2007) reduced intrusion-related gold deposits are best developed in intrusions that were emplaced in to the region behind an accretionary orogen and in to rocks of the deformed continental margin backstop. As summarized in Robert et al.(2007) the intrusions and associated intrusion-related gold mineralization exhibit a wide range of characteristics that indicate a range of magmatic and hydrothermal environments at depths most between 4 and 6 kilometers. Although they share a large number of associated features with orogenic gold systems, the reduced intrusion-gold model deposits are a product of local-scale fluids derived from a cooling pluton and they differ from orogenic deposits that are considered to result from crustal-scale fluids derived through metamorphic dehydration (Groves et al., 1998; Stuwe, 1998). Another most distinctive style of gold mineralization in reduced intrusion-relater gold systems are sheeted arrays of parallel, low-sulphide, single-stage quartz veins which are found over 10s to 100s of meters and preferentially located in the pluton's cupola which are unlike multidirectional interconnected stockworks that are characteristic of porphyry systems or antithetic tensional vein arrays typical of orogenic deposits (Hart, 2005).

1.5.3.3 The oxidized intrusion-related model

This model includes the well-known porphyry and high-sulfidation epithermal gold deposit types, as well as skarn and manto type deposits, formed in continental and oceanic convergent plate settings (Robert et al., 2007). According to Sillitoe and Thompson (1998) the Au-Fe oxide–Cu and Au–Cu–Mo–Zn, Au–Te–Pb–Zn–Cu, and Au–As–Pb–Zn–Cu associations are all related with oxidized intrusions where the former to highly oxidized calk-alkaline intrusions emplaced in subduction related arcs, the middle to similar setting but linked to less oxidized intrusions, and the later with highly oxidized intrusion but of alkaline composition and back-arc location. The oxidized intrusion related deposits are, therefore, best regarded as components of large hydrothermal systems centered on high-level, generally oxidized, and intermediate to felsic porphyry stocks (Robert et al., 2007). In the last decade, the genetic connection between porphyry and high-sulfidation epithermal deposits have been more firmly established (Heinrich et al., 2004), and it has been suggested that the largest deposits if this clan form in compressional arcs (Sillitoe and Hedenquist, 2003).

Other types of globally important gold deposits include low- and intermediate-sulfidation epithermal, carlin type, gold-rich volcanic massive sulfides, and Witwatersrand type deposits. Epithermal deposits are now subdivided in to low-, intermediate-, and high-sulfidation categories, on the basis of mineralization and alteration assemblages (Sillitoe and Hedenquist, 2003). Intermediate-sulfidation deposits, like high-sulfidation ones, are interpreted to be a component of large oxidized intrusion-related systems, as is the case for some deposits. Carlin type deposits have been regarded either as being distal parts of large oxidized intrusion-related systems or as standalone deposits (Cline et al., 2005). Work on modern sea floor has provided additional insight in to the formation of gold-rich volcanic massive sulfide deposits, with the identification of a number of favorable settings (Huston, 2000; Hannington, 2004). The recognition that some gold-rich volcanic massive sulfide deposits are effectively submarine equivalent of high-sulfidation deposits (Sillitoe et al., 1996) puts them in the oxidized intrusion related model of deposits and has significant exploration implications. The controversy remains regarding the origin of the unique Witwatersrand gold deposits, with both modified paleoplacer and hydrothermal origins being proposed (Frimmel et al., 2005; Law and Philips, 2005).

1.5.4 History and production of gold in the world and in Ethiopia

1.5.4.1 History and production of gold in the world

Gold has been a large part of human history. It has been traded, worshiped, fought over, and prized for a long period of times. It was among the first metals to be mined by early human beings (the earliest gold miners being Sumerians who were working with deposits in present day Iran and the Egyptians) because gold commonly occurs in easily extractable native form, it is beautiful and imperishable, and beautiful objects are made from it (Misra, 2000). During the primitive time the major source of the metal was placers and people of the time were attracted by its beauty, durability and malleability, and they used it for decoration purpose. As tribal development progressed through the Paleolithic, Mesolithic and Neolithic ages, and as people assembled in to civilized centers, gold appears to have taken on a sacred quality because of its enduring character, being worn initially as amulets and later fashioned to religious objects (idols) (Boyle, 1987). But the first significant rise in gold production followed the discovery of America, when Mexico, Peru, Bolivia, and Chile poured forth streams of yellow and white metal to enrich the capitals of Europe (Jensen and Bateman, 1981).

As summarized in Jensen and Bateman (1981) and Boyle (1987) a similar discovery of placer gold in Australia in 1851 pushed the world output to over 6 million ounces in 1850 to 1860 (1 ounce = 28.349 grams). Even though such production was quickly declined, it was counterbalanced by other discoveries in western United States which brought another significant gain in United States' output, which was surpassed by the even more sensational rise in South Africa, the discovery of the great Rand in 1886. According to Misra (2000) there was a decrease in productivity of gold in the middle ages but increased again due to the large economic expansion of the 16th century. The " Gold fever" of the middle and late 19th century lead to the discovery of many rich placer deposits in Siberia, Alaska, California, Australia, and South Africa and it was probably triggered by the adoption of gold as the monetary standard by the British Empire in 1821(Jensen and Bateman, 1981).

One hundred ten years data (1900 up to 2010) from the US Geological Survey indicate that world gold production has been steadily risen, except for four periods (Fig. 1.3). Responsible for production increases are, among others, technological advancements with respect to construction of mines and the excavation of gold from soil materials and improved means to locate gold deposits. Figure1.3 reveals four drops in gold production: during the two world wars, gold production naturally declined. A third major decline started in 1970 and lasted for five years. Thereafter, gold production stood at a constant level of around 1,200 annual tons. For the fourth decline, 2002 - 2008, are responsible rising production costs.

Data from the USGS further indicate that the decline in world gold production set in when the gold price already started to rise. Mining companies were first reluctant to step up production, as it was not clear whether the greater interest in gold was only a shortterm trend. Besides, increasing gold mining needs preparation and time. The US dollar become the world's monetary standard at gold parity of $30 per troy ounce in 1944, a situation that continued until 1968 when the US government declared a de facto abandonment of the gold standard (Jensen and Bateman, 1981).The gold price rose slightly at first to about $40 per troy ounce, but very rapidly after 1971 when the US officially comes off the gold standard and its citizens were again allowed to own gold. The price peaked at $843 in 1980, and then felt erratically, to an average price of around $300-$ 400 per troy ounce, a price which has been fairly stable since 1981(Misra, 2000).

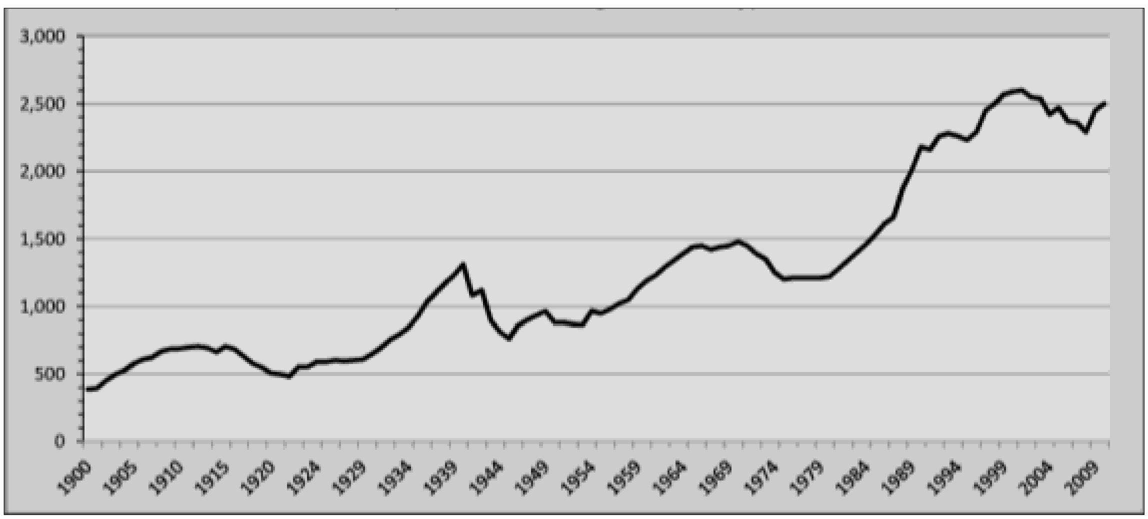

Figure 1.3 Global production trends for gold in tons from 1900 up to 2010. [Source: USGS]

1.5.4.2 History, distribution and production of gold in Ethiopia

Gold, currently being one of the most important export mineral in Ethiopia, has a long history in the country. It has been traditionally mined from placer deposits and semi-mechanized gold mining began in 1930s after the discovery of placer gold in Bedakessa valley in the Adola belt (Hundie, 2010). After this time several prospecting activities as well as geological mapping and geochemical prospecting were undertaken in several regions of the country with the prime aim of locating favorable geological environments and prime target areas for gold exploration. Primary gold sources were discovered in the 1980s during detailed exploration in the Adola gold field by EMRDC (Ethiopia Mineral Resources Development Corporation) that resulted in the discovery of the Lega Dembi and sakaro primary gold deposits and many other primary gold occurrences (Solomon, 2009). Even though primary and placer gold deposits and occurrences have been reported from the Pan-African volcano-sedimentary sequences in the northern, western, and south-western Ethiopia, at present the Adola gold field is the only existing active gold producing area except for small-scale placer gold mining activities by artisanal miners in the above mentioned regions (MoM, 2010; Solomon, 2009).

The most important terrain for gold exploration and exploitation in Ethiopia is the Proterozoic basement rocks that are distributed in different parts of the country and hosting nearly all known gold occurrences of the country. Even though the occurrence of gold is reported from the different parts of the country, significant gold mineralization in Ethiopia is concentrated in three main greenstone belts (Fig. 1.4). These are the northern, western, and southern greenstone belts. All of these main greenstone belts contain syn- to post-orogenic intrusions of intermediate to acidic composition, in association with which intrusion-related gold deposits may be found (MoME, 2007).

The northern greenstone belt is located in Tigray Region and comprises the gold occurrences of Terakimti, Adizeresenay, Mai Hanse, and Zeger areas. The most promising discovery in this greenstone belt is the Terakimti prospect, which is located in the western part of the Northern Greenstone belt and occurring in a sequence of meta-volcanic, meta-sedimentary and intermediate to acid intrusive rocks where systematic exploration by GSE and Ashanti accompanied by trenching and drilling discovered auriferous quartz veins that revealed grades up to 4-16 grams per ton (MoME, 2007; MoM, 2010). The western greenstone belt comprises Tulu-Kapi, Oda-Godare, Dul, Akobo, Baruda, Gizen-Mengi, Ankore, Beles-Dendir and Sirkole gold deposits and occurrences. Even though many of these greenstone belts host promising gold showings, the most promising gold occurrences so far are located in Tulu-Kapi and Sirkole areas that are underlain by meta-sediments, which consists of sandstone, phyllites and quartzite at the central part, followed by metamorphosed intrusive units including granites, synites, diorite and grano-diorite to gabbro in western and eastern parts (MoM, 2010).

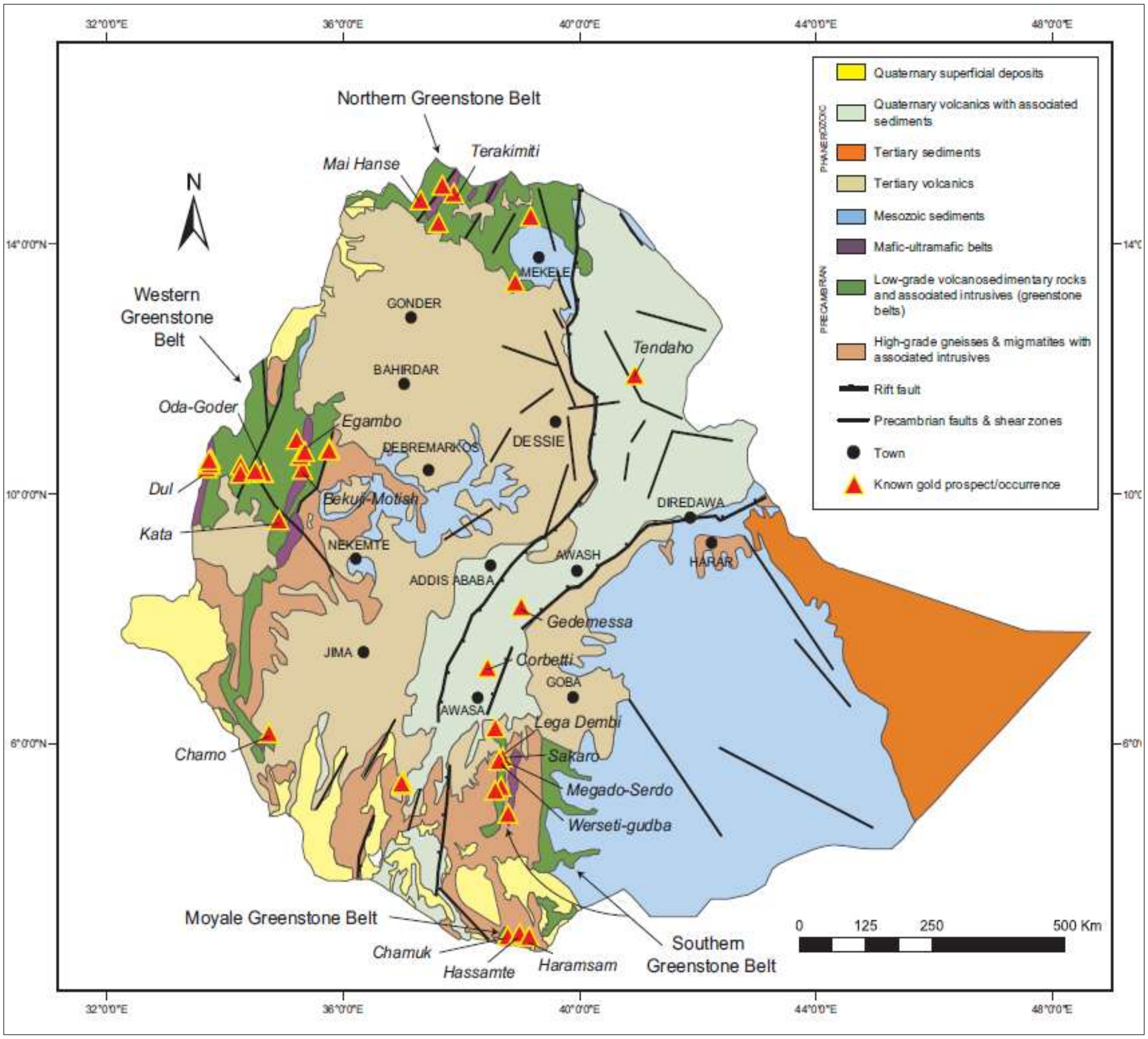

Figure 1.4 The distribution of principal gold prospects and occurrences in Ethiopia. [Source =from MoME, 2007]

The southern greenstone belt, on the other hand, hosts the Lega Dembi, Sakaro, Megado-Serdo, Dawa-Digati, Okote, Hassamte, and Chamuk gold deposits and occurrences. The Adola gold field of southern Ethiopia, which also hosts the Lega Dembi primary gold mining, is by far the largest gold supplier of the country. As stated in Debele and Koeberl (2004) the gold mineralization occurs in intensely sheared, hydrothermally altered, green schist facies N-S trending volcano-sedimentary rocks of Megado belt, which forms part of the late-Proterozoic Adola granite-greenstone in southern Ethiopia. According to

Ministry of Mines Mineral Licensing Administration Department (2010) there are both open pit and underground mine in the Lega Dembi gold field. The open pit mine has proven gold reserves of ca. 66 tones with an average grade of 3.7 grams per ton within200m depth. The mine began pilot-scale operation in 1987 and upgraded to industrial scale in 1989. Following the new investment policy of Ethiopia, the mine was privatized in 1998 after extraction of ca. 12 tons of gold by the government. Currently the annual production of the mine is 3500 kg of gold per year. Underground work began in 2000, and today the present length of tunnels is 8.8 km. The gold reserves are estimated to be ca. 11 tones with an average grade of 3.59 grams per ton. The actual operation started in June 2009 and has an average annual gold production of 1086 kg.

1.5.5 Previous work done in the study area

As stated by the 2008 annual report of the Geological Survey of Ethiopia (GSE, 2008) magnetic and spectral induced polarization (SIP)/ resistivity survey was done in Burikaro prospect in 2007 by the Geological Survey of Ethiopia geophysics department for National Mining Corporation. It was done as part of the Dawa Digati gold exploration project of the National Mining Corporation. The objective of the total magnetic field and dipole-dipole induced polarization (SIP)/ resistivity survey employed was to get lateral and depth information of the auriferous zones covered by deeply weathered regolith and to suggest possible test drill sites by integrating with geological information.

The results of the geophysical survey have indicated two well defined anomalous IP-chargeability regions in the north-central and south-central parts of the Burikaro prospect which are associated with different lithological units. Both regions are characterized by relatively high IP and high apparent resistivity. The north-central anomalous zone is within the zone of flat quartz vein system and the major lithologic units are quartz-mica-graphite phyllite, graphitic-talc phyllite, and graphite-sericite-chlorite phyllite. The high chargeability and resistivity anomaly component is dominantly within the graphite-sericite-chlorite phyllite. The south-central anomalous zone is within mica phyllite, meta-conglomerates, and quartz- mica-graphitic phyllite. The central part of the anomaly is within the conglomerates and the west and east components are in the mica phyllite and quartz-mica-graphitic phyllite. In both cases of the anomalous zones, the contact regions of the lithologic units are good targets for gold mineralization.

Basson (2006) conducted a structural analysis of selected areas in the Dawa Digati prospect area (that includes Okote, South Ejersa, and Burikaro sub-areas) through the contracted agreement between National Mining Corporation and Tect Geological Consulting. The aim of the study was to determine the structural nature and potential continuity of gold bearing quartz veins and/or mineralized zones in the Dawa Digati prospect. Accordingly, he summarized that the Burikaro sub-area is continuous along strike with the Ejersa area and mineralization is hosted in quartz veins mainly dipping to east and west with some veins directly attributable to cross-cutting, NNE-trending, late tectonic shears. Veins also have apparently imposed a degree of alteration, in the form of silicification, chloritization, and even carbonitization on the host meta-sediments. The study also concluded that the mineralization at Ejersa south is associated with the contact zone between a thick amphibolite unit and metasedimentary sequence.

A summary of exploration work report in 2004 by National Mining Corporation Dawa Digati gold exploration project indicates an exploration work accompanied by drainage heavy concentrate, chip samples, and trenches in Ejersa and trench work in Burikaro was conducted. The majority of the samples show gold-positive results. Though low grade, the trench results show that the mineralization of south Ejersa prospect is well defined and consistent usually represented by quartz veinlets infesting the meta-volcanics/meta-sediment contact zone.

According to a report on mineral exploration in Dawa Digati area, an exploration work was conducted by Ethiopian Institute of Geological Survey (EIGS, 1995). This work touches western part of the Ejersa ridge (western part of the present study area) and is accompanied by geophysical, geochemical, and trenching works. The results of this work suggested the occurrences of placer gold in the upper parts of Ejersa river. Most of the first and second order streams that drain from the meta-sediments and the amphibolites/gabbro-amphibolites show the maximum number of gold grains suggesting the upper and lower parts of Ejersa river and other areas like the Wachu Dima areas of Chebi Botera river, the lower parts of Chebi river, and Kursu river to be the most potential areas for placer gold. Hence, this condition strongly implies the occurrence of primary gold either in the meta-sediments or the amphibolite with their quartz veins outcropping east of Wachu Dima extending further to the Ejersa ridge.

1.5.6 Significance of the study

As stated earlier, there are only few organized and compiled works in the study area either for scientific interests or economic considerations. Therefore; this research work is intended to benefit the following people and organizations in a direct or indirect way.

- Governmental organizations (Mines Bureau of the region as well as the country) for further work in the region.
- Exploration/mining companies and Research institutions
- To develop the basic philosophy and skills of research undertaking in geosciences for the researcher
- As a reference material for the students and other researchers may be after publication.

1.5.7 Scope and limitations of the present study

Because of inadequate finance and shortage of time which clearly have significant effect on any research work activity; isotope, fluid inclusion, sulfide geochemistry, and many other related studies are not incorporated in this research work although they are important components of the study of ore genesis. As clearly stated in the methodology section, this thesis work is therefore solely based on detailed field identification and description of rocks and structures, thin section studies, polished section studies, chemical analysis through Atomic Absorption Spectrophotometer, and a thorough review and interpretation of previous exploration works conducted in the area.

CHAPTER TWO

2 METHODOLOGY

2.1 Introduction

Undertaking research works in mineral exploration can be carried out using one or combinations of geological, geochemical, geophysical, and remote sensing methods and in most cases involve a team of mineral exploration professionals. Geological mapping with associated structural data being the fundamental tasks in any exploration work irrespective of the type of methodology one may follow. It also needs the utilization of different types of equipments, computational ability and/or software. Whatever methodology we adopted, it is necessary to follow a continuous and interlinked set of procedures and activities that are performed in the different stages of the proposed research work. Geological and geochemical methods are employed in this research work. Accordingly, three main investigation stages are followed to achieve the general and specific objectives of the proposed research work, namely the pre-, field, and post-field stages. The various activities employed in each stage are discussed as follows and flow chart showing summary of the different activities performed in each stage is also provided at the end of this chapter.

2.2 Pre-field work

The key activities carried out prior to the actual field work of this study are the following:

- The first step toward this thesis work was research title selection and setting of the objectives which was followed by searching working area with appropriate secondary data that are helpful for the proposed research study and cannot be produced by the researcher himself.
- After getting the working area, all known and available works previously done in the study area were collected from the National Mining Corporation, Ethiopian Geological Surveys, and online published articles in different journals.

- The next step was a thorough review of relevant and related literature that concentrate, among others, on the following major points:
  - Major theories of ore genesis
  - History and production of gold in the world
  - General geochemistry, occurrences, uses, and properties of gold
  - The different types of auriferous deposits and proposed models
  - The distribution and production of gold in Ethiopia
  - Geologic setting and geodynamic evolution of the Adola region
- Following the collection of necessary information and literature review was preparation for the field work. The first job in this respect was aerial photo interpretation, field base map preparation, preparation of exploration/traverse lines. Using aerial photo interpretation the overall topography, drainage systems, and some structural information of the area were obtained. A 1:100,000 geological map of the Adola area that was produced by Ethiopia Institutes of Geological Surveys (MoME, 1992) was used to prepare a base map for the field work.
- Then the necessary field equipment including, among others, compass, hand lenses, geological hammer, GPS, field notebook, photo camera, acid, and sample bags were collected.
- Finally, the necessary finance for the field work and other logistics were made ready.

2.3 Field work

During the field work which was conducted for two weeks, the following major activities were carried out:

- Through the prepared exploration/traverse lines, identification and description of each lithological unit were done based on their color, texture/grain size, composition, and field relationships with other rock units.
- Orientations of important structural parameters such as bedding planes, foliations, shear zones, joints, quartz veins, and mineral lineations were measured.

- Important field photographs of rocks and structural features were taken to support the above descriptions.
- Preliminary geological map of the area was prepared by delineating each rock unit on the base map (by using the parameters listed above) following their strike length and width.
- Furthermore; rock alterations, structures, rate of weathering, breccias, favorable rock types and topographic features suggesting anomalous rock conditions were also studied to further identify and interpret:
    - Rock types, facies of those rocks, stratigraphic successions, method of emplacement, the relationship between the different rock types, i.e., their boundaries, structure and others.
    - Alteration minerals, assemblages, and intensity
    - Structures and rock units which may control mineralization in the study area

2.3.1 Methods of sample collection

A total of 42 representative surface samples were collected from each lithological unit, quartz veins, and the mineralized contact zone. More than one sample was collected from a single rock unit where variation in lithology and/or certain other parameters are observed/suspected. The sampling was done by using the prepared traverse lines that were drawn in E-W direction, the direction perpendicular to the general strike of the rocks. Each sample was properly labeled and their locations were also recorded using GPS.

2.4 Post-field work

The key activities of the post-field work stage are laboratory works/primary data analysis, interpretation of secondary data results, finalizing the geological map of the study area, discussion of the overall obtained results, writing the thesis work report after incorporating all available data, submission of the finalized report, and defense. The detail procedures followed in each activity are briefly presented below.

2.4.1 Primary data analytical methods

2.4.1.1 Thin section preparation and rock petrography

Out of the collected surface rock samples during the field work, 12 samples were selected for petrographic study and submitted to Addis Ababa University where thin sections of these samples were prepared in the school of earth sciences laboratory. After the thin sections were prepared, descriptions and study of the thin section are made by using petrographic microscope in Addis Ababa University and Geological Surveys of Ethiopia. The detailed descriptions undertaken using thin section study includes the determination of:

- The type and modal percentages of minerals present in each thin section
- Structural features including shearing, foliation, deformation and recrystallization, twinning, and other intragrain and intergrain phenomena like rimming, mineral inclusions, and secondary porosity.
- Observed alteration phenomenon and relative stability of minerals
- Metamorphism and metamorphic mineral assemblages
- Presence and distribution of opaque minerals
- Taking photomicrographs using digital camera to post and support report writing.

Finally, mineral abundances, mesoscopic structures (e.g., in schists), and composition and the nature of the protolith (e.g., in meta-conglomerate) are employed as a major criteria for naming the rocks of the study area.

2.4.1.2 Polished section preparation and ore petrography

From the collected surface rock samples during the field work, 13 surface rock samples indicating mineralization were selected for polished section preparation and they were sent to the Ethiopian Geological Survey Central Laboratory. After the preparation of the polished section, the detailed description of these polished sections was carried out using reflected light microscope both in Ethiopian Geological Survey and School of Earth sciences, Addis Ababa University. The detailed descriptions performed during ore petrography session include:

- Identification of the different types of ore minerals present in each view of the studied polished sections
- Identification and interpretation of the different types of textures of ore minerals and associated gangue minerals to understand:
  - The processes responsible for initial ore deposition and determining the sequence of events or depositional history
  - Understanding the timing of formation of the ore minerals relative to the associated gangue minerals
  - Studying post depositional histories such as deformation, annealing, and weathering
  - The different types of structures in the host rock such as veins and open spaces
  - The spatial relationship between ore mineral grains
- Studying alteration and/or replacement phenomena
- Taking necessary photomicrographs using digital camera

2.4.1.3 Surface sample chemical analysis

Out of the collected surface samples during the field work, 10 samples (six rock and four quartz vein) were selected for chemical analysis through atomic absorption spectrophotometer (AAS) and sent to Ezana Mining Development plc, Mekelle. The elements analyzed are Au, Ag, Cu, Co, Pb, Ni, and Zn. The main reason for the surface sample chemical analyses was to understand the surface distribution/manifestation of the gold mineralization, identify the differences in gold mineral distribution between the different lithologies, and the relationship of gold with few other base metals. The analysis was performed with a Varian atomic absorption spectrophotometer, spectra AA240FS. Accredited methods were employed in the preparation which uses aquaregia digest (AA74D1 and AA74D2) for base metals and gold. The preparation code is PG210 that involves drying samples, crush to 2 mm, split 1000 g, and pulverize to 75 mm. The means of quality control includes: bowls are cleaned using barren quartz chips between each sample to minimize cross contamination, second splits, reject duplicates and pulp duplicates are also used to monitor the quality of sample preparation, standard reference materials, internally prepared in-house standards and repeat samples are used in all sample batches. The detection limit for gold is 0.02 ppm, for silver 0.2 ppm, and 1ppm for the rest of the base metals.

2.4.2 Secondary data analytical methods and interpretation of results

The analyses of several trench channel samples were conducted in the study area by the National Mining Corporation (NMiC, 1996-1998) as a part of the Dawa Digati Gold Exploration Project work. The samples collected (108 samples) were analyzed by Atomic Absorption Spectrophotometer (AAS) and Fire Assay methods (FA) in the Adola Mineral Exploration Group and Ethiopian Institute of Geological Surveys laboratories. The reliability of these laboratories was counter checked by sending duplicates of some of the samples analyzed by one of the laboratories to the other and vice versa. External control analysis was conducted by Geomet Laboratory, Zimbabwe, to ensure the reliability of the two laboratories. The efficiency of the analytical methods was also checked by subjecting AAS/FA analyzed samples to BLEG (bulk leachable and extractable gold) tests at the Geomet Laboratory. Some of the selected trench analytical results and cross-section data are used in this thesis work to understand and interpret:

- ✓ The spatial distribution of gold mineralization between the different rock types
- ✓ The nature of gold mineralization
- ✓ Structures controlling gold mineralization
- ✓ The different alteration phenomenon and ore genesis

2.4.3 Report compilation

This was performed in the last phase of the proposed research work. After collecting the results of all analyzed samples and incorporating it with available secondary data, interpretations are made and the report on the geology and genesis of gold mineralization in the study area is prepared. ERDAS IMAGINE 9.2, ArcGIS 10, Surfer 10, Stereonet Version 9.0.2, Microsoft Excel, and Microsoft Word are among the softwares utilized in the mapping, discussion of analytical results, and report writing.

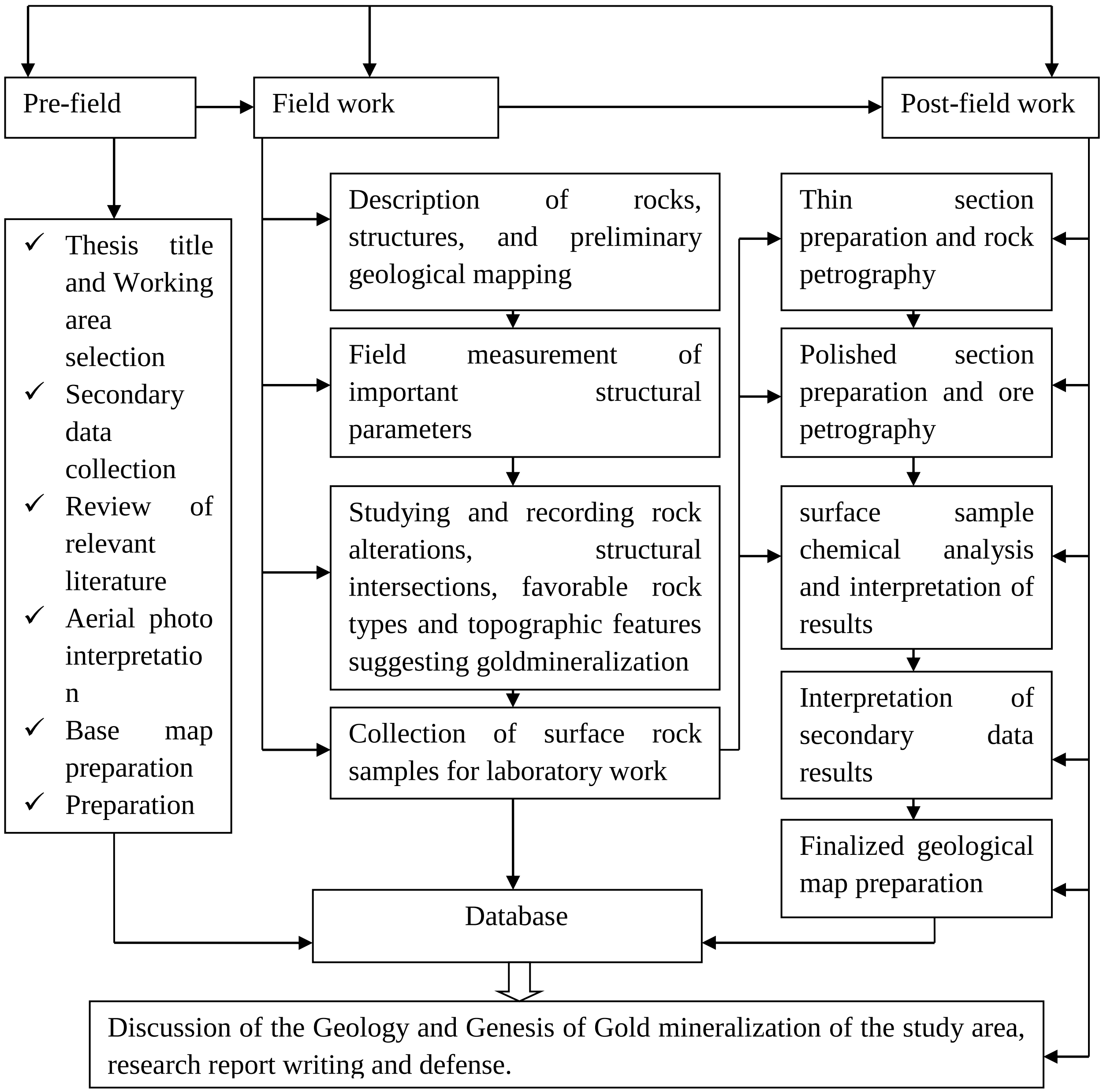

Figure 2.1 Flow chart summarizing the different activities carried out in the different stages of the proposed research work.

CHAPTER THREE

3 REGIONAL GEOLOGY AND TECTONIC SETTING

3.1 Introduction

The geology of Ethiopia can be categorized in three major divisions that document the long geologic history of the country from Precambrian to the present time. These are the Precambrian metamorphic rocks with their associated granitoids, the Paleozoic-Mesozoic sedimentary rocks and the Cenozoic volcanic and volcano-sedimentary rocks. The Precambrian basement rocks are the oldest formations in the country and form the basal group. They are poly-deformed and metamorphosed and basically exposed in areas where the overlying rocks are eroded away, particularly in the peripheral parts of the country and in some deep river gorges. According to Mogessie et al.(2002) the basement rocks in the south and west Ethiopia, where granitic rocks and gneisses predominate, has been higher metamorphosed than the Precambrian sequence in the north which is metamorphosed to green schist facies. The late Paleozoic to Mesozoic sedimentary rocks are widely distributed in the northern, central, eastern and southeastern parts of the country unconformably overlying the basement rocks and mainly composed of sandstone and limestone and are exposed mainly in the Ogaden, Abay and Mekele Basins (MoME, 1995). Phanerozoic sedimentary and volcanic rocks cover much of the country's central highlands, rift valley and eastern lowlands; whilst the Tertiary to Quaternary volcanics are the youngest formations in the country and are associated with the evolution of the East African Rift System and the main rock types of this class are basalts, trachytes and associated dyke swarms, andesites, rhyolites, ignimbrites and pumiceous ash (Gebremichael, 2006).

3.2 Regional Geologic Setting

The study area is located in the Adola ore district which marks an important terrain in the Precambrian of southern Ethiopia where the northeast branch of the Mozambican belt is supposed to merge with Arabian-Nubian Shield. The Adola area marks an extensive exposure of both high-grade gneissic terrain of Mozambique belt and low-grade metavolcano-sedimentary sequences of the Arabian-Nubian Shield. As discussed in the works of Worku and Yifa (1992); Yibas et al.(2002) the Adola area of southern Ethiopia is made up of two main tectonostratigraphic units that are separated by repeatedly reactivated deformation zones: high grade and complexly deformed gneissic terrains that are intruded by syn-to post-tectonic granitoids and green schist to amphibolite facies metamorphic grade ultrabasic rocks that undergone relatively simple deformation state. The greenstone belts form synclines while those of the gneissic terrain lies in the anticlinal sides.

Many classification schemes have been proposed for the Precambrian rocks of the region. Early studies of the rocks of southern Ethiopia by (Gilboy, 1970; Chater, 1971; Kazmin, 1972; Kazmin, et al., 1978; as cited in MoME, 1994; Worku, 1996a; Yihunie and Tesfaye, 2002) classified the rocks in to three groups: Lower, Middle and Upper complexes on the basis of characteristic contrast in lithology, metamorphism and structural style. According to Kazmin (1972, 1975) and Kazmin et al.(1978) the lower complex is made of mainly high grade gneisses and assumed to be Archean age. The same work indicates that the middle complex consists of psammitic and pelitic meta-sediments and regarded to be Palaeo-to-Mesoproterozoic; whilst the upper complex is made of low grade rocks of island arc-ophiolite association of Neoproterozoic age and correlated to the Arabian-Nubian-Shield (Worku, 1996a). This interpretation and traditional classification of the Precambrian rocks into an Archean cratonic basement, Palaeoproterozoic and Neoproterozoic has not been supported by recently obtained geochronological and isotope investigations (Ayalew et al., 1990;Ayalew and Gichile, 1990; Teklay et al., 1993; as cited in Worku, 1996a) and Worku (1996a) who revealed that the rocks of southern and western Ethiopia, some of which were previously assumed to be Archean, show the same age like the arc and back-arc complexes of the Arabian-Nubian-Shield.

Schmeroled (1988); as cited in EIGS, 1993 proposed a five-fold classification, grouping the rocks of Adola area in to western basement, meta-volcano-sedimentary belt, central basement, ultramafic belt and eastern basement, which later redefined by Hailu and Kinetibeb (1989) as the western gneissic domain, the meta-volcano-sedimentary domain, the Burjiji-Gariboro domain, the ultrabasic domain and the eastern gneissic domain, respectively. But, a two-fold classification proposed by the works of Ghebreab (1992); MoME (1993); Worku (1996a); Billay et al.(1997); Yibas et al.(2002) is preferred for the purpose of description of the regional geological setting of the region. Accordingly, the rocks of Adola area are grouped in to two general categories: the high-grade gneissic terrain and the greenstone terrain. The proposed classification is briefly presented below.

3.2.1The Gneissic Terrain

The gneissic terrain occurs surrounding and separating the two greenstone belts (Billay et al., 1997) and it consists of relatively high grade rocks which occupy three N-S trending anticlinal zones separated by two intervening narrow N-S trending synclinal greenstone belts (MoME, 1993).The geology of the terrain comprises para- and ortho-gneisses, including monotonous quartzofedsphatic biotite gneisses with subordinate muscovite quartz schists, staurolite-garnet-biotite schists, impure marbles, and amphibolites (Gilboy, 1970;Chater, 1971; Kozyrev et al., 1985; Ghebreab, 1989; Worku and Yifa, 1989, as cited in Billay et al., 1997). According to a report by the Ministry of Mines and Energy (MoME, 1993) quartzofedsphatic gneisses (both of sedimentary and igneous origin), biotite, and quartz biotite gneisses/schists with some sporadic interlayer of amphibolites form the dominant geologic units of the gneissic terrain. In addition to the para- and orthogneisses and associated ultramafic complexes, the gneissic terrain is also intruded at places by large bodies of deformed and metamorphosed granitoids/tonolites (Billay et al., 1997; Yibas et al., 2002). These granitoids intruding the gneissic terrain are relatively younger syn- to post-tectonic and are generally migmatized (MoME, 1993). Sporadic Tertiary basalts also unconformably cover the northern parts of the gneissic terrain (MoME, 1993; 1995).

With references to the greenstone belts, the gneissic terrain is present in the western, central and eastern parts of the area. Based on metamorphic grade and structural position, the gneissic terrain rocks are believed to be older than the greenstone belt rocks even though it has not yet been ascertained whether there is a sedimentation gap or not between the two rock associations (MoME, 1993).

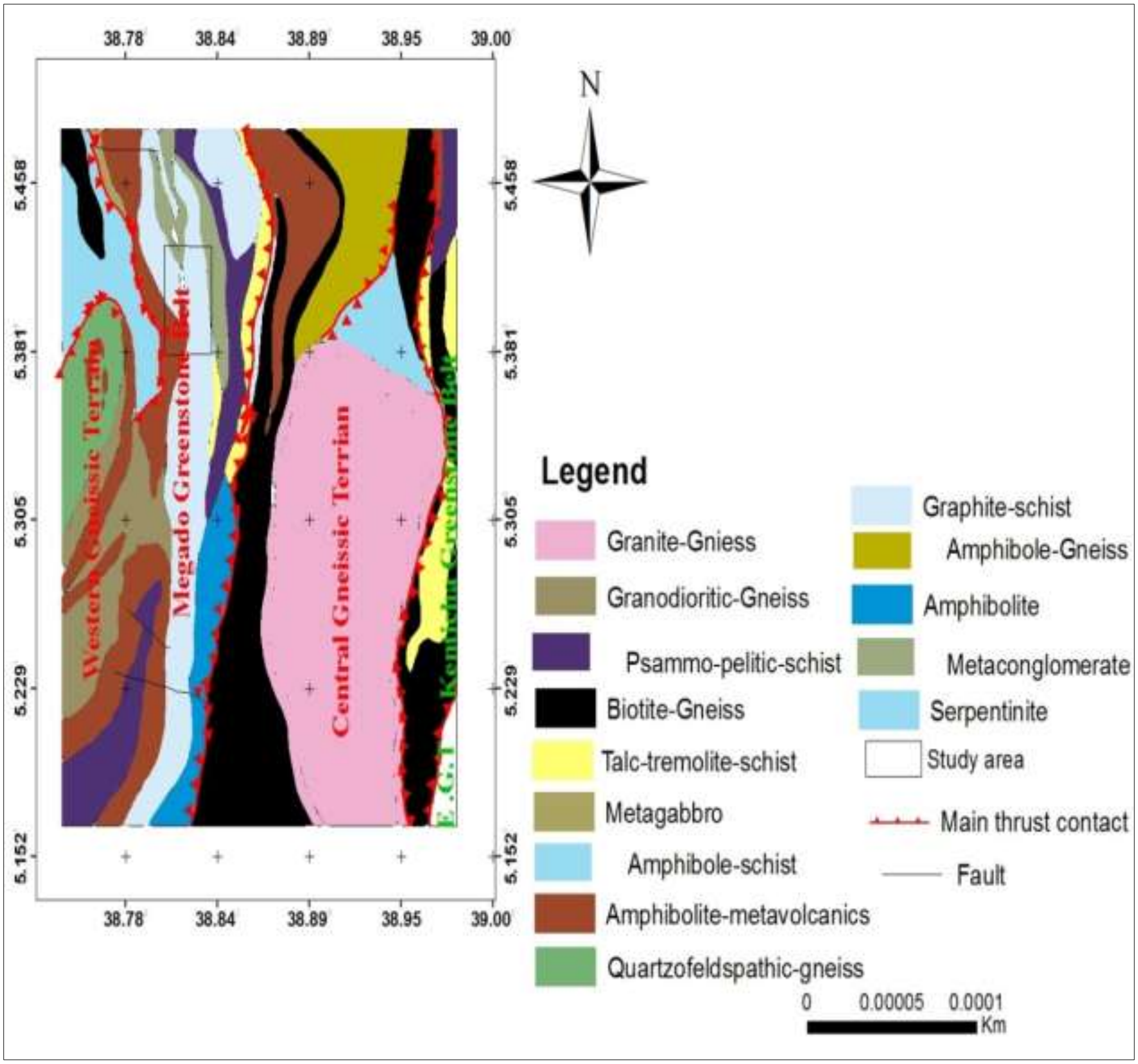

Figure 3.1 Simplified geological map of Adola region (modified from MoME, 1992). (E.G.I = Eastern Gneissic Terrain)

3.2.2 The greenstone terrain

The greenstone terrain is located between the gneissic terrains that are separating and enveloping it from east and west. It consists of a succession of meta-volcanics and pyroclastics, graphitic schists, graphitic quartzites, meta-sandstone, meta-conglomerates, ultramafic rocks, and intruded by gabbro and tonalite (Worku, 1996a; Adugna et al., 2010). As discussed in Billay et al.(1997) the Adola greenstone terrain is characterized by two linear, closely spaced, N-S trending belts of metamorphosed supracrustal rocks, namely the Megado volcano sedimentary belt in the west and the Kenticha ultramafic belt in the east. The greenstone sequence of the Megado zone and the Kenticha zone appear to represent rocks of slightly different depositional environment, i.e., two separate discrete basins, in that the Kenticha zone encompasses rocks that have different geochemical affinities (MoME, 1993). Metabasic and metasedimentary rocks (predominantly of arkoses, feldspathic quartzites, quartzites, perlites, and polymictic conglomerates and grey wackes) are dominant over ultramafic rocks in the former one; whilst ultramafic rocks such as serpentinite, talc-tremolite and talc-anthophyllite schists are dominant over the mafic rocks in the Kenticha belt (Billay et al., 1997; Yibas et al., 2002and references there in). Apart from the large Gariboro syn-tectonic batholith which is situated between the Kenticha and Megado zone, small syn-tectonic granitoids, meta-gabbros, and subcircular post-tectonic granitoids align particularly along the western boundary of the Megado zone (MoME, 1993). The mafic–ultramafic–sedimentary assemblages can be referred to as fold and thrust belts in view of their deformational styles and as ophiolites in as far as their origin and lithological associations are concerned (Yibas,2000; Yibas et al., 2000c; as cited in Yibas, 2002).

The thrust bounded rock assemblages of the greenstone terrain are thought to represent southern extensions of the arc/back-arc Arabian-Nubian Shield sequences (Kazmin, 1976; De Wit and Chewaka, 1981; Berhe, 1990; Gichile, 1991; Worku, 1996, as cited in Yihunie et al., 2006). Excluding the intrusive and ultramafic rocks of the greenstone terrain, the rock association was considered to form the Adola group (which is further subdivided to Chakata and Finkilcha Formations) and the Kajimiti Beds (Kozyrev et al., 1985, as cited in Worku, 1996a).The mafic meta-volcanics and associated volcanoclastic deposits constitute the Chakata formation whereas the Finkilcha formation is made of mainly graphitic schists and graphitic quartzites (Worku, 1996a).

Table 3.1 Summary of the simplified stratigraphy of Adola region

	Basalt
	——Unconformity——
	Post-tectonic granitoids
	Syn-tectonic granitoids
	Metasediments -semi-pelitic schist
Green stone	-graphitic schist
Belt	-metaturbidites(metaconglomerates, meta - sandstone, metasiltstone)
(Upper Proterozoic)	-Fe-Mn sediments and minor calcareous sediments (marble, dolomite)
	Metaplutons - mafics (dominantly gabbro)
	- ultramafics (mainly altered equivalents)
	Metavolcanics-metabasalts
	- amphibolites
	-minor felsics
	——Tectonic contact—— (Unconformity?)
Gneissic Terrain	Gneisses - biotite, quartz-biotite gneiss
(Middle Proterozoic or	- amphibolite(biotite) gneiss
Older)	- minor graphitic and micaceous schists

[Source: from Ghebreab et al.(1992)]

3.3 Regional Tectonic setting

3.3.1 Geotectonic evolution of the region

The Precambrian of eastern Africa is composed of two Archean cratons, namely the Tanzanian and the Nile cratons, and two mobile belts known as the Mozambique Belt (MB) and the Arabian Nubian Shield (ANS) (NMiC, 2004). The polycyclic Proterozoic

Mozambique mobile belt, a major geotectonic unit with a dominant northerly structural trend, extends for some 5000 km along the eastern margin of the African Precambrian shields (Holmes, 1951; Clifford, 1970; Kroener, 1977; as cited in Warden and Horkel, 1984).A bifurcation in southern Ethiopia separates a northeastern branch, extending from southern Kenya into the Horn of Africa and southern Arabia, from the main belt which continues into western Ethiopia and the Sudan and these two branches, composed mainly of polymetamorphic continental lithosphere, are separated by the Adola belt, comprising crust of fundamentally different origin (Warden and Horkel, 1984).

The Neoproterozoic belts of Ethiopia, therefore, occur at the interface between the Mozambique Belt in the south and the Arabian–Nubian Shield to the north (Tsige, 2006). The Precambrian of southern Ethiopia also occupies an important position within the Pan-African Mozambique Belt and the Arabian–Nubian Shield, which together form the East African Orogen (Stern, 1994; as cited in Yibas et al., 2002).The East African Orogen, extending from southern Israel, Sinai and Jordan in the north to Mozambique and Madagascar in the south, is the world's largest Neoproterozoic to Cambrian orogenic complex (Fritz et al., 2013). The current understanding is that Tibetan style collision between East and West Gondwana occurred along the Mozambique Belt and a contemporaneous oblique collision occurred in the Arabian–Nubian Shield (Stern, 1994 and references there in; as cited in Tsige, 2006). This accounts for the differences in lithospheric thickness, grade of metamorphism and intensity of deformation that is generally higher in the Mozambique Belt relative to the Arabian–Nubian Shield (Stern, 1994; as cited in Tsige, 2006).

The East African Orogen (EAO) marks one of earth’s greatest collision zones, a global feature in space and time (Stern, 1994; Jacobs et al., 1998; Kroner et al., 2000, as cited in Stern, 2002), the disappearance of a major ocean basin (the Mozambique Ocean), the formation of a vast tract of juvenile Neoproterozoic continental crust, and where East and West Gondwana joined to form the supercontinent ‘Greater Gondwana’ or ‘Pannotia’ at the end of Neoproterozoic time (Rogers et al., 1995; as cited in Stern, 2002). The great rifts of Africa, the Red Sea, and the Indian Ocean itself were spawned along the EAO (Stern, 2002). Therefore, as pointed out in Tsige (2006) generally the following three major evolutionary stages explain the geodynamic evolution of the N-trending Neoproterozoic belts of southern Ethiopia: (i) early stage rifting, associated sedimentation and ocean basin formation, (ii) subduction and island arc formation and (iii) finally continent–continent collision (Fig. 3.2).

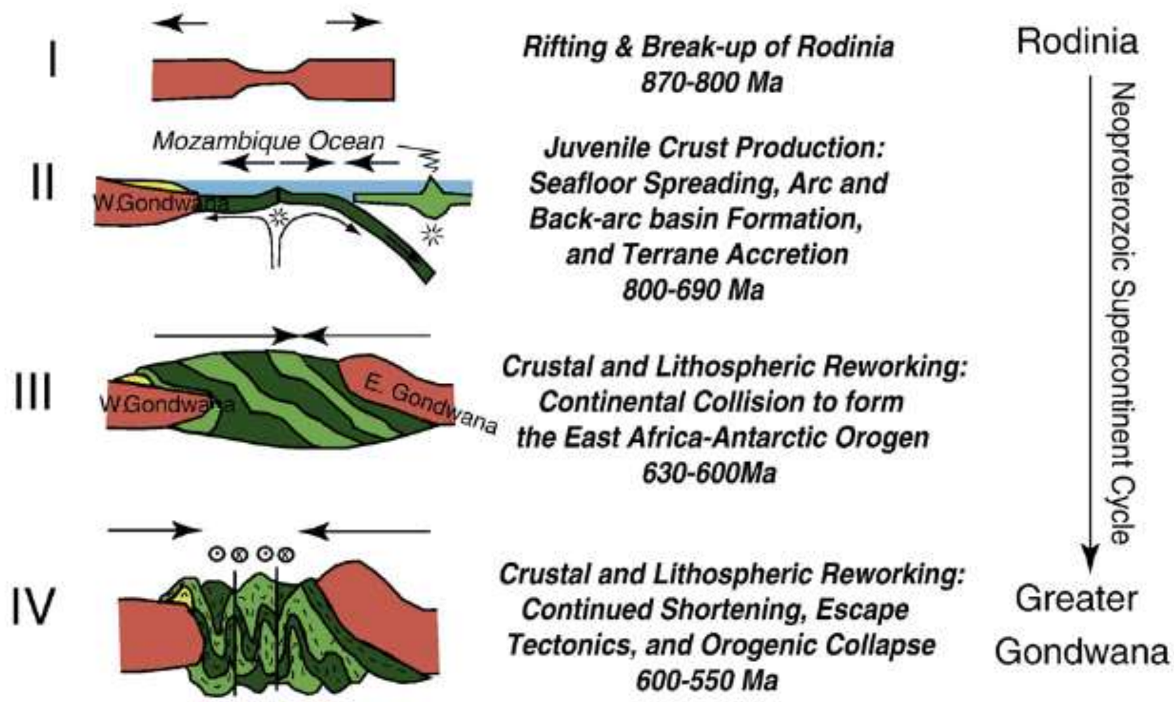

Figure 3.2 Greatly simplified model showing the evolution of the East African Orogen (from Stern and Johnson, 2010).

As summarized by a report in the National Mining Corporation (2004) four north-south trending tectonic faults resulting from the late stage Arabia Nubian Shield evolution (escape tectonics) favored the five litho-structural domains of Adola Gold belt. Two low grade greenstone belts known as Megado greenstone belt (known for its gold and base metal mineralization) and Kenticha greenstone belt (known for its rare earth elements mineralization) form grabens; whilst three high grade gneisses, known as central (Gariboro/Bourjiji/Ujima), western, and eastern high grades form horsts. Each domain is separated by a tectonic contact, N-S trending fault and/or shear zone. Most of the gold mineralization of the southern greenstone belt, such as Lega Dembi, Sakaro, Buri-Ejersa, Digati, Okote, etc. is associated with the aforementioned Megado belt.

3.3.2 Deformation, metamorphism and sequence of events

As pointed out by Abdelsalam and Stern (1996) deformation belts in the Arabian-Nubian shield are divided in to: (1) those associated with sutures, both arc-arc and arc-continental; and (2) post-accretionary structures which include north trending shortening zones ad northwest trending strike-slip faults. Bonavia and Chorowicz (1993), as cited in Abdelsalam and Stern (1996), correlated the evolution of the Adola-Moyale suture with that of the Mozambique belt in the northern Kenya and suggested that the structural history of the Adola-Moyale region started with collision related deformation at ~ 830 Ma. This was followed by strike slip faulting developed between ~ 620-530 Ma in the form of early north trending and late northwest trending shear zones (Abdelsalam and Stern, 1996).

The Pan African Orogeny in southern Ethiopia is characterized by three major deformational episodes, comprising an earlier fold- and thrust event (D_1), a subsequent event (D_2), which folded and/or reactivated the D_1 thrust zones and associated structures and, a final event D_3, which produced a set of strike-slip shear zones, invaded by ubiquitous quartz veins (Worku and Schandelmeire, 1996; as cited in Debele and Koeberl, 2004). But as discussed in (Ghebreab et al.1992, MoME,1993, 1995), beside the above D_1-D_3 phases, there is also a fourth phase, D_4, deformation characterized by locally observed steep N-S/NE-SW trending mainly brittle conjugate shear systems and formation of regional scale E-W warps (Table 3.2). As stated by Hailu and Kinetibeb (1989) the deformation sequence in the Adola belt was initiated by extensional faulting and formation of sedimentary basin as a result of thinning and stretching of the continental crust and lithosphere and is followed by a rifting stage as shallow basin was fragmented in to several fault bounded basins which is evidenced the present distribution of the volcano-sedimentary and ultrabasic suites.

Apart from the Cenozoic volcanics and the post-deformational intrusive bodies, all the rock types encountered in the Adola area have been subjected to varying degrees of metamorphism (MoME, 1993).As discussed in the reports of the Ethiopian Institute of Geological Surveys (MoME, 1993; 1995) three metamorphic domains are proposed for the rocks found in the Adola belt based on mineral assemblages of major lithologies, namely the gneissic domain, the Megado greenstone belt domain, and the Kenticha belt domain. The report also indicates that the equilibrium mineral assemblages commonly observed in the Gneissic Domain represent the medium temperature part of the amphibolite facies; whilst mineral paragenesis of the Megado greenstone belt indicates the maximum grade of metamorphism attained is of the order of greenschist-amphibolite facies, with a few mineral assemblages particularly those containing kyanite suggest equilibration towards the higher part of the amphibolite facies assemblage. The Kenticha belt domain, on the other hand, reflects a medium grade metamorphism, although the pelitic schists within this domain suggest a prograde sequence very close to the boundary between medium and high grade metamorphism. The gneissic terrain rocks were locally subjected to granitization and migmatization (Wurku, 1996b).

Although earlier works (e.g., Gilboy, 1970; Chater, 1971; Baraki et al., 1989; as cited in Worku, 1996a) recognized two metamorphic events (M_1 and M_2) related to different orogenic cycles, detailed textural and petrological work by Worku (1996a) revealed five distinct metamorphic segments (M_0 - M_4) in which M_0 representing a relict texture which might represent an early or pre-pan-African metamorphism whereas M_1 - M_4 are related to a continuous pan-African cycle. According to this study M_1 is a prograde regional metamorphism while M_2 and M_3 respectively represent isothermal decompression and isobaric cooling events. As summarized in (MoME, 1993) M_1affected the gneissic domain to give rise to the higher grade of metamorphism observed in the area and $M_2$is possibly separated by a period of uplift and erosion from M_1 and affected all the lithologic units of the area, but probably with various intensities of the P-T regime.

Table 3.2 Summary of sequence of events in the Adola region

D_1 deformation	Isoclinal tight NNE/SSW recumbent F_1 folds; longitudinal reverse and/or thrust faults; M_1 green schist facies metamorphism; compatible moderate to sub-horizontal E or W plunging tectonic lineations.
D_2 deformation	
(D_{2a})	Broadly N-S upright F_2 folds dominate, produce type-3 fold interference pattern with F_1 folds.
(D_{2b})	Dominantly ductile N-S/NE-SW trending sinistral transcurrent shear and associated steep S- folds common.
(D_{2c})	Dominantly ductile N-S/NE-SW trending dextral transcurrent shear and associated steep Z-folds locally observed. M_2 amphibolite and amphibolite-schist facies metamorphism Steep and sub-horizontal, N/NE trending tectonic lineations such as striations, mineral stretching. Lineations, quartz boudins, etc. associated with transpressional type tectonism.
D_3 deformation	E-W generally sub-horizontal up right F_3 cross folds often verticalized by the D_4 event. E-W/NW-SE brittle to brittle ductile conjugate shear system; M_3 retrograde metamorphism.
D_4 deformation	Steep N-S/NE-SW mainly brittle conjugate shear system; retrogression perhaps continued; complete recrystallization of minerals; formation of regional scale E-W warps.

[Source: compiled from MoME (1993); Ghebreab et al.(1992)]

CHAPTER FOUR

4 GEOLOGY OF THE STUDY AREA

4.1 Lithology and petrography

Field observation and thin section study results revealed that the major rock units of the study area comprises of meta-gabbro, meta-conglomerate, quartz-biotite schist, graphite-quartz-mica schist, talc-tremolite-actinolite schist, and amphibolite (Fig. 4.1). Meta-sandstone and phyllite are the other minor units mainly occurring as intercalations. The meta-conglomerate, quartz-biotite schist and graphite-quartz-mica schist rocks form the upper stratigraphy and separated from the underlying rocks such as amphibolites by a shear contact characterized by intermixing of rocks from both sides. The contact zone is highly sheared, deformed, and hydrothermally altered and have a N-S general strike while dipping between 50^0- 63^0 to the west. The detail description of each rock unit is presented below.

4.1.1 Amphibolite

This rock is the other dominant unit in the study area and is located in the western part of Ejersa, separated by a shear contact from the graphite-quartz-mica schist from the east and has a sharp contact with the meta-intrusives. The rock disappears in the northern part of Ejersa and the whole Burikaro sub-areas, probably covered by the overlying meta-sediments. It is relatively more competent, highly weathered, and occurs as a ridge forming unit. The amphibolite has medium grain size, black fresh color, and mainly occurs as a blocky material. Thin section study result indicated that the rock is composed of about 40% tremolite-actinolite, 20% hornblende, 10% plagioclase feldspar, 8% quartz, 8% epidote, 4% opaque minerals, 2% biotite, and minor amounts of chlorite and calcite (Fig. 4.2 a). The hornblende minerals are highly fractured and at places replaced by quartz, calcite, and opaque minerals.

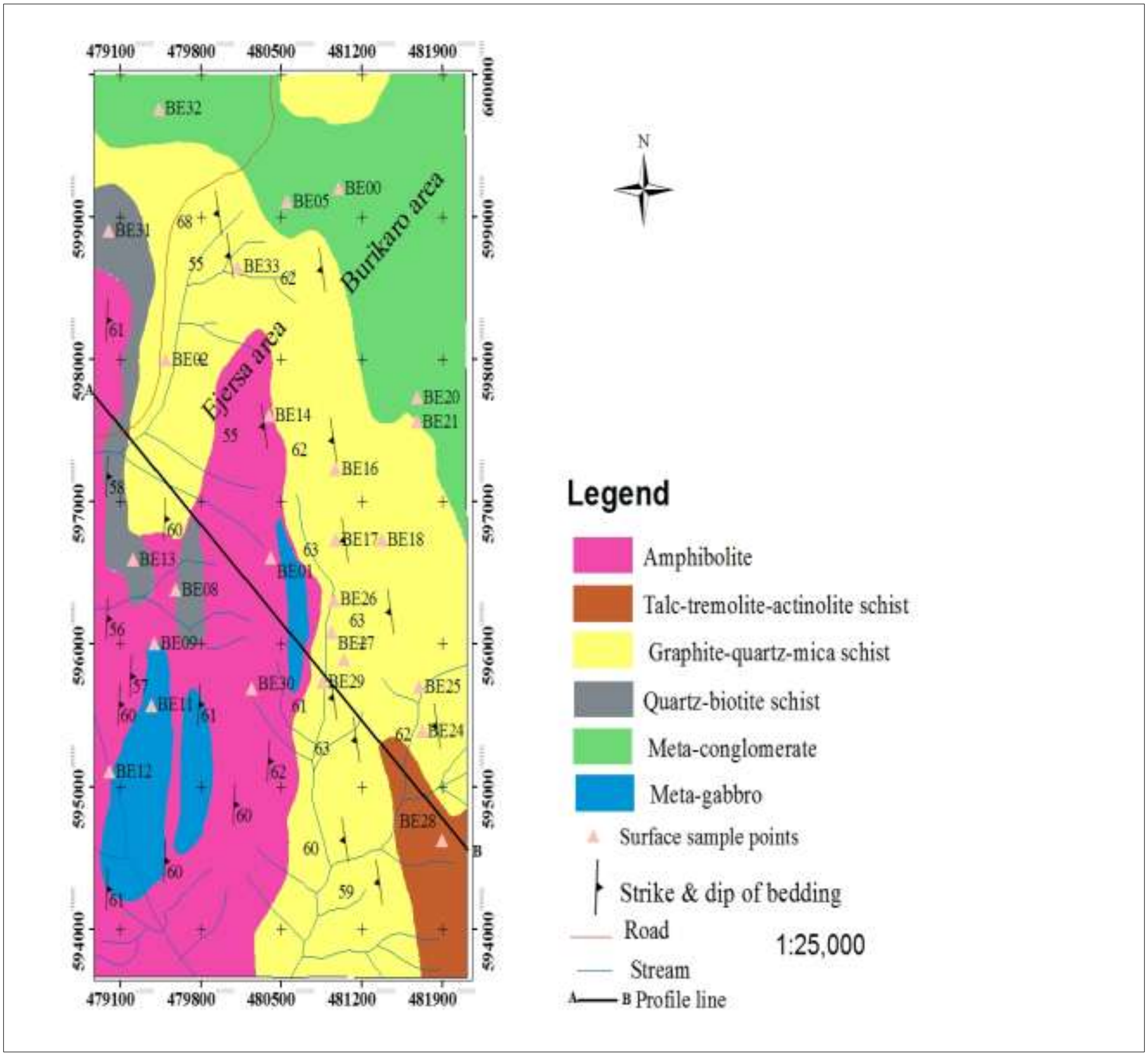
479100
479800
480500
481200
481900
Burikaro area
Ejersa area
N
Legend
Amphibolite
Talc-tremolite-actinolite schist
Graphite-quartz-mica schist
Quartz-biotite schist
Meta-conglomerate
Meta-gabbro
Surface sample points
Strike & dip of bedding
Road
Stream
A—B Profile line
1:25,000

Figure 4.1 Geological map and cross section of Burikaro and Ejersa areas

The hornblende minerals in the amphibolite rock are also rimmed by actinolite-tremolte producing a characteristic pattern in which a central hornblende is surrounded by actinolite-tremolte. The plagioclase is also highly fractured and crowded by calcite and quartz clouds which masked its appearance and only traces of its twinning are observed. The amphibolite is a sheared, deformed and/or folded rock containing swarms of quartz and carbonate veins, veinlets, and stringers; which themselves are extremely folded and at places crenulated. The rock is generally massive but it becomes slightly schistose (amphibole schist) as one approaches toward the contact with graphite-quartz-mica schist (Fig. 4.2 b). The bedding in this rock generally strikes N-S (between 350^0 up to 355^0 azimuth) and dips 54^0 - 62^0 to the east.

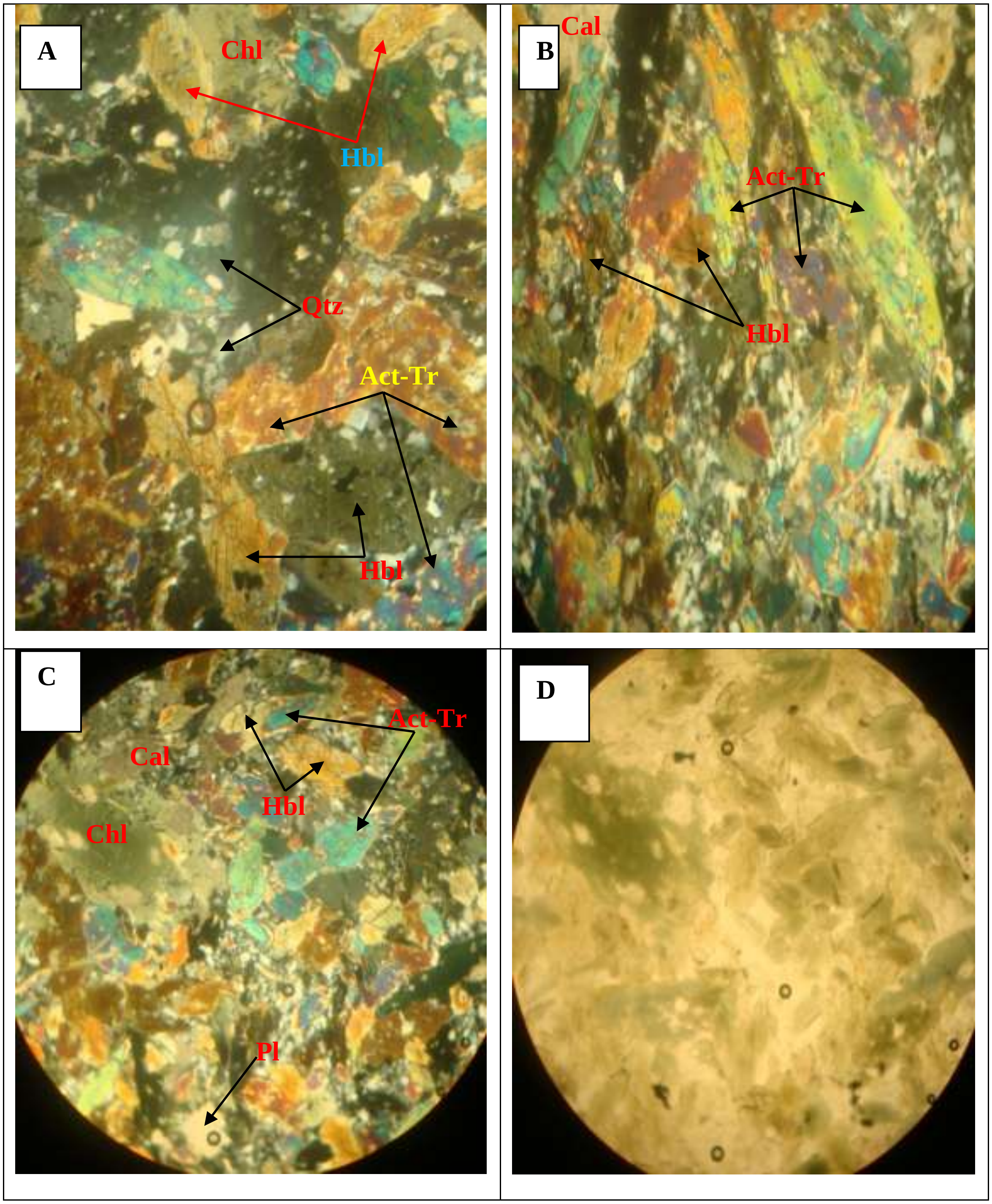

Figure 4.2 Photomicrographs from the amphibolite a) hornblende as a dominant constituent and replaced at places by quartz and opaque minerals (XPL) b) slightly schistose part from the contact with graphite-quartz-mica schist (XPL) c) a typical view from relative highly altered part (XPL) d) PPL view of part c. (Sample numbers: A, C & D = BET30, location: 480247E, 0595693N; B = BET14; locations: 480397E, 0597610N). (X100)

4.1.2 Talc-tremolite-actinolite schist

Besides its minor lensoidal occurrences in the northwestern part of Ejersa sub-area, the talc-tremolite-actinolite schist is located mainly in the southeastern part of the study area. Field observation indicated that it is medium grained, has greenish-grey fresh color with shiny and soapy appearance and is relatively less affected by weathering. The rock is relatively less schistose compared to the other schists of the area and the schistosity is mainly developed by preferred parallel alignment of elongated needle shaped tremolite-actinolite minerals. Thin section study result revealed that the rock is composed of 72% tremolite-actinolite, 22% talc, and minor amounts of chlorite, biotite, and quartz (Fig. 4.3 a). The tremolite-actinolite minerals have mostly acicular to fibrous form and various color shades as displayed in figure 4.3(a). At places, the tremolite-actinolite minerals are altered in to mainly talc and some chlorite minerals. The quartz in this rock is very limited and disintegrated in to smaller grains that are dispersed in the rock. The talc is soft, highly fibrous, and more affected by the shearing and at places slightly fragmented and replaced by opaque minerals (Fig. 4.3 b).

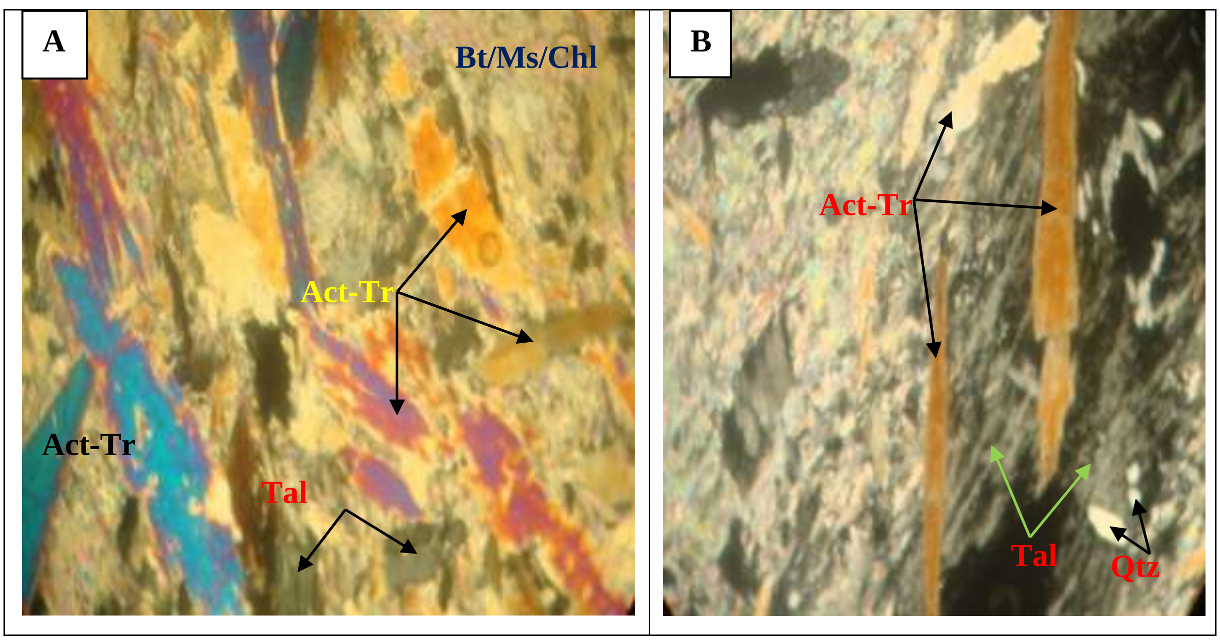

Figure 4.3 Photomicrographs from the talc-tremolite-actinolite schist (XPL) a) with a dominant, variable colored, and acicular to prismatic shaped tremolite-actinolite minerals b) with a highly fragmented talc mineral. (Sample number: BET28; location: 481900E, 0594626N). (X100)

4.1.3 Graphite-quartz-mica schist

Being exposed at the contact zone between the amphibolite and meta-sediments of Ejersa and the southern parts of Burikaro, the graphite-quartz-mica schist is the most schistose rock of the study area. In the rest parts of Burikaro sub-area, this rock is overlain by the meta-conglomerates and thick soil cover except its patchy occurrence in the northwestern parts. It is one of among the dominant rock types of the study area. The rock is composed of bigger, relatively not deformed pre-tectonic crystals mainly made of 47% biotite, 34% quartz, and minor amounts of muscovite and plagioclase feldspar; 11% later coming opaque minerals replacing mainly the biotite crystals; and strongly sheared fine grained fabric material at places wrapping around the bigger pre-tectonic crystals and composed of biotite, quartz, and sericite (Fig. 4.4 a). It is also graphite bearing which is easily observable even in the hand specimen level and give, together with the flaky micas, smooth and shiny appearance to the rock. It is fine to medium grained, highly weathered, fractured, sheared, and invaded by quartz veins, veinlets and stringers that are mainly discordant with the host rock and have variable thickness and length. The degree of shearing in this contact zone decreases as one goes towards east and the rock becomes more of quartz rich, britley deformed where fractures are filled with iron oxides. These iron oxides are mainly filled within the fractures of the rock and gave a reddish brown shade to it (Fig. 4.4 b). It displays relatively well developed and generally N-S oriented schistosity produced by preferred alignment of mainly biotite and muscovite minerals. The schistosity is parallel to the bedding of the rock which is dipping 50^0- 63^0 to west.

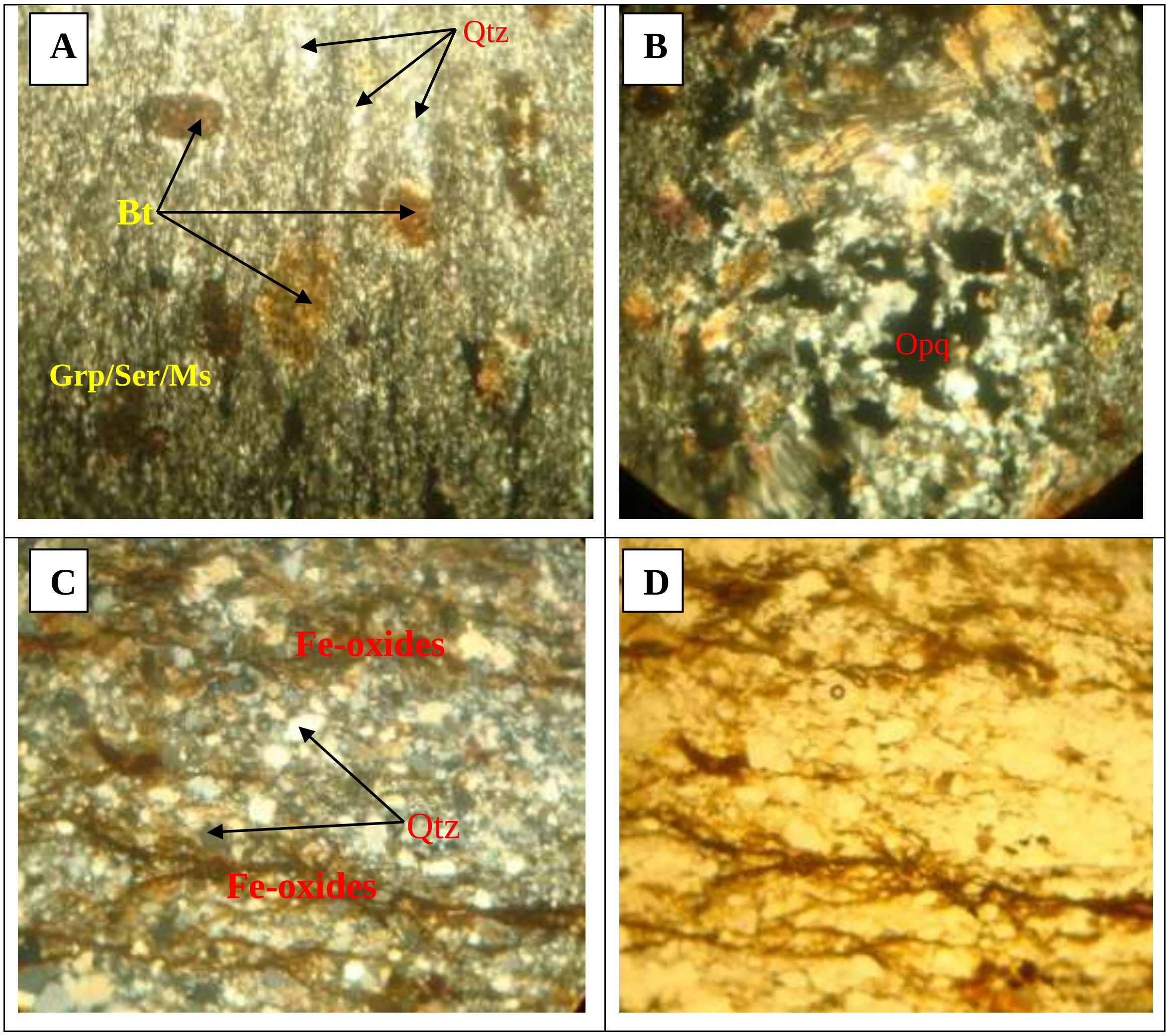

Figure 4.4 Photomicrographs from the graphite-quartz-mica schist a) a typical schistose external fabric at places wrapping round the pre-tectonic biotite crystals (XPL) b) with opaque minerals selectively replacing biotite crystals elsewhere in the same rock (XPL) c) a fracture zone filled by iron oxides (XPL) d) PPL view. (Sample numbers: A & B = BET23; C & D = BET16; locations: BET23: 481045E, 0595893N; BET16: 480975E, 0596734N). (X 100)

4.1.3.1 Phyllite

This rock is located in the northwestern part of the study area intercalated with the graphite-quartz-mica schist. It is fine-grained, graphite bearing, have lustrous sheen, and display well developed schistosity resulting from parallel alignment of mica minerals (Fig. 4.5). The phyllite rock becomes more of talc bearing as one traverse toward the contact between the meta-dolerite and graphite-quartz-mica schist. Since the rock is extremely weathered and fragmented because of easy cleavable nature, getting representative fresh sample for further laboratory work is seldom possible.

Figure 4.5 Field photograph showing a highly sheared and cleaved phyllite rock intercalated within the graphite-quartz-mica schist.

4.1.4 Quartz-biotite schist

This is rock located in the northwestern part of the study area in a sharp contact with the amphibolite and graphite-quartz-mica schist rocks. It also occurs intercalated within the graphite-quartz-mica schist. The less development of schistosity, the absence of graphitic material, and the abundance of quartz makes the rock different from the graphite-quartz-mica schist. The quartz-mica schist is medium grained, light grey colored with black spots, and slightly schistose. It is highly deformed and at places boudinaged (Fig. 4.6). The rock is composed of 40% quartz, 36% biotite, 15% epidote, 3% plagioclase, 3% opaque and accessory amounts of calcite, olivine, and sericite. The quartz grains are recrystallized quartz type with irregular (sutured) grain contacts and show undulose extinction. At places, the rock is rich in magnetite even reaching up to 20 % of the total constituents. The magnetite is subrounded to elongated in shape and at places forming bands. The rock is intersected by many quartz veins and stringers generally aligned along the fracture lines.

Figure 4.6 Field photograph showing boudinaged quartz-mica schist in which magnetite mineral grains form bands alternating with fine grained silica.

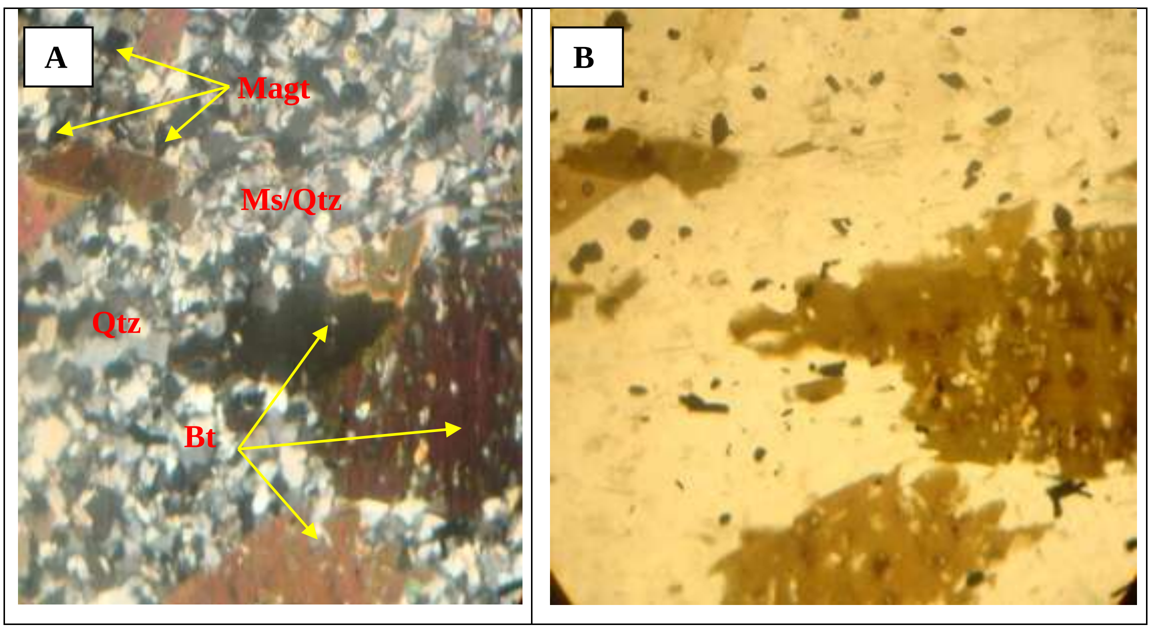

Figure 4.7 Photomicrographs from the quartz-biotite schist a) magnetite bearing quartz-biotite schist (XPL) b) PPL view. (Sample number: BET33; location: 480122E, 0598650N). (X 100)

4.1.5 Meta-conglomerate

This unit covers most parts of Burikaro plain area and it is highly weathered and fragmented that the rock lacks its identity, which makes its sampling a difficult job. Except in few areas where blocks of the rock that are survived from fragmentation are present, the rest are covered by a thick reddish soil, at places reaching more than 10 meters depth. The rock is characterized by the presence of sub-rounded to well-rounded gravel sized clasts that are surrounded by a matrix. It is slightly sheared, deformed and exposed to a lesser degree of metamorphism compared to the other rocks of the study area, which is evidenced by the presence of original rock relict features. Due to deformation, most of the clasts are elongated and aligned generally in N-S direction. However; some of the elongated minerals slightly changed their orientation to NE-SW direction, with an average of about 15^0 from the NS.

Thin section study result indicated that the clasts in the meta-conglomerate are composed of 50% quartz, 18% biotite, 12% plagioclase feldspar, 10% opaque, 4% calcite, and accessory amounts of chlorite, sericite, muscovite, and epidote. The finer matrix, on the other hand, is composed of muscovite and welded rock fragments made of quartz, biotite, and feldspar and all together cemented by silica (Fig. 4.8 a). However; it should be noted that these percentages represent the average of many views of a single thin section and otherwise at places, for example, the feldspar can reach up to 30% (Fig. 4.8 b).The quartz grains in this rock are mainly recrystallized quartz type having irregular (sutured) grain contacts, probably formed by grain boundary deformation and it also show wavy type extinction. At places, the plagioclase feldspar is altered and replaced by sericite minerals. The plagioclase is also pseudomorphed by biotite and other gangue minerals. The opaque minerals are relatively abundant in this rock and occur by replacing mainly biotite minerals (Fig. 4.8 c and d).

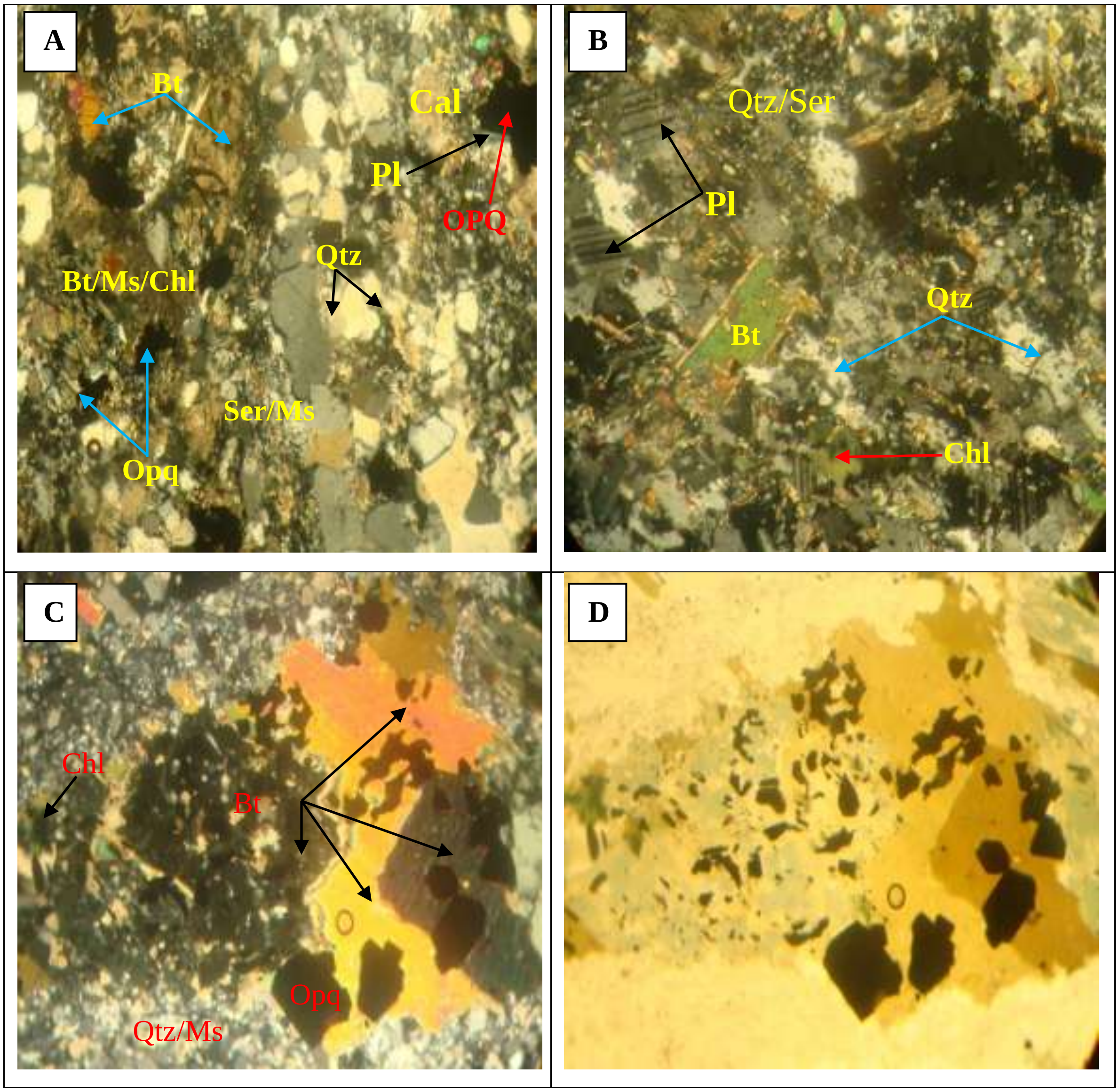

Figure 4.8 Photomicrographs from the meta-conglomerate a) with aligned clasts embedded in a relatively fine-grained matrix (XPL) b) at places with abundant plagioclase feldspar showing polysynthetic twinning (XPL) c) opaque minerals selectively replacing biotite (XPL) d) PPL view of c. (Sample number: BET05; location: 480553E, 0599120N). (X 100)

4.1.5.1 Meta-sandstone

The meta-sandstone occurs as intercalation in the above-mentioned meta-conglomerate rock. It is generally fine-grained rock and composed of quartz, feldspar, and some biotite. The meta-sandstone is coated with graphitic material and generally it has a grey to reddish brown weathered color. Even though this rock is harder and does not show prominent fragmentation, it is extremely weathered that getting representative fresh sample is seldom possible (Fig. 4.9).

Figure 4.9 Field photograph showing highly weathered meta-sandstone rock occurring intercalated with the meta-conglomerate.

4.1.6 Meta-gabbro

The meta-gabbro is located in the southern and central parts of the study area. It has a sharp contact with the amphibolite rock and generally occurs as a lenses of metapluton intruding the overlying amphibolite rock. The rock is coarse grained, granular in texture, and greenish black to dark gray in color. Thin section study result indicated that it is composed of about 30% actinolite-tremolite, 20% plagioclase, 18% biotite, 15% clinopyroxene, 8% hornblende, 6% quartz, 3% opaque minerals and accessory amounts of calcite and chlorite. It is slightly weathered, sheared, and intruded at places by veins and stringers mainly of carbonate composition. At places, the hornblende and clinopyroxene are replaced by chlorite, epidote, and tremolite-actinolite, and opaque minerals (Fig. 4.10).

The quartz in this rock is also recrystallized quartz with irregular grain contacts and show wavy type extinction. The plagioclase is highly altered and partly field with epidote and quartz. The rock becomes more sheared and loses its primary texture, such as grain size, as one approach to the contact with the graphite-quartz-mica schist.

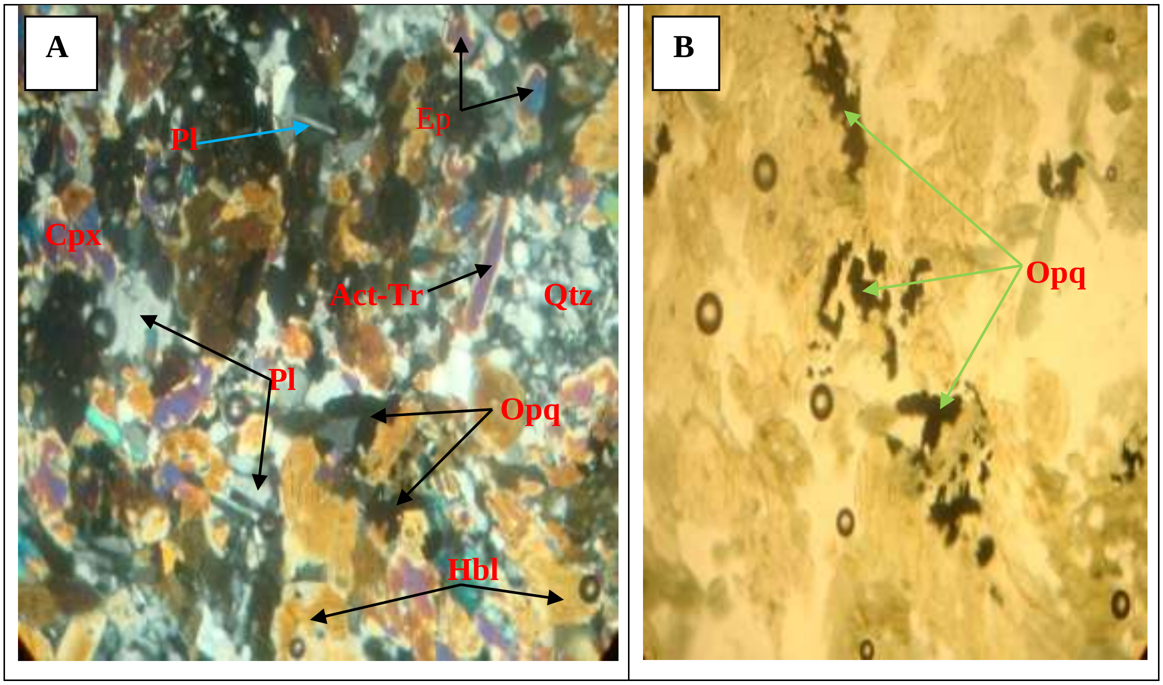

Figure 4.10 Photomicrographs from the meta-gabbro a) massive meta-gabbro in a crossed polar light (XPL) b) a typical dendritic type replacement texture produced by opaque minerals distribution (PPL). (Sample number: BET12; location: 479010 E, 0595111N). (X100)

4.2 Deformation, metamorphism and shearing

4.2.1 Deformation

The rocks of the study area display swarms of deformed quartz and/or calcite veins and veinlets, ductile to brittle shear zones, different phases of mesoscale folding, boudinaged rocks, mineral stretchings, joints, and slicken sides and brecciations indicating the occurrence of faulting. Therefore; it is possible to conclude that the study area has experienced different deformation phases.

The intensity of deformation is higher and more of ductile in the amphibolite rocks, which form the lower stratigraphy in the study area, and decreases toward the overlying meta-sediments that are mainly exposed to brittle deformation which is manifested by the presence of slicken sides and brecciations, joints, and other open fractures probably formed at the last phase of deformation. Field observations on the amphibolite rock indicate the presence of at least more than one phase of deformation, which is evidenced from the highly folded quartz veins and at places having crenulated or refolded fold limbs. The axial plane of the majority of these folds trend to NNE-SSW direction.

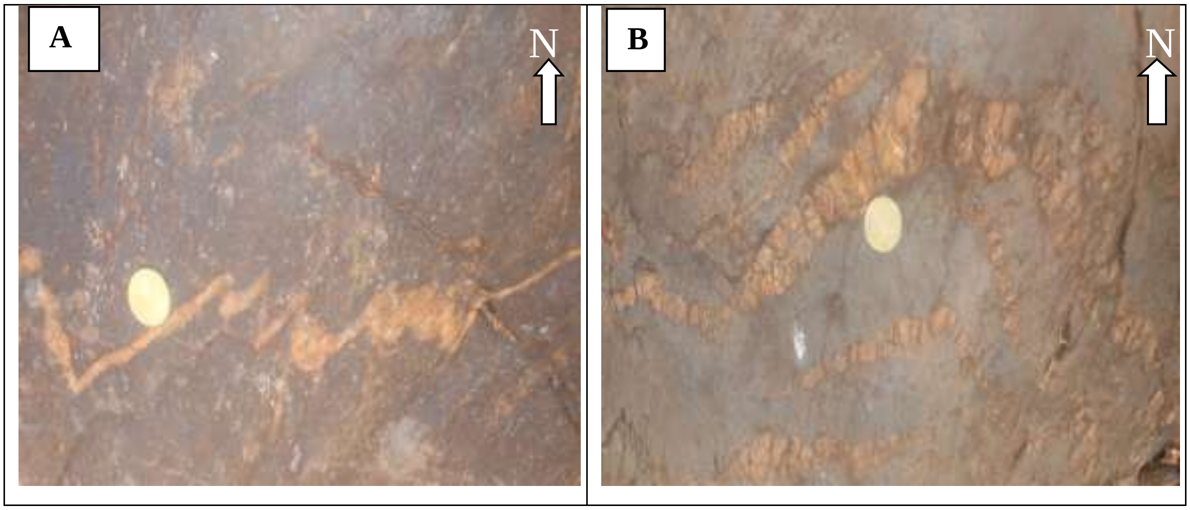

Figure 4.11 Field photographs showing folded quartz veins

Unlike the amphibolite rock described above which is generally massive, the deformation produced foliation in the schistose rocks which is generally parallel to the original bedding direction of the rocks. Field measurements of few bedding and foliation orientations are presented below using stereonet projection. From the stereonet diagram it can be observed that the calculated poles to the planar structures are clustered in the eastern and western parts indicating that these planar structures are generally dipping to the west and east directions. This probably indicates the presence of regional scale fold. Even though the intensity of deformation in the meta-conglomerate is relatively lower, it resulted in elongation and preferential N-S alignment of gravel sized clasts that are embedded in a relatively fine grained matrix (Fig. 4.12 a). The deformation of rocks of the study area is also evidenced from rock petrography, particularly displayed by quartz minerals. Thin section study of rocks indicated that most of the quartz grains are mainly recrystallized quartz type having sutured grain contacts that are probably formed by grain boundary deformation and it also shows wavy type extinction (Fig. 4.12 b).

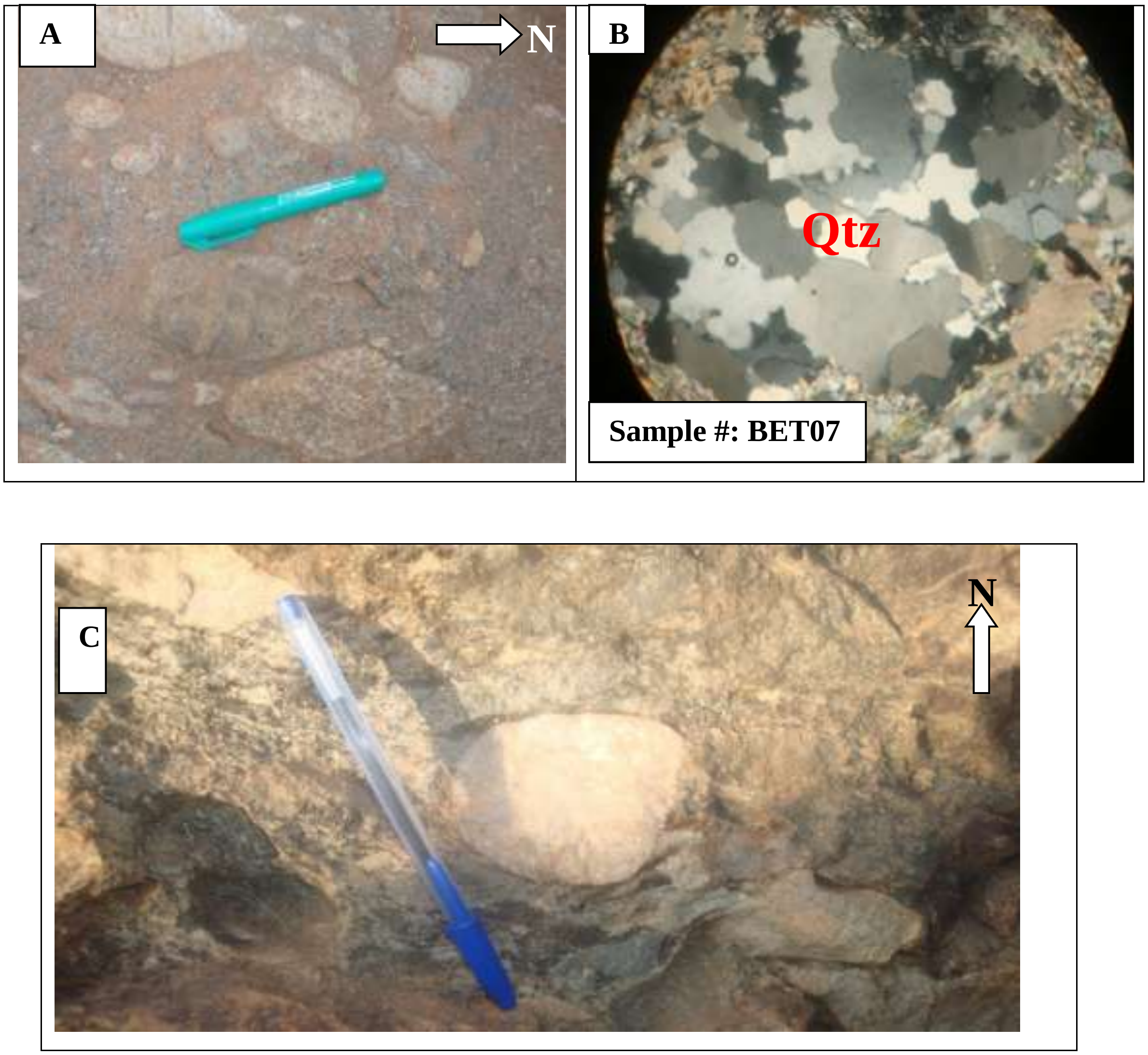

Figure 4.12 Field photographs from the meta-conglomerate (A & C) and thin section photomicrograph from the quartz-mica schist

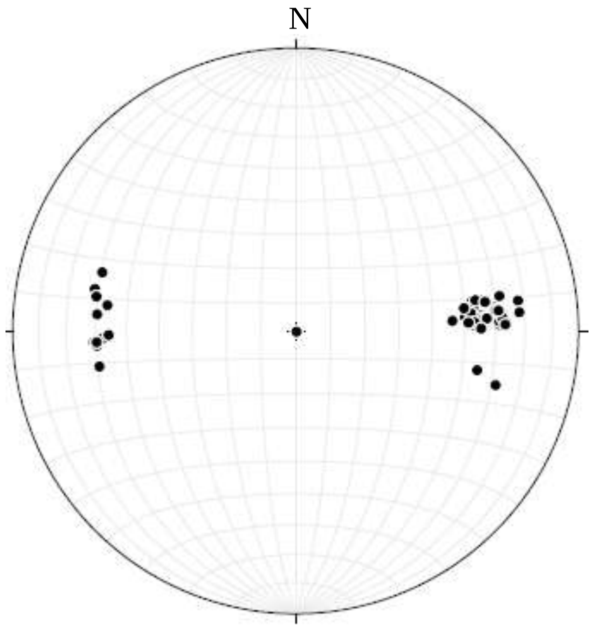

Figure 4.13 Stereonet diagram (lower hemisphere, equal area) of calculated poles to bedding and foliation within and around the contact zone between the amphibolite and the meta-sediments. (Number of data used: 53)

4.2.2 Metamorphism

The rocks of the study area are characterized by low- to medium-grade metamorphism typically of the green schist to amphibolite facies metamorphic conditions. Based on field observations and thin section studies, the metamorphism of each lithologies accompanied with their mineral assemblages are given below.

The typical mineral assemblages of the amphibolte rock are: tremolite-actinolite + hornblende + plagioclase feldspar + quartz + epidote + chlorite + biotite + calcite (Fig. 4.10). The plagioclase is highly fractured and crowded by calcite and quartz clouds which mainly masked it's twining, making its identification difficult. The biotite minerals are at places altered to chlorite, a typical green colored mineral indicating chloritization is the dominant type of alteration in this rock. Hornblende on the other hand, is altered to actinolite-tremolite at places dominated with inclusions of quartz and calcite. The mineral assemblages and the presence of hornblende may suggest epidote-amphibolite facies metamorphism for meta-basic rocks. No minerals like kyanite are generally encountered in the amphibolite rocks throughout the petrographic study suggesting equilibrium towards the lower part of the amphibolite facies assemblage.

The talc-tremolite-actinolite rock is characterized by the mineral assemblages: tremolite-actinolite + talc + biotite + chlorite + quartz (Fig. 4.9). Likewise, these mineral assemblages also indicate upper green schist facies metamorphic condition. The mineral assemblages and the lower content of quartz (< 5%) in this rock suggest that the protolith is ultramafic rock.

The mineral assemblages in graphite-quartz-mica schist are: biotite+ quartz + muscovite + plagioclase + sericite + graphite +/- pyrite (Fig. 4.7). In these rocks the percentage of biotite is highly increased compared to the meta-conglomerate and it also becomes more stable mineral assemblage. The introduction of more biotite to the assemblage probably suggests the transition from lower green schist facies to upper green schist facies metamorphism.

The mineral assemblages in the quartz-biotite schist are: quartz + biotite + epidote + plagioclase + calcite + olivine + sericite (Fig. 4.6). Similarly, this assemblage also indicates upper green schist facies metamorphic condition. The magnetite minerals in this rock are being replaced by pyrite along the central and southern parts of the contact zone.

The typical mineral assemblages in the meta-conglomerate are quartz + biotite + plagioclase + calcite + chlorite + muscovite + epidote (Fig. 4.3). Accordingly, the mineral assemblages: chlorite + muscovite + biotite + quartz + albite + calcite indicate a characteristic upper green schist facies metamorphism of meta-sedimentary rocks. The biotite in this assemblage is highly altered, dominated by quartz and plagioclase inclusions, and usually altered to chlorite and muscovite indicating its unstable condition. The rock is characterized by silicification, carbonatisation, and chloritization which are manifested by the presence of secondary quartz, calcite, and chlorite minerals, respectively.

The meta-gabbro has mineral assemblages: tremolite-actinolite + biotite + plagioclase + clinopyroxene + hornblende + quartz + calcite + chlorite + zoisite/ (epidote) (Fig. 4.2).

According to Winkler (1976) the metamorphic mineral assemblages: albite +actinolite + chlorite + zoisite/clinozoisite (epidote) + quartz are typical assemblages of upper green schist facies for those derived from meta-basaltic rocks.

4.2.3 Shearing

Although its intensity varies which is probably related to the relative differences in response to deformation among the different rocks, most of the rocks of the study area are exposed to shearing. The most important with respect to gold mineralization being the contact between the meta-volcanics and the meta-sediments of Ejersa sub-area and the bedrocks in the Burikaro. Generally, three types of shearing (a dominant and two minor) are observed in the study area during field geological mapping. Those shear zones associated with amphibolites are dominantly ductile while those lower grade meta-sediments are generally exposed to brittle shearing. This may suggest that the amphibolite rocks are more competent than the meta-sediments. The identification of the different shear zones is mainly based on observations of shear zone materials, rotated porphyroclasts, and shear zone foliation. The shear zones are few to several meters wide, the wider being the one associated with the contact zone even though it is difficult to determine its width because it is weathered and characterized by the presence of rocks of various types.

The most important and frequently encountered among these shearing are the dominant N-S striking ductile-brittle shear zones that are invaded by quartz and/or calcite veins of variable orientations and occur cross-cutting the host rocks and some of which are folded and crenulated. As will be discussed in the coming sections, only those quartz/calcite veins that are not deformed are associated with gold mineralization. This may be because further deformation of these quartz/calcite veins may result in the redistribution of their ore constituents such as gold to the neighboring rocks. The dominant N-S shear zone is mainly recognized from the shear foliation in the graphite-quartz-mica schist rock of the contact zone that is manifested by the realignment of micas. In addition to this, the shear zone is also characterized by fault planes containing mineral stretching and wider breccia zones occupied by shear zone materials.

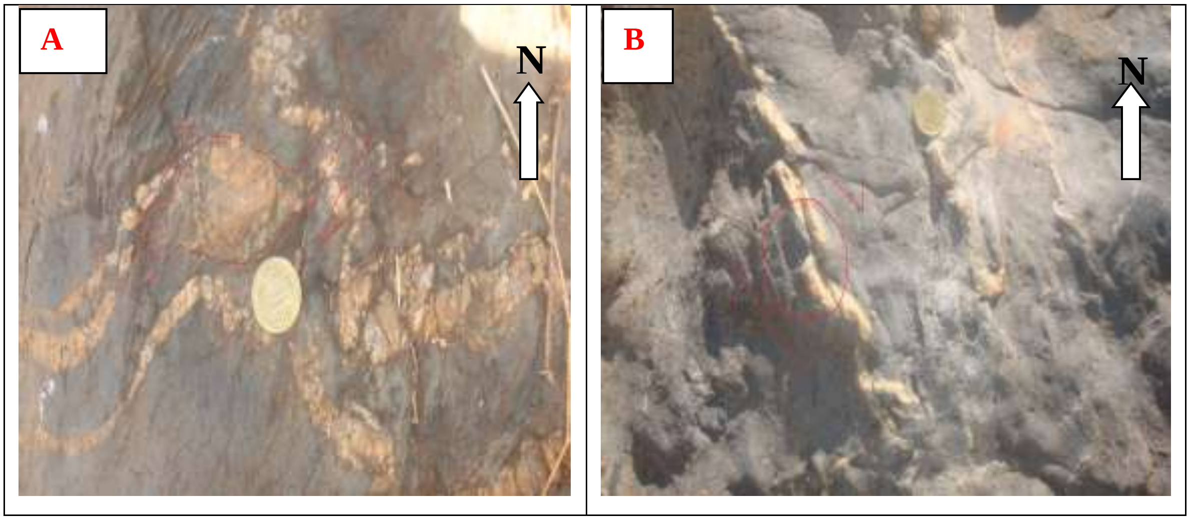

Figure 4.14 Field photographs showing a) a ductile deformation and locally crenulated quartz vein in the amphibolite rock and displaying N-S/NE-SW trending dextral shear system b) a NW-SE trending ductilely deformed dextral shear zone with associated locally observed Z-folds indicating dextral shear system.

The other types of shear zone are the NW-SE and E-W trending and relatively less frequently encountered during the field geological mapping. Although the data density is not a lot, stereonet projection of few shear zone orientation measurements are given below in figure 4.17. From figure 4.17 it can be observed that there are three categories of shear zones that are discussed above.

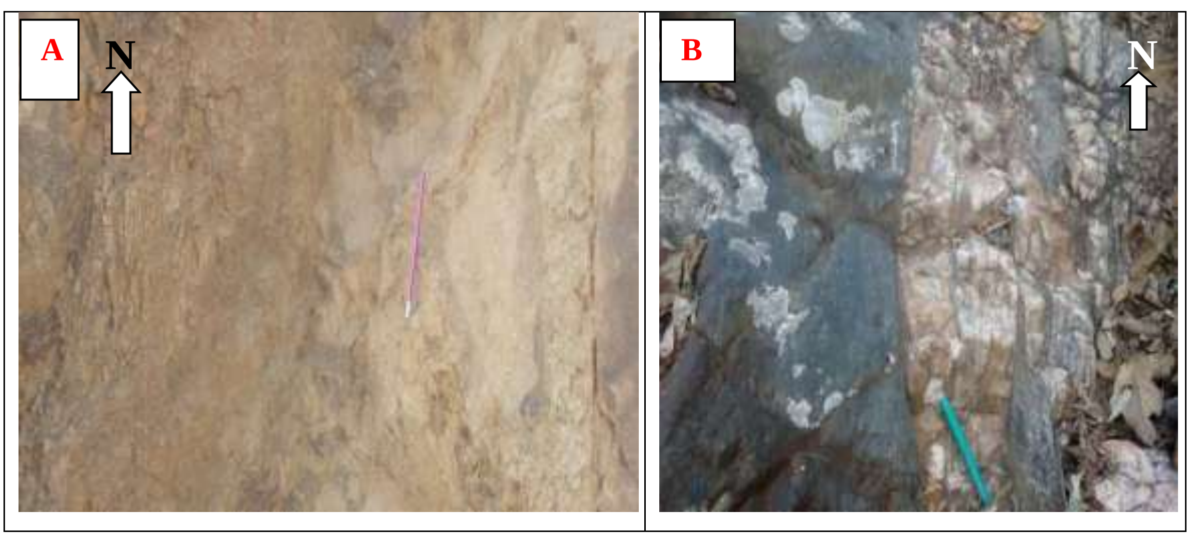

Figure 4.15 Field photographs showing brittle shearing in the graphite-quartz-mica schist

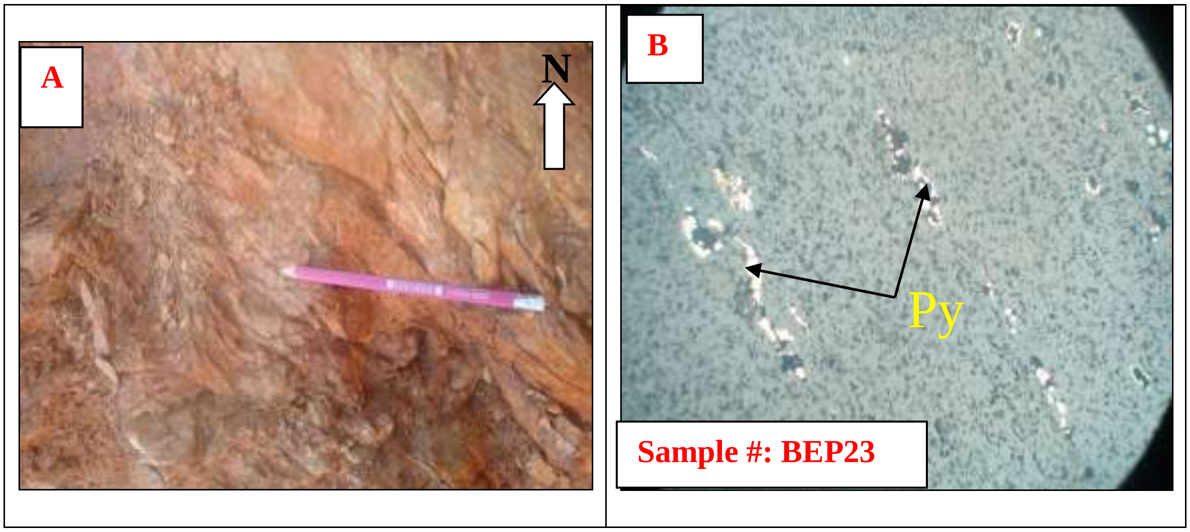

Figure 4.16 a) field photograph showing an intensely sheared and altered graphite-quartz-mica schist rock containing brecciated shear zone materials b) a polished section photomicrograph indicating shear zone associated quartz vein mineralization (X100).

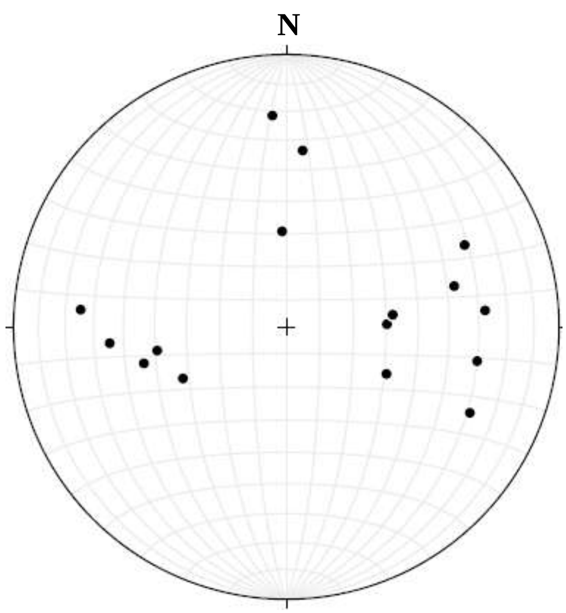

Figure 4.17 Stereonet diagram (lower hemisphere, equal area) of calculated poles to shear zones within and around the contact zone between the amphibolite and the meta-sediments. (Number of data used: 16)

CHAPTER FIVE

5 GOLD MINERALIZATION AND ASSOCITEDFEATURES IN THE STUDY AREA

5.1 Hydrothermal alterations

The rocks of the study area are considerably altered by hydrothermal solutions that are focused upward and invading sideways mainly through the quartz/calcite veins, veinlets, and stringers probably due to deformation and/or squeezing of materials created at the lower parts. The mineralization is also clearly associated with these alterations. A simple designation based on the most abundant or most obvious mineral observed in the altered rock is used to separately discuss each alteration types. Silicification, carbonatization, and tourmalinization are, respectively, the most prominent types of alterations over others such as chloritization, sercitization, and kaolinization. The discussions of the different types of hydrothermal alterations observed in the study area are presented below.

5.1.1 Silicification

Silicification is the dominant type of alteration in the study area. It is genetically similar to the carbonatization (will be discussed latter) but mainly occurring in meta-sediments of the contact zone in Ejersa and also in the Burikaro sub-areas. Similar to the carbonatization, the silicification also occurs through quartz veins and stringers and invading and altering the surrounding rocks (Fig. 5.1). As clearly depicted in figure 5.1 below, the hydrothermal solutions were migrated considerable distance sideways from the major quartz vein altering the nearby country rocks, which is evidenced by the change in composition/color of the host rock. As revealed from field work observation and trench data results, this is one of the important types of alteration with which the gold mineralization of the study area is associated.

Figure 5.1 Field photograph showing a typical silicification alteration in which the hydrothermal fluids have invaded considerable distance in to the country rock material.

5.1.2 Carbonatization

This is the second dominant type of alteration in the study area and the more prominent type in the meta-volcanic rocks (e.g., meta-gabbro). It is basically occurred when those carbonate materials focused upward and migrating though veins and stringers were invaded and altered the neighboring country rock materials (Fig. 5.2). As shown in figure 5.2 below (lower central and lower left parts), the graphite-quartz-mica schist is highly invaded by calcite veins and stringers through which hydrothermal solutions containing carbonate material are circulating in to the host rock materials. This phenomenon is mainly disclosed when one breaks the rocks and enter a little deeper parts since the rocks are exposed to high degree of weathering. The carbonate materials are tested in the field by their intense reactions with hydrochloric acid. This is another type of hydrothermal alteration with which gold mineralization is associated (Table 5.1).

Figure 5.2 Field photograph showing an intensely carbonatized, folded and slightly sheared graphite-quartz-mica schist rock.

5.1.3 Tourmalinization

Tourmalinization is the third dominant type of alteration in the study area. As evidenced from field observations and the cross-sections of various trenches dug in the study area, this type of alteration is generally restricted to the quartz veins of Burikaro sub-area. It is clearly observed from hand specimen that the dark colored and acicular shaped tourmaline minerals are invading the quartz veins in Burikaro sub-area and cross-cutting them indicating that the tourmaline minerals are younger and/or latter coming (Fig. 5.3). As observed from the polished section studies conducted in this research work, the prominent ore mineral associated with this quartz-tourmaline vein is pyrite, giving the alteration mineral assemblages: quartz-tourmaline-pyrite. As revealed from the trench cross-sections done by the National Mining Corporation (Table 5.1) and a compilation report of the Dawa Digati gold exploration by Basson (2006), such quartz-tourmaline veins are associated with gold mineralization in the Burikaro sub-area. Gold analysis results of tourmalinized quartz veins from Burikaro sub-area (BEA00) yielded a 0.2 ppm Au supporting the association of gold with tourmalinization (Table 5.2). Such tourmalinization alteration is associated with medium to high temperature deposits, e.g., many tin and some gold veins have a strong development of tourmaline in the wall rocks and often actually in the veins as well (Evans, 1993).

Figure 5.3 A hand specimen photograph of a mineralized quartz vein material from the quartz-tourmaline veins located in the sheared meta-conglomerate bedrock of Burikaro sub-area.

5.1.4 Chloritization

This is another type of alteration that mainly occurs in the graphite-quartz-mica schist rock and meta-conglomerates. Chloritization is characterized by the introduction of green to yellowish-grey colored chlorite minerals in to the host rocks. The chlorite minerals mainly occur as surface coatings in the schist rock and also as inclusions within quartz and biotite minerals. It is also observed through thin section study that the chlorite minerals are produced through the alteration of biotite mica minerals.

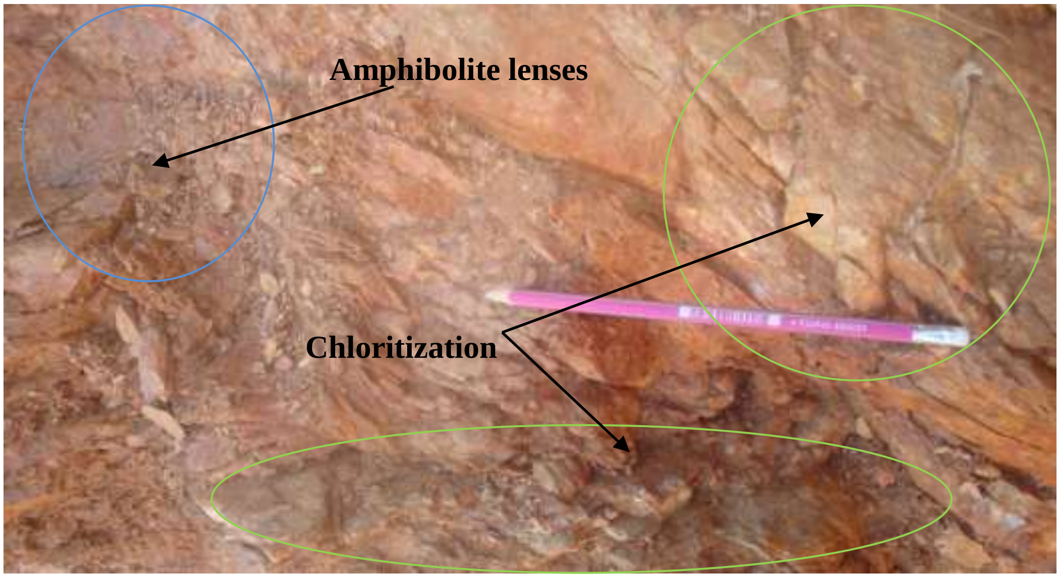

Figure 5.4 Field photograph showing an intensely sheared graphite-quartz-mica schist rock showing chloritization alteration (top-right and south-central parts) and containing amphibolite lenses (top left).

5.1.5 Sericitization

Sericitization is another alteration type observed in the study area characterized by the introduction of a very fine grained sericite mineral which is probably produced due to the alteration of the plagioclase feldspars in the meta-sediments (Chapter 4). As evidenced from polished section study works, such alteration assemblages are at places accompanied with pyrite. The introduction of such sericite mineral at places gave a very sheen appearance to the graphite-quartz-mica schist rock. The sericite micas mainly occur as sub-rounded to rounded nodules by filling cracks and pore spaces between other mineral grains in graphite-quartz-mica schist and at places it is silicified and makes the rock relatively strong.

5.1.6 Kaolinization

Kaolinization is also another minor type of alteration mainly present in the meta-sediments of northern parts of Ejersa and Burikaro areas. It is characterized by the presence of white colored kaoline minerals mainly in the phyllite rocks that are intercalated with the graphite-quartz-mica schist (Fig 5.5). According to Evans (1993) such alteration is an intermediate argillic alteration type and the dominant kaoline minerals are the products of hydrothermal alteration of plagioclase.

Figure 5.5 Field photograph showing kaolinization alteration in the graphite-quartz-mica schist rock of north Ejersa characterized by the development of white colored kaolin minerals.

5.2 Quartz veining

Field work investigations, polished and thin section studies, surface sample analytical results, and trench cross-sections indicate that the gold mineralization in the study area is clearly hosted within and/or directly adjacent to quartz veins of various types that have dissimilar color, width, length, and orientations. They also possess various relationships with the host rock. Some of the veins are massive while others are folded and brecciated. The majority of these quartz veins observed in the field through outcrop, available trenches, and many excavations and hand dug holes indicate that they are four major categories: dull-white, sugary, transparent/glassy, and milky-white quartz veins. At places, quartz veins of rose color are also observed. Field observations and measurements indicate that these quartz veins have a variable width ranging from few centimeters up to about four meters. Although there are quartz veins with continuous length and that are up to hundred meters long, the majority are pinch and swell type having discontinuous length that repeatedly dies out for a considerable distance and again appears back. Irrespective of their type and length, the quartz veins described above have variable orientations, that is, variable strike and dip. There are vertical, horizontal, and inclined quartz veins; whilst still there are quartz veins that are diffused within available fractures mainly in the graphite-quartz-mica schist, meta-conglomerates, and meta-sandstones. Based on their relation with the regional tectonics and mineralization, the quartz veins of the study area can be grouped in to two categories: early-tectonic and late-tectonic.

5.2.1 Early-tectonic quartz veins

These are predominantly folded and at places having extremely crenulated or refolded and highly sheared fold limbs (Fig. 5.6). They are believed to be exposed to the D_1 to early D_2 regional events in the Adola Gold belt (Table 3.2). These veins are generally dull-white in color and located mainly in the amphibolite rock while few exist in the transition from amphibolite to the graphite-quartz-mica schist of the contact zone. Trench and surface sample analysis from these quartz veins indicated that they are not mineralized or at least much less mineralized compared to those quartz veins occurring elsewhere in the study area, which will be discussed later.

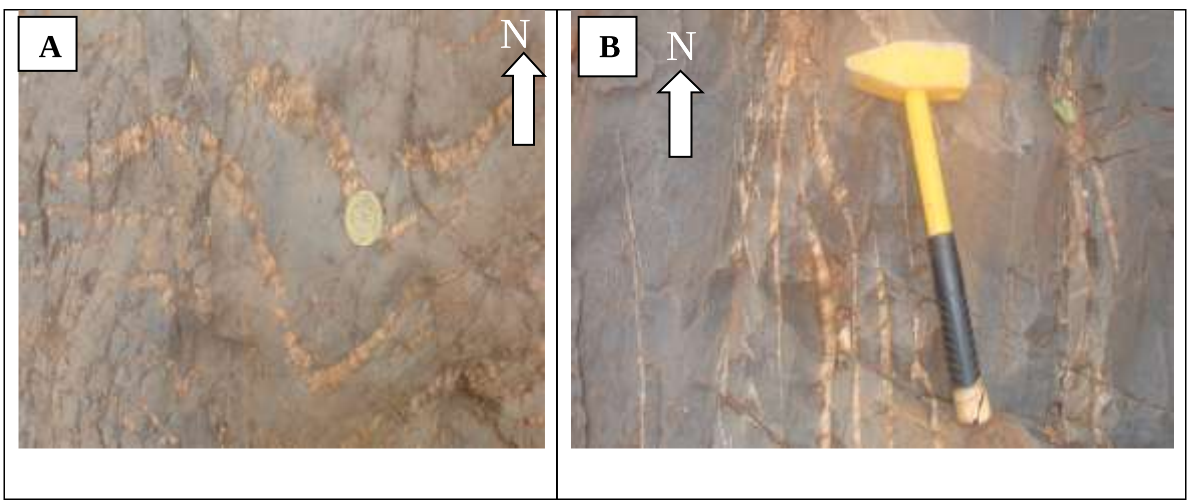

Figure 5.6 Sample field photographs showing a) a folded dull-white quartz vein in the amphibolite rock of the transition from amphibolite to the graphite-quartz-mica schist of the contact zone b) slightly folded quartz veins and veinlets from the same rock.

5.2.2 Late-tectonic quartz veins

These category of quartz veins are generally not deformed (or, if any, at least much less than the above category) and are mineralized veins (Fig. 5.7). Therefore; it is possible to say that they are not closely associated (or affected by) with the regional D_1- D_2 deformation events (Table 3.2). They are generally sugary, transparent/glassy, and milky-white colored quartz veins. Trench and surface sample analytical results from these quartz veins and the extensive exploitation by the local artisanal gold miners indicated that the gold mineralization is associated with such vein categories that are intern associated with carbonaceous matter, pyrite, tourmaline, and other sulphides. They are mainly located in the meta-sediments such as the graphite-quartz-mica schist, meta-conglomerate, and meta-sandstone and predominantly occur in a britley deformed shear zone. The quartz veins located in Burikaro sub-area are at places rich in dark colored tourmaline minerals diffused throughout and penetrating the quartz in the veins. In addition to the quartz veins described so far, there are also so many veinlets and/or stringers invading the host rocks, particularly the amphibolite and quartz-mica-graphite schist units.

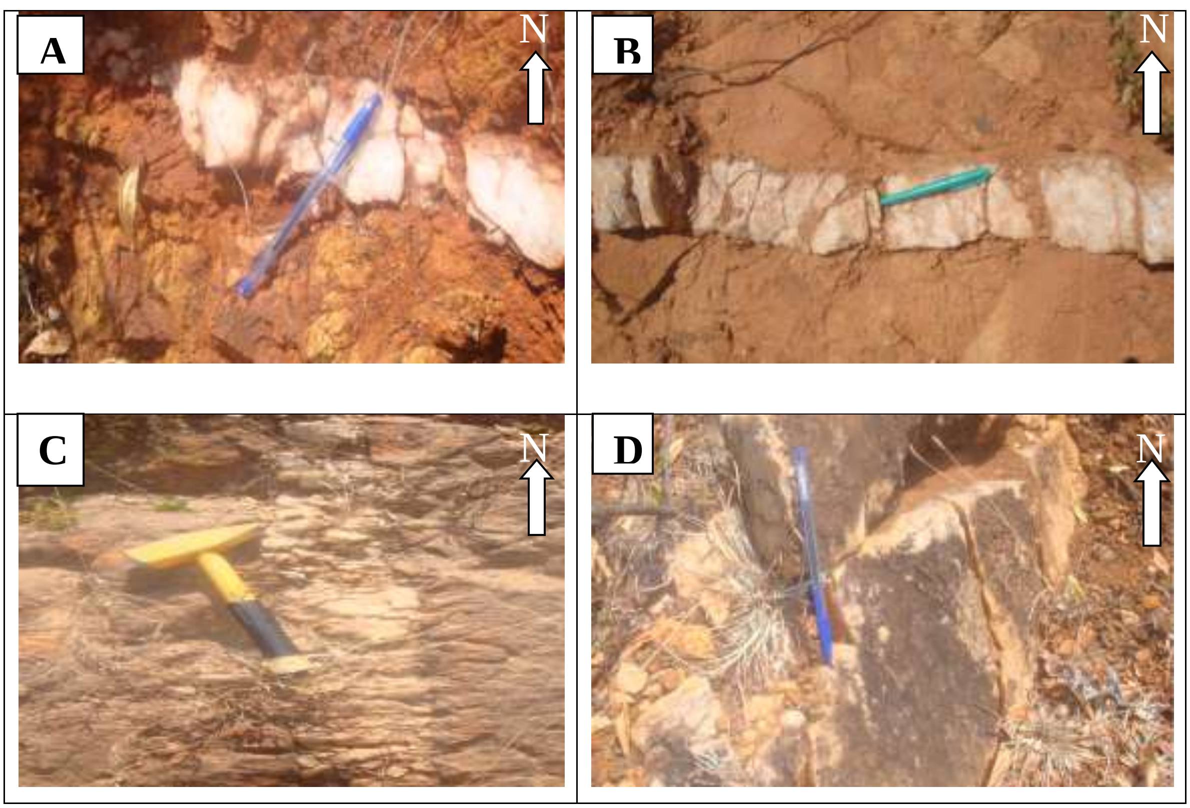

Figure 5.7 Field photographs showing (a) an eastward dipping glassy/transparent variety quartz vein (b) horizontally oriented milky-white quartz vein (c) a verical sugary quartz vein exposed along road cut (d) a southeast dipping quartiz vein in the graphite-quartz-mica schist.

5.3 Geochemical analysis results

5.3.1 Interpretation of trench results

One of the strong evidence of gold mineralization in the study area is the trench data results. As clearly indicated in the methodology section, a number of trenches were dug by National Mining Corporation in the study area as part of the Dawa Digati Gold Exploration project. Eleven trench data results are used to elaborate the discussions on gold mineralization. Analyses results are found in appendix1.The average gold results of each of these trenches is calculated for the purpose of discussion and are indicated in table 5.1 below against the lithology they crossed.

Table 5.1 Average gold values of selected trenches dug in the study area

S. No.	Trench number	Sample numbers	Lithology crossed	Average Au (ppm)	Comments on the lithology crossed
1	6FTR-585	01 - 07	Amphibolite	0.025	the amphibolite contain local carbonatization
		08 - 12	Graphite-quartz-mica schist	0.014	containing no quartz veins and stringers
		13 - 19	Graphite-quartz-mica schist	0.844	with many quartz veins and stringers
		20 - 31	Graphite-quartz-mica schist	0.0575	only at places containing quartz veins and stringers
2	6FTR-	01 - 07	Amphibolite	0.026	containing quartz/calcite stringers
		08 - 19	Graphite-quartz-	0.879	invaded by many quartz

	584		mica schist		veins and stringers
		20 - 31	Graphite-quartz-mica schist	0.065	with few quartz veins and stringers
3	6FTR-564	01 - 05	Meta-gabbro	< 0.01	containing no quartz/ calcite veins and stringers
		06 - 14	Meta-gabbro	0.488	carbonatized and silicified at places containing quartz veins with pyrite crystals
		15- 36	Graphite-quartz-mica schist	0.157	with quartz/calcite veins and stringers
4	6FTR-545	01 - 03	Meta-gabbro	0.103	with few quartz/calcite veins and stringers
		04 - 11	Graphite-quartz-mica schist	0.143	carbonatized and at places silicified
5	6FTR-591	01 - 02	Amphibolite	0.200	Carbonatized and at places containing quartz/calcite veining.
		03 - 08	Graphite-quartz-mica schist	0.435	at places containing quartz veinlets and stringers
6	6FTR-550	01 - 05, & 08	Graphite-quartz-mica schist	0.103	only with few quartz veins and stringers
		06, 07, & 09 - 12	Graphite-quartz-mica schist	0.268	containing quartz veins and at places with pyrite crystals
		01 - 05,	Tremolite-	0.024	covered by thick soil and/or fragments of

7	6FTR-547	& 21, 22	actinolite schist		quartz and only at places containing quartz veins and veinlets
		06 - 20	Quartzite	0.254	covered by soil and/quartz fragments
8	6FTR-551	01 - 10	Graphite-quartz-mica schist	<0.01	only at few places having quartz veins and stringers and covered by soil
		11 -21	Meta-sandstone	0.146	containing quartz veins and stringers and also covered by soil
9	6FTR-580	01 - 20	Meta-sandstone	0.1335	only at few places having quartz stringers
		21 - 38	Graphite-quartz-mica schist	0.257	containing quartz veins and stringers
10	6FTR-573	01 - 31	Graphite-quartz-mica schist	0.931	tourmaline disseminated bed rock and at places containing quartz veins
		32 - 35	Finely laminated bed rock soil	0.020	having schistose relict and underlain by the schist rock
11	6FTR-575	01 - 17	Weathered bed rock with micaceous relict	0.056	no quartz veins have been observed
		18 - 27	Weathered bed rock intercalated with talc-tremolite schist	0.369	at places containing quartz stringers

Three key information about gold mineralization in the study area can be obtained from the analytical results of the trenches and from their average gold values against the type and nature of rocks they crossed. The first information is that the gold mineralization of the study area is clearly associated with quartz/calcite veins, veinlets, and stringers. To make the interpretation more clear, graphical illustrations of trench number 6FTR-550 and sample numbers 01 up to 14 of trench number 6FTR-564 that are located on the same meta-gabbro rock are presented below.

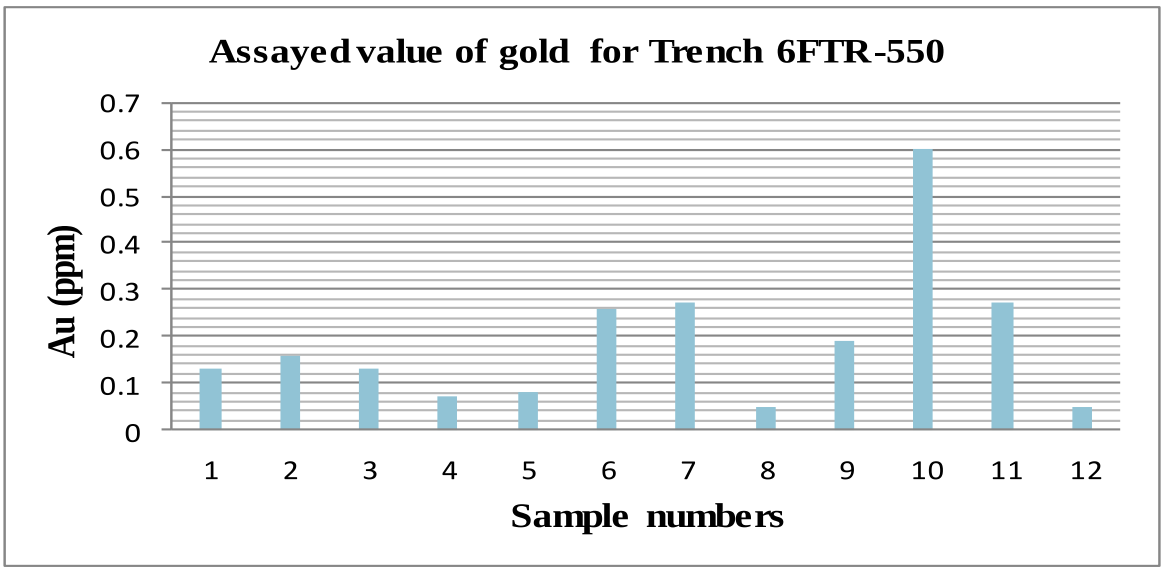

Figure 5.8 A graph showing the distribution of gold in the graphite-quartz-mica schist for trench number 6FTR-550

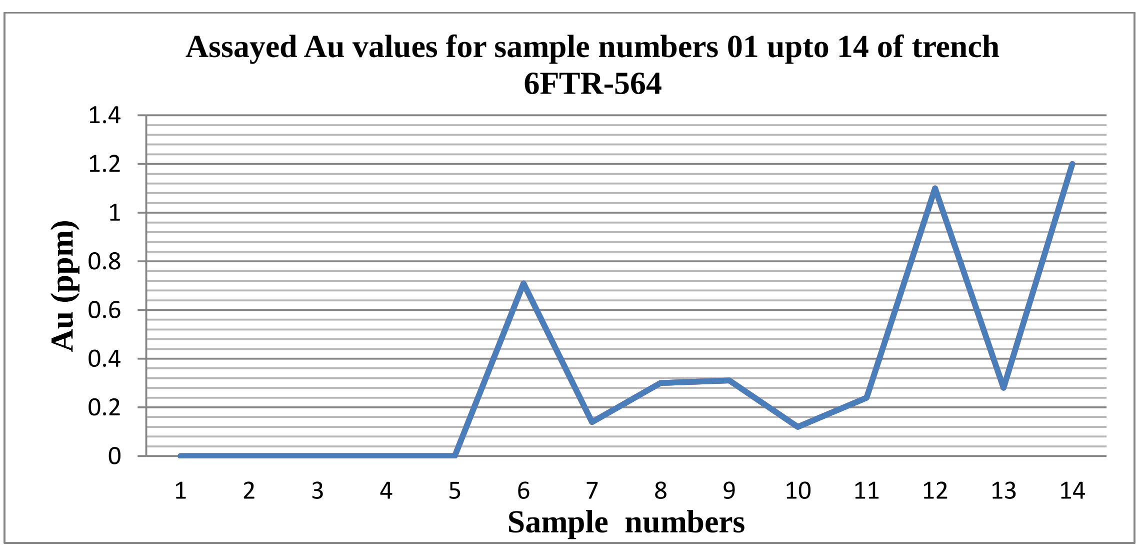

Figure 5.9 A graph showing the distribution of gold in the meta-gabbro for sample numbers 01 up to 14 of trench number 6FTR-550

Figure 5.8above clearly indicate that within the same graphite-quartz-mica schist the assayed Au value in sample numbers 01 up to 05 are <0.18ppm; whereas most of those sample numbers above 06 have gold values > 0.2 ppm. This is because as depicted in table 5.1 and appendix1, the former sample numbers are located in graphite-quartz-mica schist containing only few quartz veins and stringers whereas the latter are located in the same rock type but containing more quartz veins and even at places the veins contain pyrite crystals which often can create ore shoots. The same is also displayed in figure 5.9 in which sample numbers 01 up to 05 are located on meta-gabbro with no quartz/calcite veins and stringers and the assayed Au results are all less than the detection limit (<0.01 ppm); whilst those sample numbers greater than 06 are in the same rock type but with carbonatization, silicification, and at places containing quartz veins with pyrite crystals and have average Au value of 0.488 ppm.

The second important information is the association of gold mineralization with lower grade metamorphic rocks as long as quartz/calcite veins, veinlets, and stringers are present. It is observable from table 5.1 and the gold analytical results of the trenches in appendix 1 that the gold mineralization of the study area is generally associated with lower grade metamorphic rocks of the area such as schists, meta-conglomerates, and meta-sandstones compared with higher grade rocks such as amphibolites and meta-gabbroic lenses within the amphibolites. This is also evidenced from the extensive artisanal gold panning by the local people in the schists of the contact zone and the meta-conglomerate and meta-sandstone of Burikaro sub-area. No such mining activities are present in the amphibolites, meta-gabbro, or meta-dolerite rocks. To make the interpretation unambiguous, graphical presentations of trench numbers 6FTR-584 and 6FTR-591 are given below (Figs. 5.10 & 11).

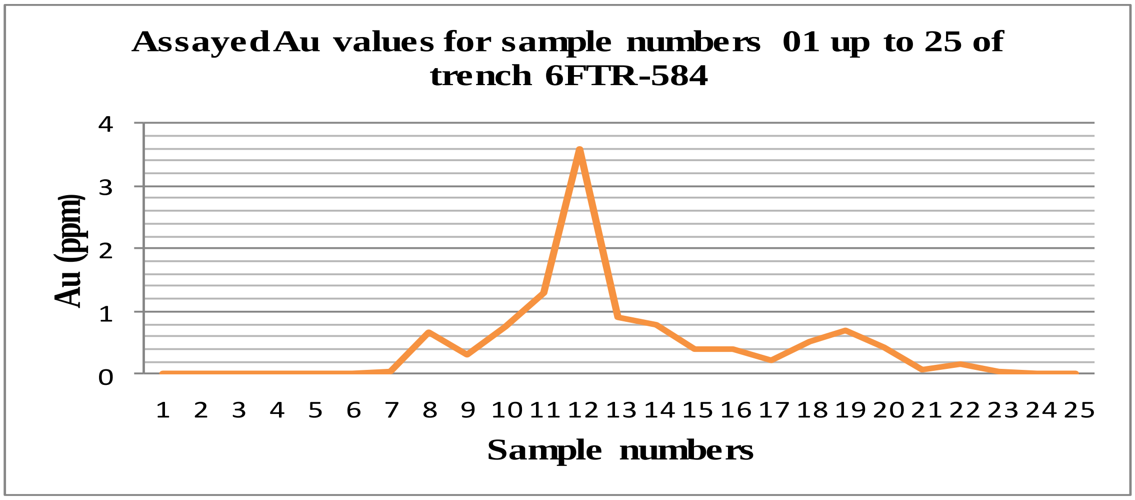

Figure 5.10 A graph showing the distribution of gold in the amphibolite and graphite-quartz-mica schist rocks crossed by trench number 6FTR-584

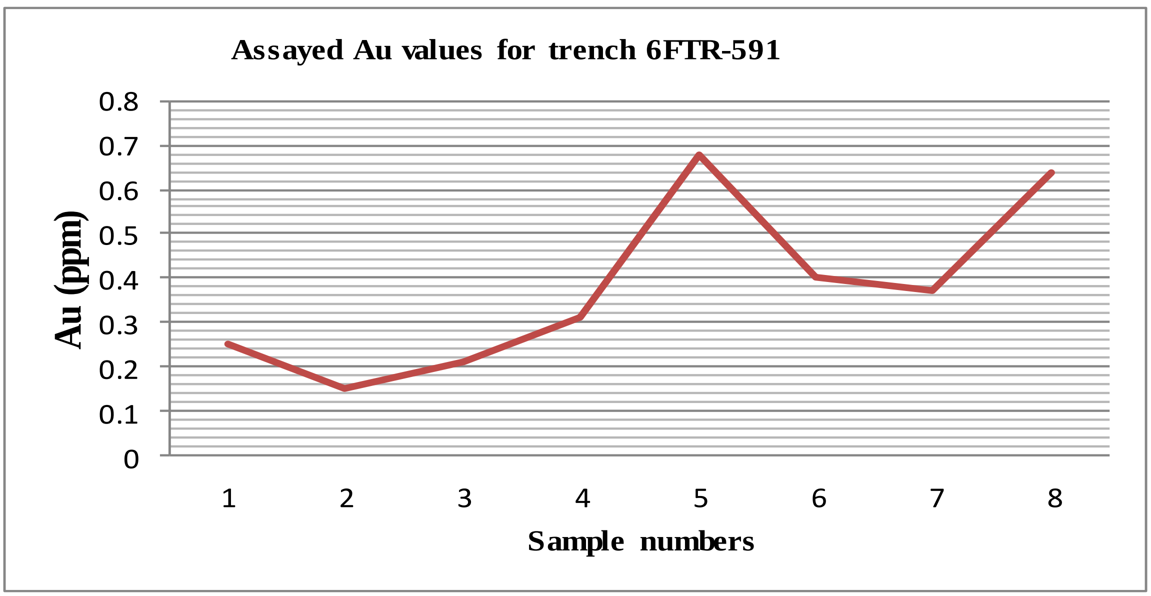

Figure 5.11 A graph showing the distribution of gold in the carbonatized amphibolite and graphite-quartz-mica schist rocks crossed by trench number 6FTR-591

In figure 5.10, sample numbers 01 up to 07 are located on amphibolite rock at places containing calcite/quartz stringers and have average gold value of 0.026 ppm (Table 5.1). Sample numbers 08 up to 19 are on graphite-mica schist invaded by many quartz veins and calcite/quartz stringers and have average gold value of 0.879ppm. The rest of the sample numbers (20 up to 25) are on graphite-quartz-mica schist at places containing quartz veins and calcite/quartz stringers and have an average gold value of 0.065ppm. The same is portrayed in figure 5.11 where sample numbers 01 up to 03 are on amphibolite rock with an average gold value of 0.2 ppm whereas those sample numbers 04 up to 08 are on graphite-quartz-mica schist having an average gold value of 0.435 ppm. Both rock types at places contain quartz veinlets and stringers, the former is also carbonatized.

The third key information that one can extract is that after getting its peak at major quartz veins, the gold mineralization goes down symmetrically on the either side of these veins. Such a symmetrically decease in gold mineralization on either side of the veins suggest that ore constituents are channeled upward from the deeper part through major veins and then further distributed laterally through mainly brittle fractures of the upper part. In addition to the above-displayed graphs such as figures 5.8 and 5.9 displaying this phenomenon, additional graph of trench number 6FTR-545 is also given below in figure 5.12 to strengthen the interpretation.

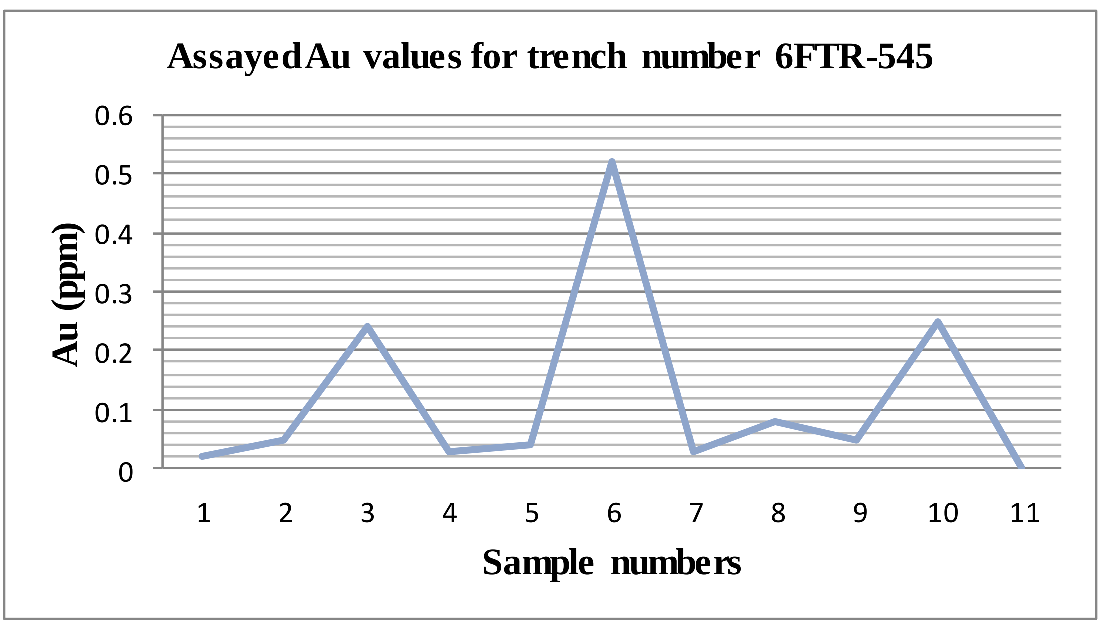

Figure 5.12 A graph showing the symmetrical drop off in Au mineralization on either side of the quartz veins hosted in meta-gabbro and graphite-quartz-mica schist rocks that are crossed by trench number 6FTR-545

5.3.2 Chemical analysis results of surface rock samples

Ten surface samples, six from each rock units and four from different quartz veins, were selected and analyzed for gold and six associated elements: Ag, Cu, Co, Pb, Ni, and Zn. The quartz veins analyzed are hosted in three different rock types: sample code BEA00 is a tourmaline rich quartz vein hosted in the meta-conglomerate, BEA17 is quartz vein from the graphite-quartz-mica schist, and BEA14 is hosted in the amphibolite. The analytical results are presented below in table 5.2.

Table 5.2 Surface sample chemical analysis results from the study area

S. N	**Sample Code**	**Au**	**Ag**	**Cu**	**Co**	**Pb**	**Ni**	**Zn**	**Sample Location**
1	BEA00	0. 20	0.3	4	7	1	24	9	Meta-conglomerate
2	BEA05	<0.02	0.8	26	16	<1	83	33	Meta-gabbro
3	BEA14	0.03	0.5	105	15	<1	28	21	Amphibolite
4	BEA17	4.45	0.7	5	2	<1	4	3	Graphite-quartz-mica schist
5	BEA20	0.03	<0.2	6	2	<1	2	3	Meta-conglomerate
6	BEA21	<0.02	<0.2	5	2	<1	3	2	Graphite-quartz-mica schist
7	BEA31	<0.02	0.9	11	23	<1	171	36	Meta-dolerite
8	BEA28	0.08	0.3	89	12	<1	67	10	Talc-tremolite-actinolite schist
9	BEA32	0.02	0.5	9	10	6	19	24	Meta-conglomerate
10	BEA33	<0.02	1.0	47	20	1	116	75	Qurtz-biotite schist
	Units	ppm	ppm	ppm	ppm	ppm	ppm	ppm	
	Det.Limit	0.02	0.2	1	1	1	1	1	

Gold values range from 0.02 up to 4.45 ppm with mean of 0.80; silver range from 0.3 up to 1.0 ppm with mean of 0.62; copper range from 4.0 up to 105 ppm with mean of 30.70; cobalt range from 2.0 up to 23 ppm with mean of 10.90; lead is almost undetectable except in one sample having 6 ppm; nickel ranges from 2.0 up to 116 ppm with mean of 51.70; and zinc from 2.0 up to 75 ppm with mean of 21.60.

5.3.2.1 Interpretation of surface sample chemical analysis results

As presented in table 5.2, maximum values of gold are obtained from quartz vein samplesBEA17 and BEA00, namely 4.45 and 0.20 ppm Au, which are located in the graphite-quartz-mica schist and meta-conglomerate rocks, respectively. Another quartz vein (BEA14) hosted in the aphibolite rock yielded 0.02 ppm Au, an acceptable value but much lower than the aforementioned veins. Such relatively lower gold value from this sample indicate that at present the gold mineral is not as such associated with the higher grade rocks such as amphibolites, probably because it is channeled upward through quartz veins due to deformation at the lower parts and leading to its subsequent concentration elsewhere in the overlying lower grade rocks. The maximum gold value obtained in the quartz vein from the graphite-quartz-mica schist can be associated at least with two reasons. Firstly; since the graphite-quartz-mica schist rock is highly schistose, sheared and mainly deformed in a brittle manner, probably it served as a porous medium for the concentration of ore constituents transported by hydrothermal solutions migrating upward through these fractures. The second reason is probably associated with the presence of graphitic material which always creates a conducive environment by acting as a trap for ore materials. As discussed in the previous sections, such higher values of gold mineralization in the graphite-quartz-mica-schist are also evidenced from a number of trench analytical results.

Even though lower than the gold value of BEA17, the 0.20 ppm gold value of BEA00 also can be associated with the nature of the host meta-conglomerates. In addition to the primary porosity, the meta-conglomerate rock is considerably sheared and fractured which enhanced its porosity. Similarly, these pore spaces might served as a suitable sites for ore deposition.

Besides the quartz veins discussed above, the comparison of analytical results of samples from the surface rocks also indicated that the gold mineralization is mainly associated with the lower grade rocks (schists and meta-conglomerate) than the higher grade rocks such as amphibolites and those meta-plutons hosted in these rocks. The exception is the <0.02 ppm Au value obtained in BEA33 which is from quartz-biotite schist. Such a lower analytical value from this schist can be associated to two reasons. Primarily, as discussed in the rock and ore petrography sections, the quartz-mica schist rock is magnetite bearing and ore petrography further showed that pyrite rarely occurs in this rock. Secondly, field observation and ore petrography indicated that the rock is very rarely crossed by veins and it is not graphite bearing. Consequently; these two reasons probably reduced the gold value in this rock because trench results showed that the gold mineralization is associated with quartz veins and pyrite.

Even though it is difficult to do detail statistical analysis such as graphical presentations of data because of limited sample size, correlation coefficient calculations (Table 5.3) indicated important clues about the association and genesis of gold mineralization in the study area. In the statistical correlation coefficient calculations if the calculated correlation coefficient is +1, the relationship between variables is strongly positive whereas -1 indicates a strong negative relationship. On the other hand, 0 represents no relationship between variables and values between 0 and +0.5 and 0 and -0.5 indicates weakly positive and weakly negative relationships, respectively. Lead is not considered in the calculations of correlation coefficients because it is almost not detected except one sample having 6 ppm Pb.

Table 5.3 Correlation coefficients of gold and associated base metals in the study area.

Elements	Au & Ag	Au & Cu	Au & Co	Au & Ni	Au & Zn
Correlation coefficients	0.78	-0.33	-0.56	-0.41	-0.49

From table 5.3 it can be observed that gold has nearly strong positive relationship with silver and negative relationship with, among others, cobalt and nickel. The absence of any silver ore minerals in the study area, such as argentite, and the nearly strong positive relationship between gold and silver can be interpreted that probably the silver is incorporated within the gold forming an alloy. Even though it is usually very difficult to determine the exact source(s) of the metals in hydrothermal mineral deposits (Misra, 2000), basic and ultrabasic igneous rocks are observed to be important sources of gold compared to sedimentary and acid igneous rocks (Boyle, 1987). Such basic and ultrabasic rocks are also sources for elements such as cobalt and nickel. Accordingly, the negative correlation of Au with Co and Ni can be ascribed to removal of Au from the mafic source rocks while the latter two elements remain within the source mafic-rocks. This may suggest that metamorphic dehydration is the prominent factor that resulted in the mobilization of metals incorporated in hydrothermal fluids that channeled out through fractures resulting in the precipitation of quartz veins and associated mineralization. The presence of metamorphosed mafic rocks underlying the gold mineral hosting meta-sediments of the study area strongly supports such interpretation. The nearly strong positive relationship of silver with gold probably indicates that together with gold, silver also has been mobilized upward with gold during transportation by hydrothermal fluids. On the other hand, the slightly negative correlation of gold with copper and zinc may be attributed to variation of their sources, the latter two being more of chalcophile in character.

5.4 Ore petrography

Field work investigation and polished section study results indicated that majority of the ore minerals in the study area are extremely weathered and/or altered and leached out except those samples taken from relatively fresh parts. This is best evidenced by the presence of numerous vugs or open cavities through which ore minerals such as sulfides are escaped out. Consequently, it is relatively difficult to get ore minerals not only in the field but also in the ore microscope. Most of the polished section observations indicated that the percentage of ore minerals in each polished sections rarely exceed 20%. Those majorities of available ore minerals are extremely fine grained that their identification (even with 200X magnification) is very difficult. However; the observed minerals of the Burikaro and Ejersa area are made of predominantly pyrite, magnetite and, ilmenite and consists minor amounts of hematite, chalcopyrite, and accessory amounts of sphalerite, covellite, limonite and gold. These ore minerals occur dispersed through quartz veins and other available fractures within the host rocks. Majority of the observations made indicate that the mineralization of the study area is the result of a combination of predominantly two processes: open-space filling and replacement. In some ore minerals exsolution textures are also observed.

The best indicatives of open-space filling mineralization include, among others, comb structures, symmetrically and rhythmically crustified veins, matching of fractures, and the presence of many vugs and cavities. Such open-space filling textures are formed by precipitation of ore and gangue minerals from hydrothermal fluids in pre-existing pores of various types and are primary textures of open-space deposition (Craig and Vaughan, 1994; Misra, 2000). In particular, crustification and comb structures are more pronounced indicatives of open-space filling processes in the study area. Some of the openings are irregular in outline probably because of brecciation; whilst others have regular outline and in either case the filling has well developed often sinuous boundaries. On the other hand, replacement type of mineralization is also evidenced by the presence of islands of the replaced mineral surrounded by the new (or replacing) mineral, relicts of the replaced mineral, and widening of fractures. The common gangue minerals are quartz, calcite, turmaline, and sericite.

The detailed nature and occurrence of each ore minerals is identified and briefly presented below. Since the mineralization in the study area is highly weathered and the ore minerals are very fine grained, it is generally difficult to identify ore minerals in hand specimens. Consequently; the identification was conducted based on studies of qualitative optical, structural, and morphological properties under reflected light microscope.

5.4.1 Pyrite

Pyrite is the most abundant ore mineral in the study area. It is generally yellowish white in color and mainly occurs as subhedral crystals to anhedral crystalline masses distributed in quartz veins and wall rock fractures. Generally, two distinct ways of pyrite mineralization are recognized based on textural studies: open space filling and replacement types. The open space filling type mineralization is mainly associated with quartz veins and display two well developed types of textural developments: comb structures and crustification. Figure 5.13 (a) is a typical comb structure in which euhedral pyrite crystals growing from the opposite walls of fractures are symmetrically grew towards its center developed an intermediate zone showing an appearance like the teeth of a comb. As summarized in Craig and Vaughan (1994) such comb structures are a typical primary textures resulting from open-space deposition and they are the result of the deposition from hydrothermal solutions moving through open fissures.

Another well-developed texture displayed by pyrite is cristification, the deposition of minerals in successive layers or crusts on the walls of openings in the rocks. Figure5.13 (b) shows a typical crustification texture developed by the deposition of successive layers of pyrite in a fracture and displaying growth zoning. More interestingly, the bands in figure 5.13(b) are not only symmetrical in kind on opposite walls but also equal in number. In such crustification, usually the layer next to the wall was deposited first, that is, older in age than those following successive layers (Craig and Vaughan, 1994). The younger successive layers then has grown toward the center of the fissure meeting at the lower part of figure 5.13 (b) while leaving lenticular unfilled vugs on the top parts which may be due to the difference in the size of the opening.

Replacement type of mineralization, on the other hand, mainly occurs when pyrite replaces gangue materials (mainly quartz and biotite) and at places magnetite mineral. Textural evidences of replacement type pyrite mineralization include widening of fractures, the development of zonal replacement bands and generally anhedral (or irregular) crystalline masses formed following the outline of the fissures in which they are occurring (Fig. 5.14). At places, pyrite is rimmed and cross-cut by hematite mineral indicating Pyrite is paragenetically older and giving way to hematite due to latter weathering and/or oxidation effect. Figure 5.14 (a) is a typical replacement texture in which the pyrite is replacing the magnetite mineral resulting in alternating zonal replacement bands of magnetite and pyrite. The central whitish gray vestige of magnetite minerals are implications for incomplete replacement between pyrite and magnetite. In some veins and fissure fillings, pyrite is limonitized perhaps due to oxidation effect.

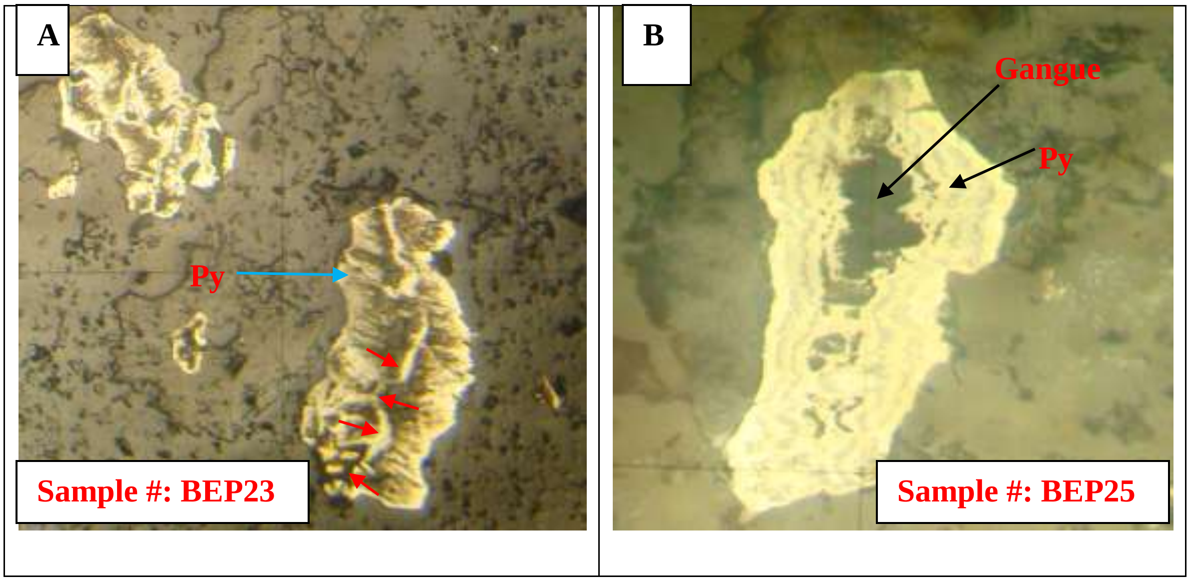

Figure 5.13 Photomicrographs showing a) a typical comb structure in which pyrite crystals are growing outward from fracture walls with perfect matching fractures (X200) b) crustification texture produced by successive deposition of pyrite (X500).

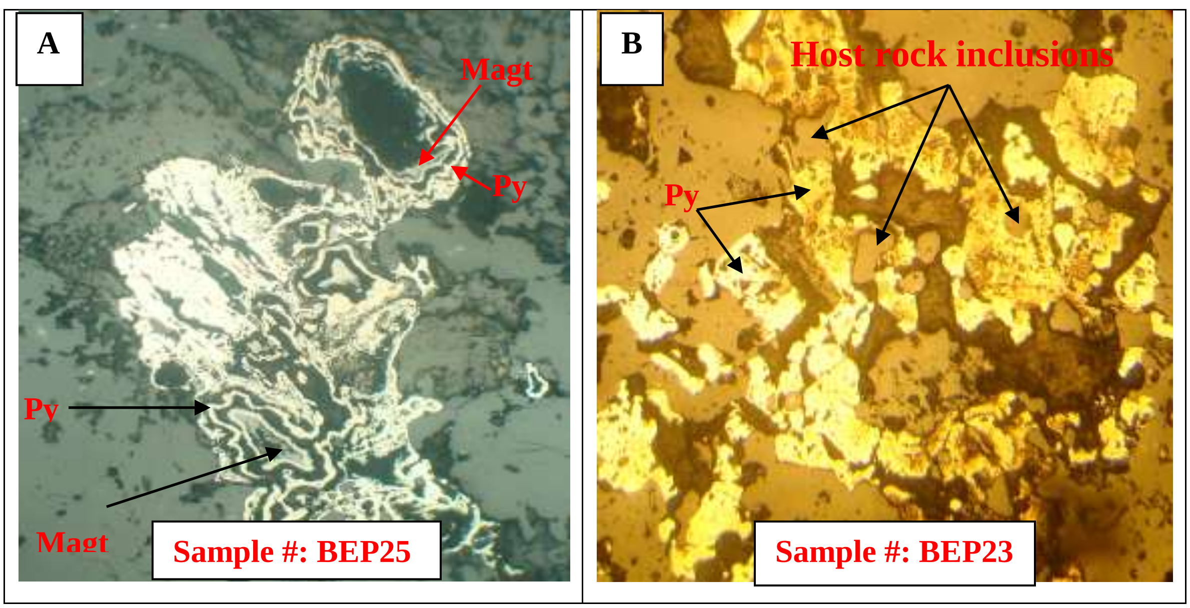

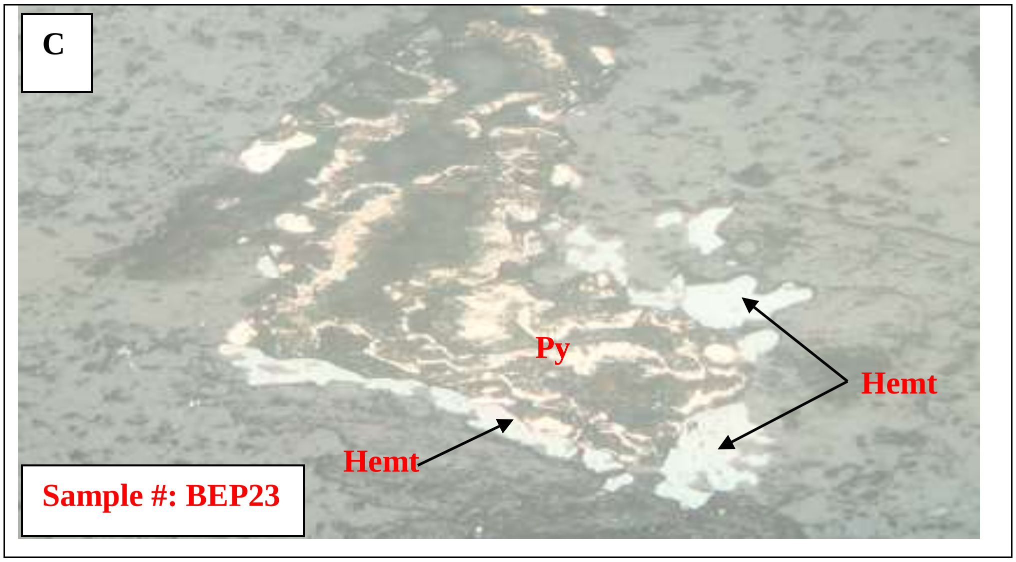

Figure 5.14 Photomicrographs showing a) a typical zonal replacement banding with alternate bands of Pyrite and magnetite displaying slight widening of fractures (X100) b) generally, an irregular crystalline masses of pyrite replacing gangue materials which is evidenced by the presence of many gangue inclusions and widening of fractures (X500) c) highly weathered vein filling pyrite rimmed by hematite (X200).

5.4.2 Magnetite

Magnetite is the second most abundant ore mineral in the study area. In particular, it is the most abundant ore mineral in the quartz-mica schist, which is at places magnetite bearing and where there is little or no pyrite mineral occurrences. The magnetite mineral is gray with brownish tint in color and occurs as euhedral and anhedral crystals and also as prismatic polycrystalline aggregates filling fractures in the host rocks (Fig. 5.15). Magnetite also occurs as a replacement type mineralization which is recognized by the presence of host rock inclusions engulfed by magnetite minerals. In the graphite-quartz-mica schist, generally it follows the schistosity (or the major N-S trending shear zone) of the rock. Hand specimen taken from the quartz-mica schist indicated that at places the magnetite minerals in this rock form a typical banding texture. As one traverses in the graphite-quartz-mica schist southward along the strike of the contact zone, the magnetite minerals are being replaced by pyrite. It is also evidenced from polished section study that at places the magnetite is altered to hematite and limonitized.

Some of the magnetite minerals show well-developed shapes and fractures within a single mineral grain that are generally aligned perpendicular to the maximum elongation direction of the magnetite mineral, probably indicating the presence of pre-tectonic magnetite (Fig. 5.15 a). The magnetite mineral in figure 5.15(a) is typically euhedral with well-developed diamond shape and occurring disseminated in a place where there is no quartz veining or any other prominent shearing, perhaps indicating a primary texture resulting from crystallization of a melt. As discussed in Craig an Vaughan (1994) primary magnetite is among the minerals that are refractory enough to retain their original textures, often occurring as well-developed equant euhedral grains interspersed in the host rocks.

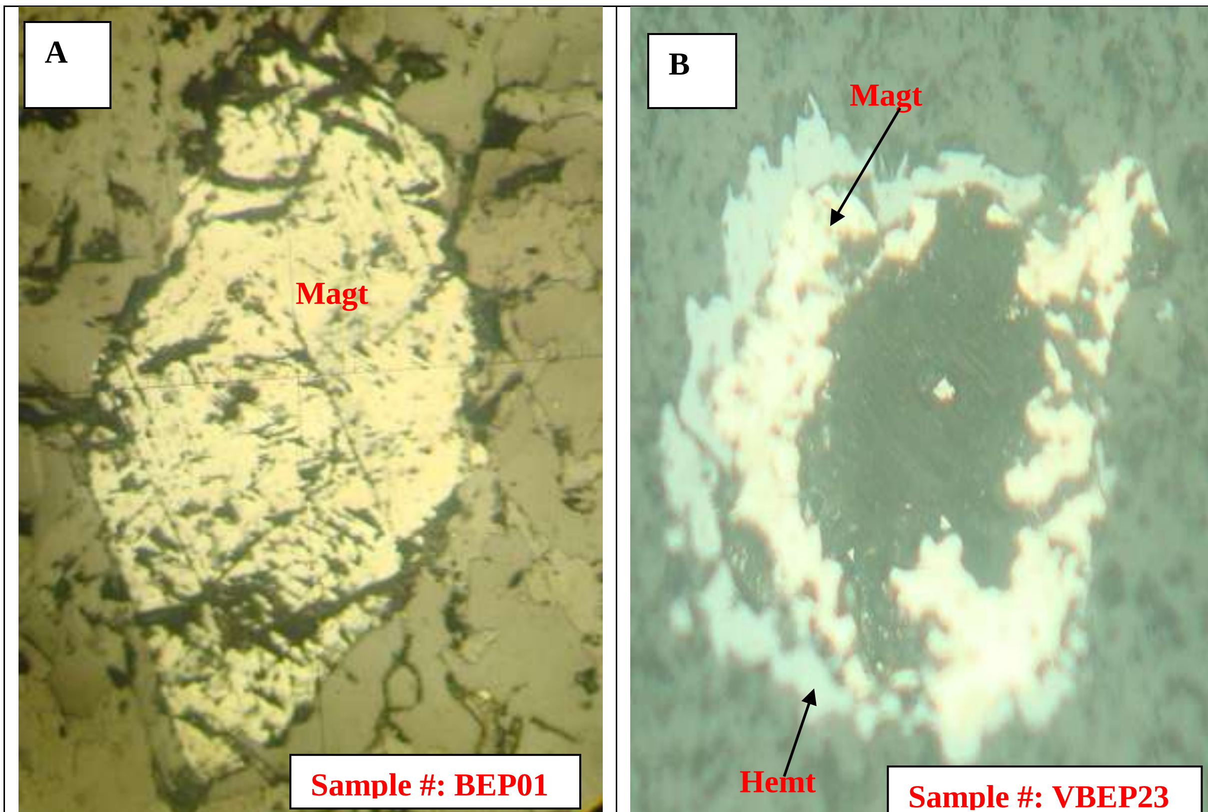

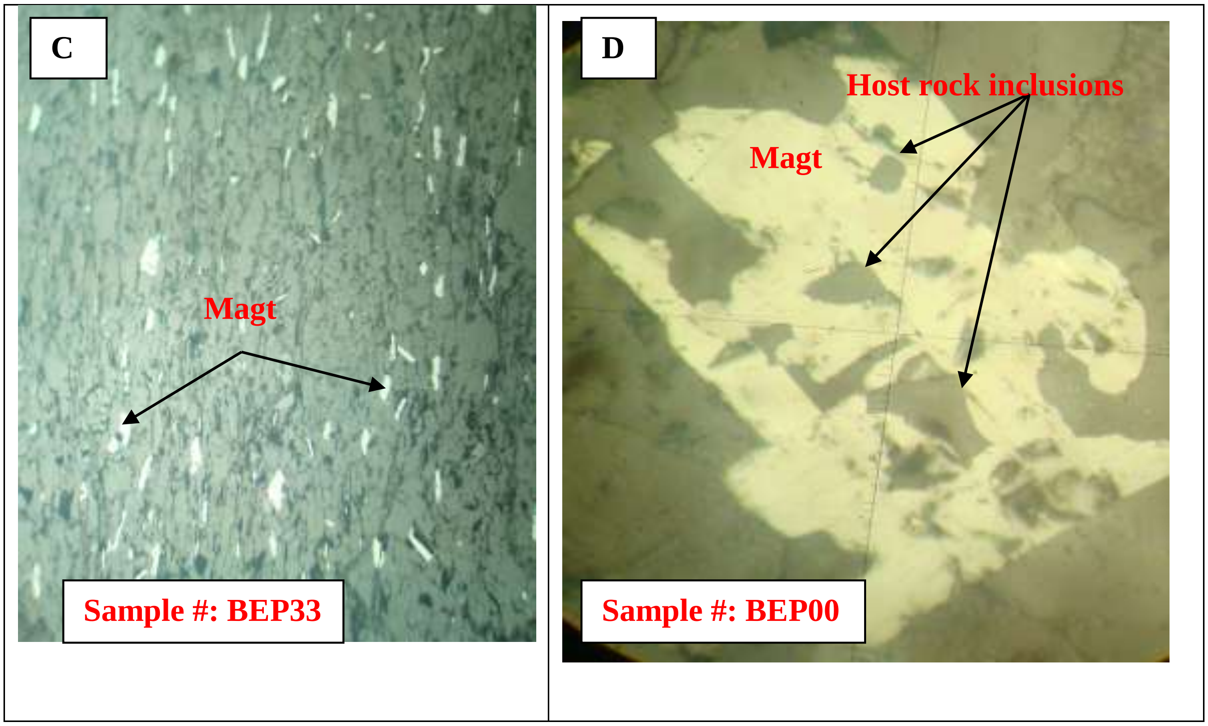

Figure 5.15 Photomicrographs a) a euhedral magnetite with well-developed diamond shape and containing fractures (X200) b) a magnetite mineral is altered and being replaced by hematite (periphery, gray-white with bluish tint) (X100) c) elongated (prismatic) magnetite minerals aligned along the schistosity of quartz-mica schist (X100) d) anhedral aggregates of magnetite minerals containing host rock inclusions, indicative of replacement texture (X200)

5.4.3 Ilmenite

Ilmenite is the third most abundant ore mineral of the study area. It has brownish with pink tint color and occurs mainly as subhedral to anhedral grains and "dendritic" masses. It also occurs pseudomorphously replacing feldspar in the meta-conglomerate rock, where it displays the elongated tabular morphology of feldspar (Fig. 5.16).The ilmenite mineral is commonly associated with hematite; particularly hematite occurs as exsolution lamellae in the host ilmenite. Such a relationship between ilmenite and hematite produced a typical exsolution texture, secondary texture resulting from the cooling of minerals from their temperatures of initial crystallization or the maximum temperature of metamorphic recrystallization (Craig and Vaughan, 1994). In this relationship, hematite is expelled from the host ilmenite probably due to incomplete miscibility as temperature cools down and displaying a characteristic pattern of lens-like lamellae. At places, the anhedral ilmenite minerals contain so many inclusions of other minerals, possibly TiO_2-minerals (rutile or anatase), having variable shape and size in addition to the hematite exsolution lamellae (Fig. 5.16 a).

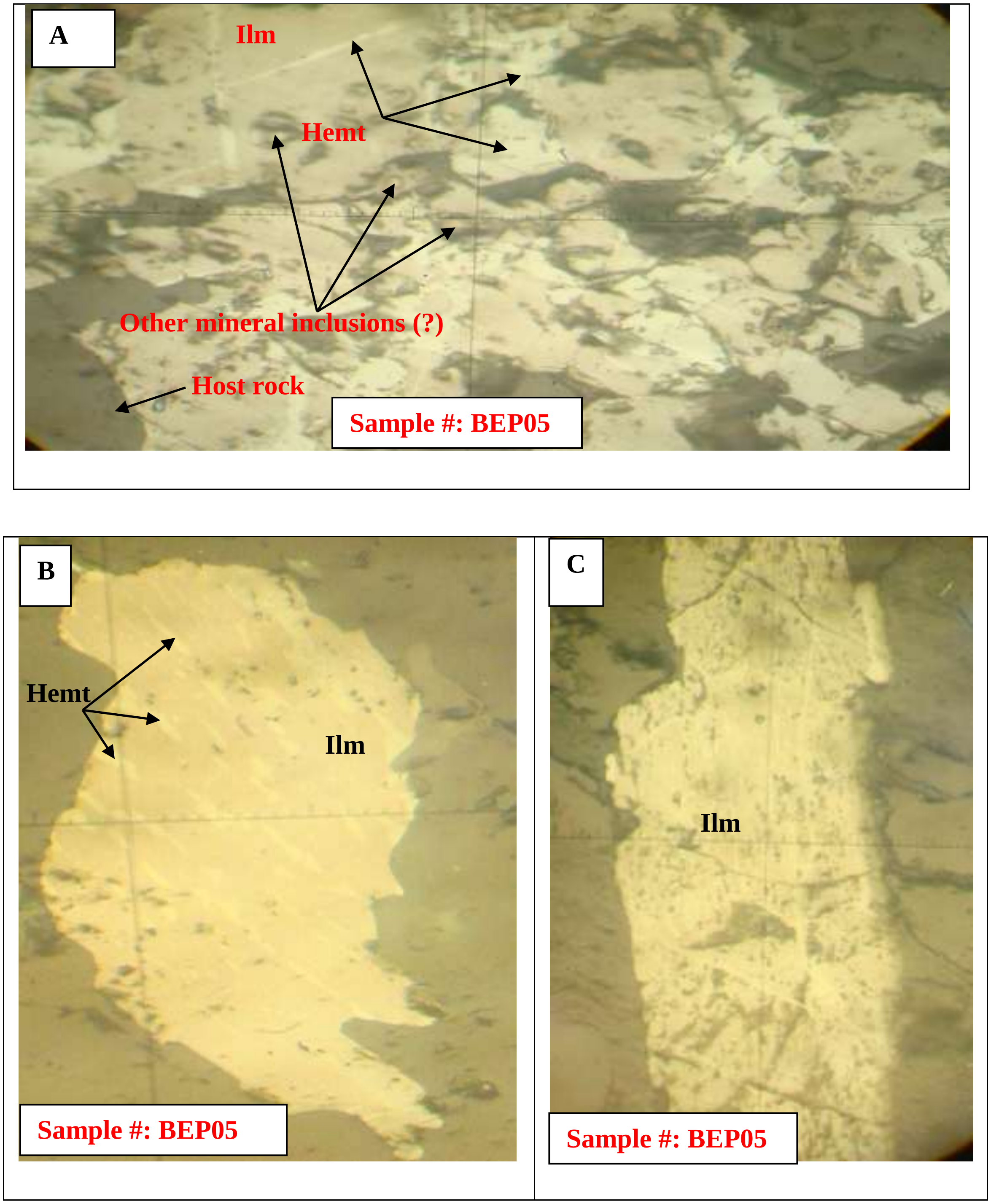

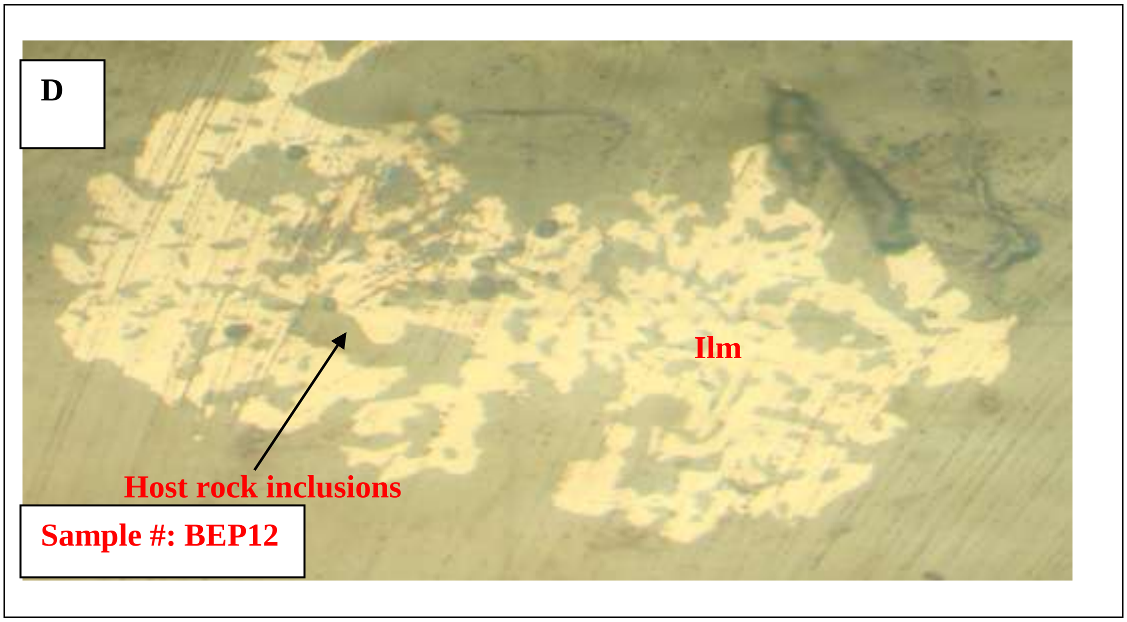

Figure 5.16 Photomicrographs showing a) ilmenite mineral hosting hematite and containing other mineral inclusions b) typical lensoidal exsolution bodies of hematite in a host of ilmenite c) a typical replacement texture produced due to pseudomorphous replacement of feldspar by ilmenite d) a dendritic pattern produced by the distribution of anhedral skeletal masses of ilmenite mineral replacing the host rock. (X500)

5.4.4 Hematite

Hematite is a minor oxide ore mineral observed in the study are. It has a gray-white with bluish tint color and predominantly occur in ferrugnized quartz veins and fissures displaying a typical pinch and swell type mineralization (Fig. 5.17 a). Hematite also occur as an alteration product of magnetite, pyrite, and as an exsolution lamellae in ilmenite as displayed in figure 5.17 (b). At places, it becomes limonitized leading to the formation of yellowish brown limonite probably due to hydration.

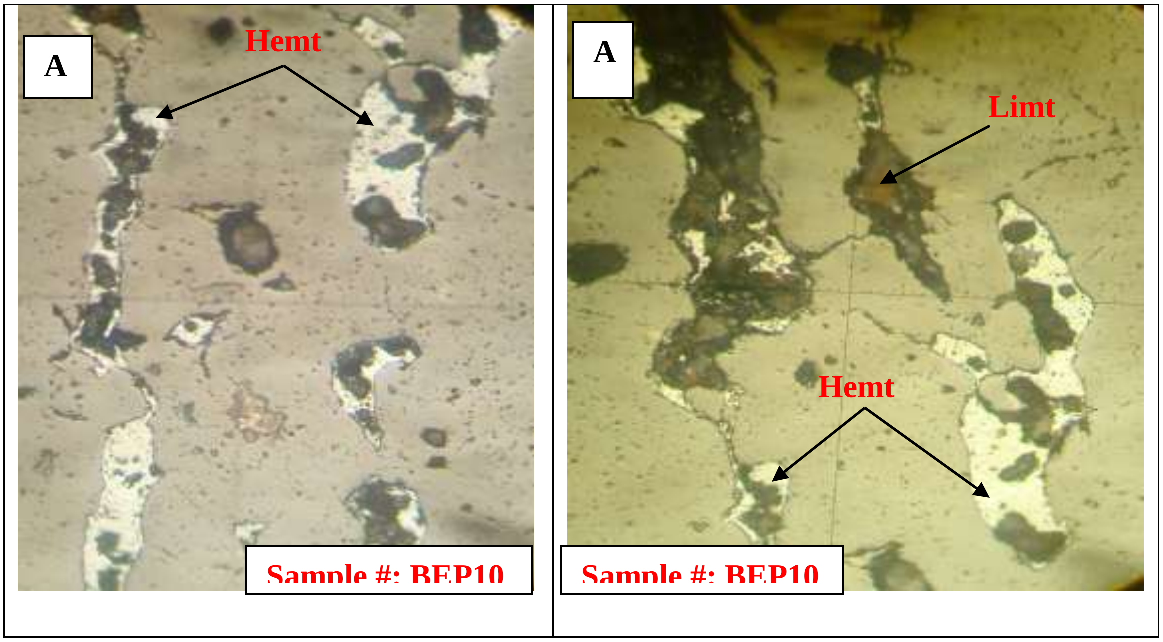

Figure 5.17 Photomicrographs showing a) a typical vein filling hematite mineral displaying pinch and swell type mineralization morphology b) a highly weathered and at places limonitized hematite mineral. (X200)

5.4.5 Chalcopyrite

This is another minor sulphide ore mineral in the study area. It has typical brass yellow to yellow color and commonly occurs as anhedral aggregates and at places with well-developed hexagonal grains. It is generally genetically closely associated with covellite and sphalerite (Fig. 5.18 a).It mainly occurs as an individual anhedral mineral in fissures replacing the gangue material which is evidenced by the presence of gangue inclusions in chalcopyrite. chalcopyrite also occur as a euhedral mineral filling open spaces in the host rock, indicated by the perfect matching of fracture walls and abrupt change in texture between the hydrothermally deposited chalcopyrite and the host rock (Fig. 5.18 b). Such well-developed crystal faces (especially of chalcopyrite) are among the evidences for primary textures resulting from open-space deposition (Craig and Vaughan, 1994). Along fracture lines and gain boundaries, chalcopyrite is commonly altered to and/or replaced by covellite and the whole sequence is then rimmed by sphalerite. Besides its general occurrence in the amphibolite and meta-plutons, chalcopyrite is also commonly associated with quartz veins in Burkaro sub-area. Chalcopyrite also occurs as atypical vein filling mineralization having pinch and swell morphology (Fig. 5.18 c).

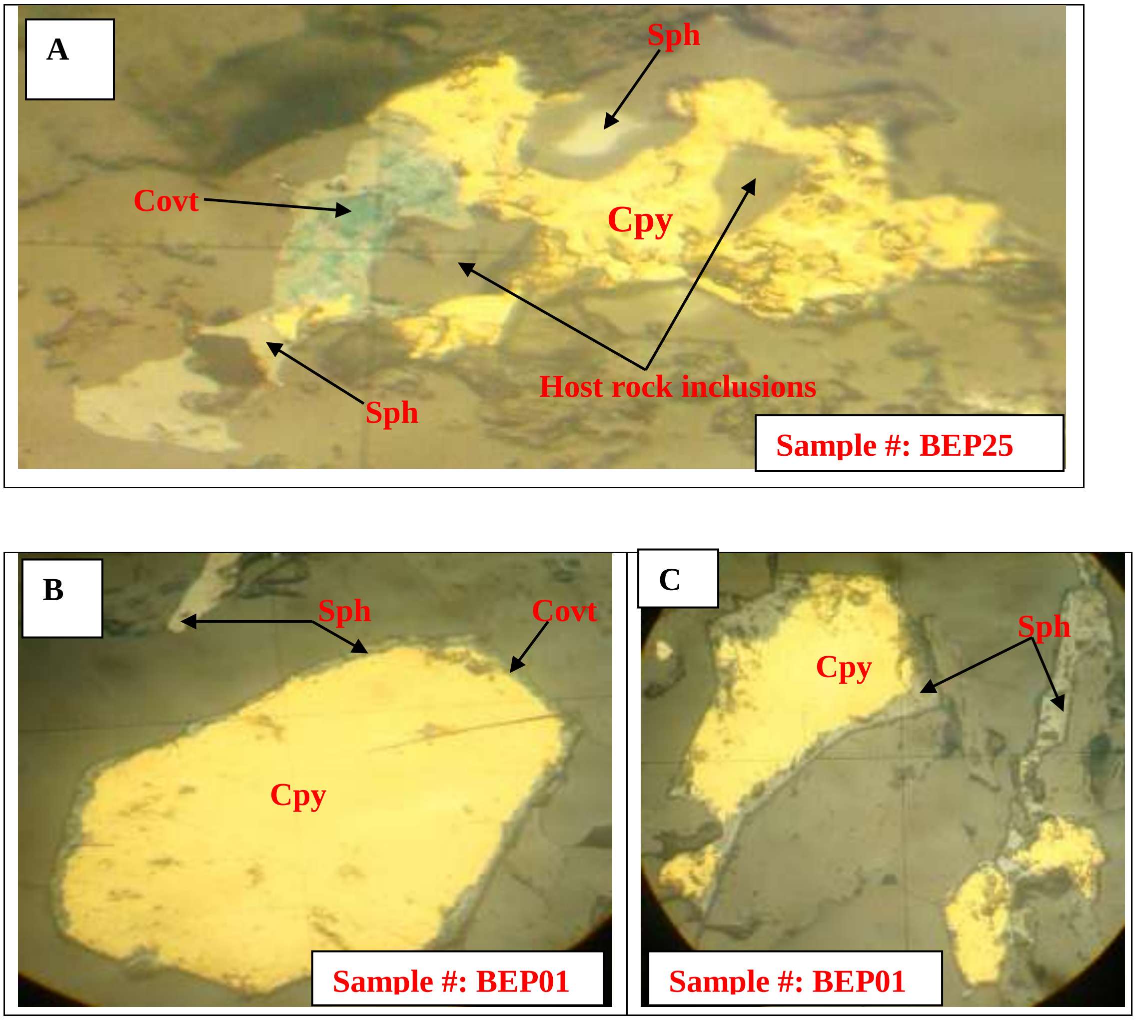

Figure 5.18 Photomicrographs showing a) anhedral aggregates of chalcopyrite containing inclusion of gangue and altered to covellite and rimmed by sphalerite (X500) b) a hexagonal shaped chalcopyrite with grain boundaries altered to covellite and rimmed by sphalerite (X500) c) a typical vein filling chalcopyrite mineralization at places replaced by sphalerite (X200).

5.4.6 Sphalerite

Sphalerite is another sulfide mineral in the study area commonly occurring as irregular anhedral masses associated with chalcopyrite. It is generally grayish-brown in color and predominantly replaces chalcopyrite, characterized by the development of a typical islands of the host (or replaced chalcopyrite) having the same orientation and surrounded by the replacing sphalerite mineral (Fig. 5.19 b). In the literature such intergrowth texture is called the "chalcopyrite diseases". Although the origin of such intergrowth texture is suggested by some writers to be exsolution of chalcopyrite from high temperature shpalerite-chalcopyrite solid solution, expermental investigations in the Cu-Fe-Zn-S system have demonstrated that the solubility of copper in sphalerite at 300^0 to 700^0c is extremely limitted, indicating that exsolution cannot account for much of the chalcopyrite diseases in natural assemblages, rather a replacemet origin is strongly supported by hydrothermal experiments in which the chalcopyrite diseases was produced by reacting iron-bearing sphalerites with copper bearing chloride fluids (Misra, 2000; and references therein). As discussed in Craig and Vaughan (1994) such type of replacement occurs in a more advanced stage of replacement because the original phase is reduced to an " island" left in a matrix of the replacing mineral. In the early stages of the replacement process, replacement may be readily identified because much of the original phase remains and the original grain boundaries, fractures, or cleavages will still visible. Furthermore; according to Misra (2000) such replacement occurs in high temperature and lower pressure conditions because since fractures, cleavages, grain boundaries, and certain crystallographic planes are preferred sites of replacement due to readily occurrence of diffusion, high temperature facilitates the diffusion while high pressure may inhibit diffusion by healing fractures. The sphalerite mineral also occurs as generally anhedral mass often together with chalcopyrite (Fig. 5.19 a). At places, sphalerite also occurs together with pyrite where the pyrite is rimmed and cross-cut by sphalerite, indicating sphalerite is paragenetically younger than pyrite (Fig. 5.19 c).

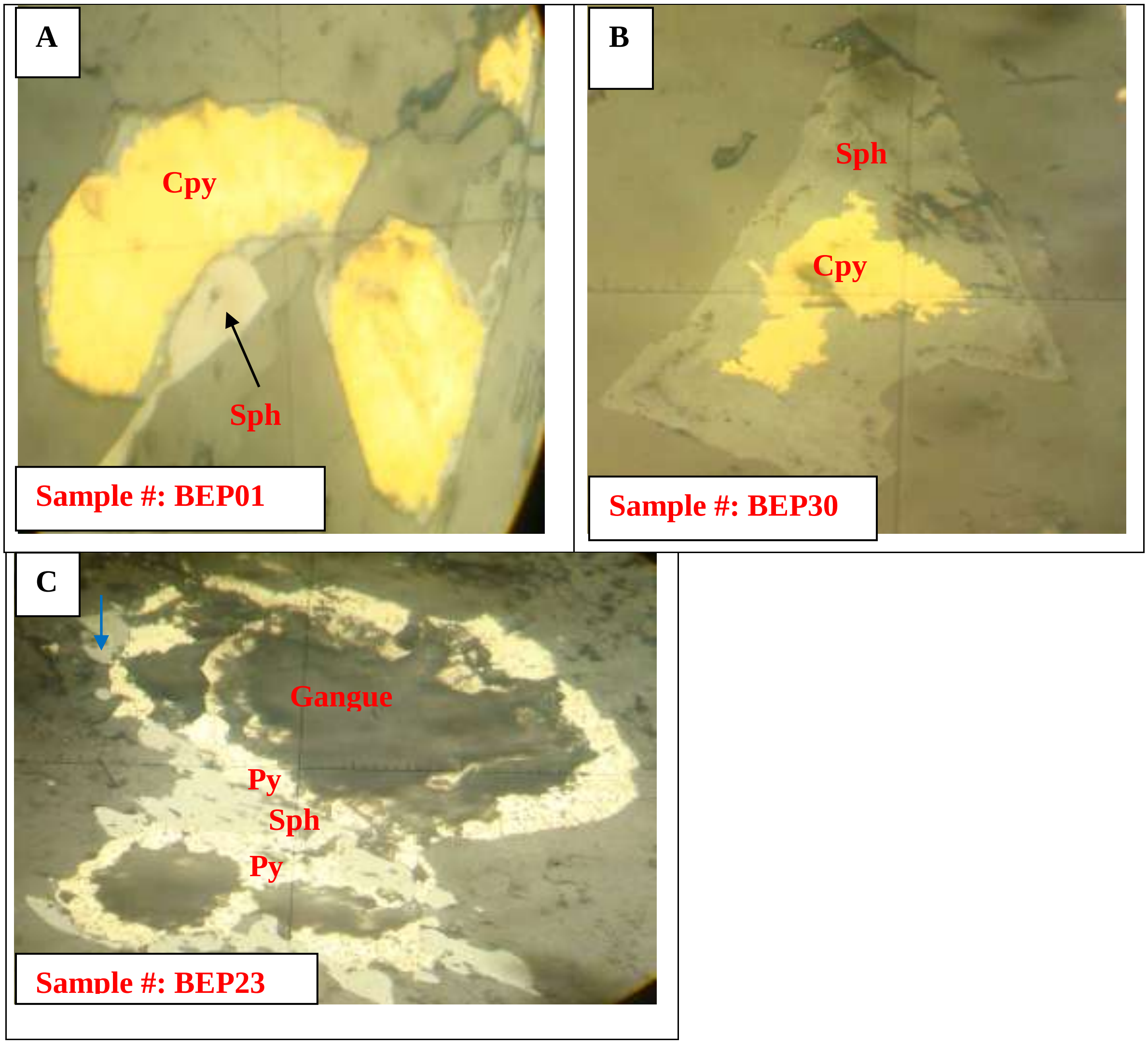

Figure 5.19 Photomicrographs showing a) anhedral sphalerite occurring together with and at places rimming chalcopyrite in fractures (X500) b) a typical replacement texture in which chalcopyrite is replaced by shalerite producing anisland of chalcopyrite in the matrix of sphalerite (X500) c) strongly weathered open-space filing type pyrite rimmed and cross-cut by sphalerite mineral (X200).

5.4.7 Covellite

It is a secondary mineral observed to be produced due to the supergene alteration of chalcopyrite (Fig. 5.18 a). Covellite has bluish-white color and occurs mainly as anhedral masses often rimming chalcopyrite and as inclusions in sphalerite where it replaced the relict chalcopyrite found in sphalerite.

5.4.8 Limonite

Limonite is another secondary mineral in the study area. It is closely associated with hematite, magnetite, and pyrite (Fig. 5.20). It can be, therefore, deduced that it is produced from hydration of hematite and magnetite and also as oxidation product of the pyrite. As stated in Craig and Vaughan (1994) the oxidation of pyrite causes the formation of sulfuric acid and ferrous sulfate, which may results in the breakdown of other sulfides the end result being a box work gossan of iron oxides and hydroxides capping the uppermost parts of veins. Generally, the limonite has a brownish-yellow color and occurs as anhedral masses.

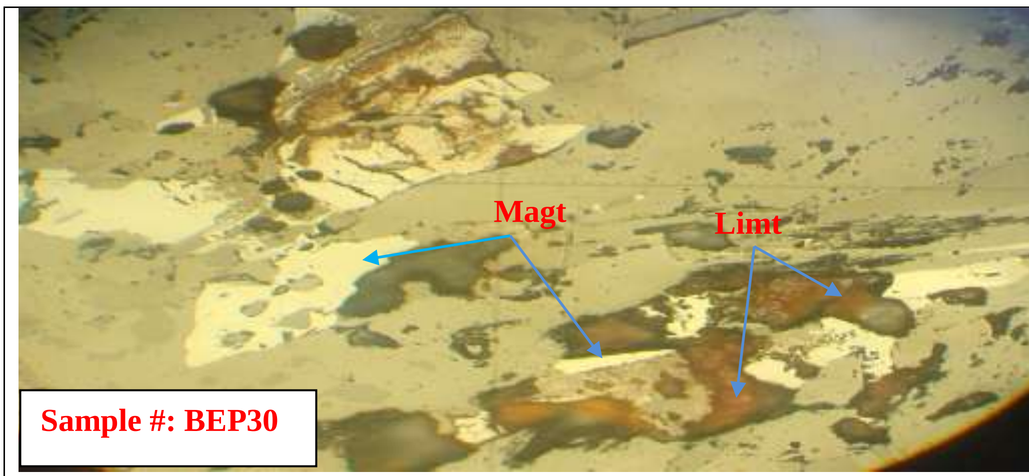

Figure 5.20 Photomicrographs showing magnetite mineral is altered to limonite probably due to hydration effect (X200).

5.4.9 Gold

Even though chemical analysis and field observation of artisanal gold panning by the local people indicated the presence of gold mineralization in the study area, particularly associated with quartz/calcite veins and stringers, none of the polished sections show clearly observed gold mineral, even under X500 magnification, because of very fine grain size. However; there are very fine grained minerals displaying a number of gold mineral characters and suspected to be gold even though it is difficult to clearly identify them. Figure 5.21 is probably a gold mineral which is characterized by golden color and very high reflectance. It is also observed that the gold mineralization in figure 5.21 is an aggregate of very minute gold grains constituting a vein material. Unlike the other ore minerals such as chalcopyrite which are relatively coarser, the gold mineral displayed below is very fine grained. The occurrence of such very fine grained gold is also observed during field work collected by the local artisanal gold miners.

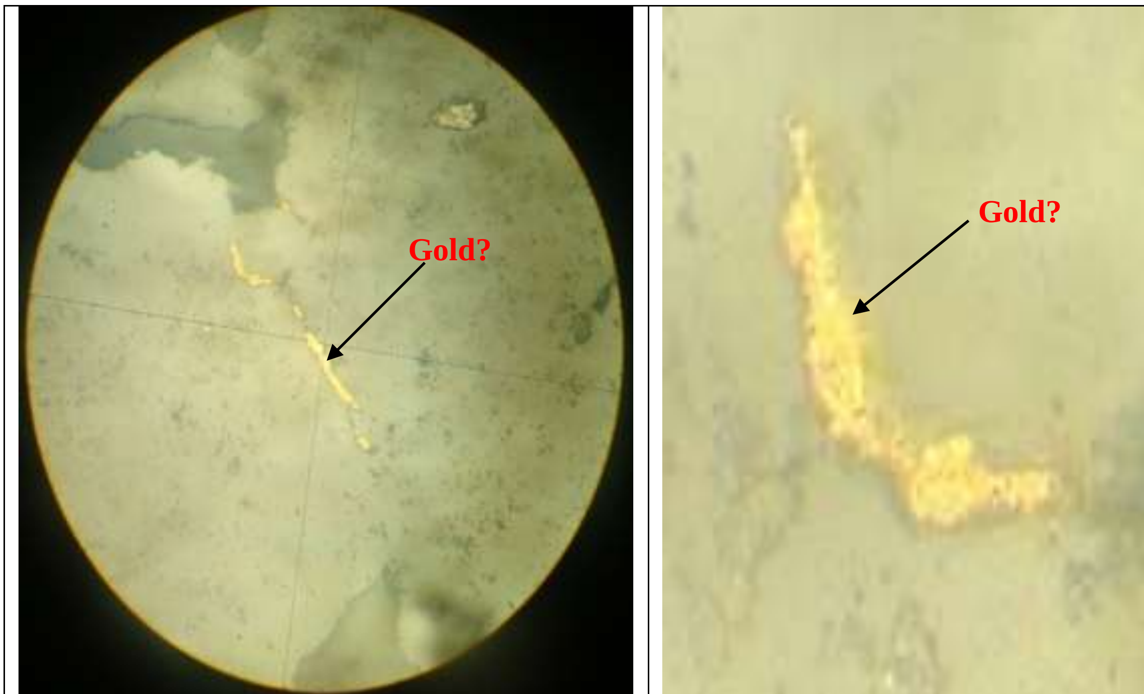

Figure 5.21 Photomicrographs showing gold mineral (?) occurring as aggregates of gold grains forming a vein material taken from a quartz vein in the graphite-quartz-mica schist rock and seen under reflected light. All the photos are taken from sample number BEP17. (X500).

Surface sample chemical analysis of the same sample, that is, BEA17 yielded exceptionally high gold value compared to the other samples, 4.45 ppm Au (Table 5.2). This supports the occurrence of gold mineral in this sample. The presence of BEA17 in the graphite-quartz-mica schist rock of the mineralized contact zone is another evidence.

5.5 Mineral paragenesis

The mineral paragenesis of the study area is prepared based on textural studies, mineral relationships and associations, and alteration processes. Accordingly, the paragenetic sequence of the ore minerals of the study area can be associated with three stages of mineralizations (i) disseminated type (ii) hydrothermal quartz/calcite vein and fracture related , and (iii) supergene mineralization.

Magnetite is the only ore mineral observed to occur disseminated in the amphibolite rock. However; since magetite and ilmenite are generally occur together, it may also be possible for ilmenite to accompany magnetite in such early formed dissemination mineralization. Consequently; even though not observed by the researcher, it is put under question mark which is represented by the dashed-lines in figure 5.21. Such magnetite minerals have well developed diamond shapes and containintragrain fractures generally perpendicular to the major elongation direction. Such features indicate that even though most of the ore mineralization is associated with hydrothermal quartz/calcite veins, magnetite also occurs as a disseminated primary mineral and suggesting its possible occurrence from magmatic process.

The hydrothermal quartz/calcite vein category mineralization is the most important type of mineralization in the study area where most of the ore minerals are associated with this stage, including pyrite, magnetite, ilmenite, hematite, chalcopyrite, shpalerite, and gold. Field observations of extensive small scale artsanal gold mining and panning activities by the local people and data from trenches indicated that gold is part of this category occurring associated with hydrthermal quartz/calcite veins, that are at places tourmaline rich. The extensive nearby alluval gold mining by the local people also indicate the occurrene of free gold because the peole recover the gold without the presence of any crushing and/or milling plant. They simply dig deep holes, take the soil material, and they wash and pan it, after many trials which may led to the recovery of very fine gold gains.

Magnetite is also part of the hydrothermal quartz/calcite vein association, occurring as an ope-space filling and replacement type mineralization. In the graphite-quartz-mica schist rock the magnetite minerals are generally aligned parallel to the schistosity of the rock. Polished section study result indicated that at places in the graphite-quartz-mica schist magnetite is replaced by pyrite, producing a typical zonal replacement banding with alternate bands of Pyrite and magnetite indicating that the magnetite is paragenetically older than pyrite. As stated in Debele (2000) such changes from magnetite to pyrite suggests that early stage hydrothermal fluids are oxidizing probably SO_2 and the reaction of the SO_2 bearing hydrothermal fluid with iron bearing host rock may result in early stage crystallization of magnetite followed by pyrite. The presence of such alteration of magnetite to pyrite (sulfidation) in a place where the graphite-quartz-mica schist is rich in iron oxides strengthen such an idea. Magnetite is also at places rimmed by hematite and altered to limonite probably due to hydration. These indicate that magnetite is paragenetically older than both hematite and limonite mineals.

Pyrite is the most dominant and important ore mineral among the hydrothermal associations where gold occurs associated with it. Besides its occurrence replacing magnetite and gangue minerals, pyrite also occurs as an open-space filling material characterized by well-developed textures resulting from open-space filling such as crustification and comb structures. According to Misra (2000) such open space filling texures are among the most reliable type of textures for determining paragenesis. At places, pyrite is rimmed by hematite and altered to limonite probably due to oxidation effect. These indicate that pyrite is paragenetically older than both hematite and limonite mineals. Pyrite is also rimmed and cross-cut by sphalerite (Fig. 5.19 c) indicating that pyrite is paragenetically older thansphalerite.

Ilmenite and hematite are often occur together showing exsolution relationship. In all observations made on such relationship, hematite occurs as an exsolution lamellae where the ilmenite is acting as a host. According to Misra (2000) pairs of minerals showing exsolution relationship must have formed essentially contemporaneosly from a high temperature solid solution. In addition to the exsolution relationship, both minerals also occur as an independent minerals filling open spaces and also as replacement type mieralization. Hematite typically occurs as a filling material in ferruginized quartz veins and at places it is limonitized perhaps due to hydration effect. As indicated above since hematite is younger than pyrite and ilmenite and hematite have formed contemporaneosly, then indirectly ilmenite is also younger than pyrite.

The other groups of minerals related with the hydrothermal quartz/calcite vein are the chalcopyrite-sphalerite association. Chalcopyrite occurs both as an open-space filling mineralization and replament type. In the majority of the observations made, chalcopyrite is rimmed by and/or altered to covellite and sphalerite indicating chalcopyrite is paragenetically older than both of them. As discussed above since sphalerite is younger than pyrite and pyrite in turn is younger than magnetite, we can establish an indirect relationship showing that shpalerite is younger tan magnetite.

The last phase of the paragenetic sequence is characterized by the formation of the secondary minerals covellite and limonite. Covellite is produced due to supergene alteration of chalcopyrite and often occurs replacing chalcopyrite along grain boundaries and fructure lines. From this relationship it can be easily understood that covellite is the youngest within the chalcopyrite-sphalerite-covellite association. Limonite, on the other hand, usually occurs as a hydration product of magnetite and hematite and it is defintely the youngest in the magnetite-ilmenite-hematite-limonite association. Limonite also observed to form as an alteration product of pyrite. On the basis of the discussions made so far, a tentative paragenetic sequece has been proposed for the gold mineralization of the study area and presented using the bar diagram below (Fig. 5.22). However; it should be noted in the paragenetic sequence diagram given below in figure 5.22 that open-space mineralization is not necessarily paragenetically older than the replacement categories and both type even can occur simltaneously. The exact distinictions of such mineralization, however, needs proper age datings which is beyond the scope of this reearch work. As discussed in Boyle (1979) calcite and opal quartz are ammong the common supergene associates of gold besides other secondary minerals such as limonite and clay minerals. Consequently; it is worth to think that these mierals may extend up to the supergene enrichent level in the paragenetic dagram given in figure 5.22 eventhough the researcer is not sure of their presence.

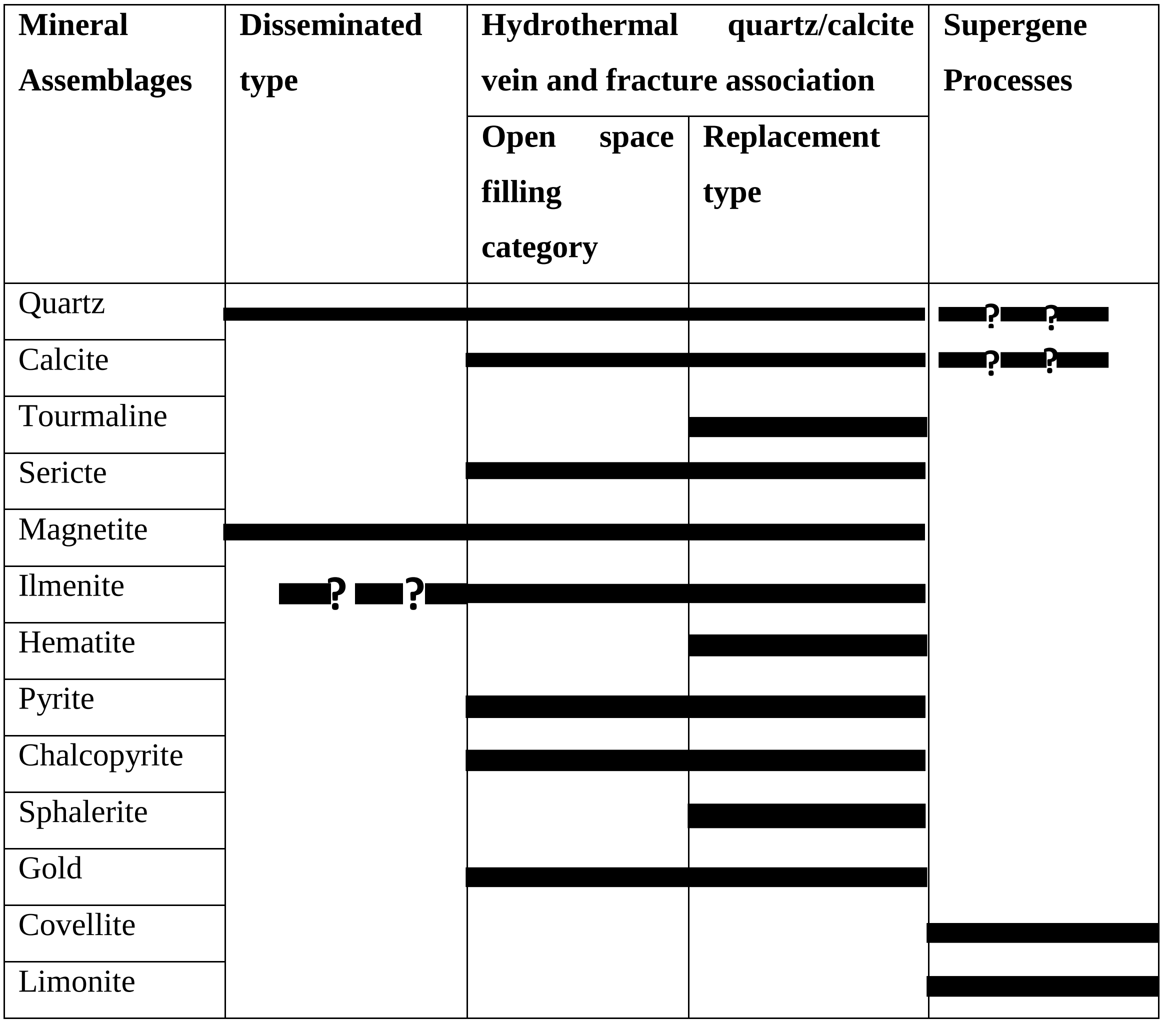

Figure 5.22 Paragenetic sequence of ore minerals related to gold mineralization

Key: - Line thickness is not to scale and has nothing to do with relative abundances of minerals

- Dashed-lines indicate probable occurrences for which the researcher is not sure (?)

CHAPTER SIX

6 DISCUSSIONS

6.1 Nature of Mineralization

As depicted from field work observations, chemical analysis, and ore petrography the mineralization in the study area is strongly structurally controlled type. It is associated with shear zones hosting ubiquitous quartz and/or calcite veins and stringers. The prominent one is the major N-S trending shear zone that affected most of the rocks of the study area. The ore minerals observed by petrographic study include sulfides such as pyrite, chalcopyrite, sphalerite; oxides like magnetite, ilmenite, and hematite. As clearly indicated in the micro-textural studies of the above-mentioned ore minerals, the mineralization is associated with hydrothermal fluids and the introduction of these fluids brought a change in mineralogy in the host rocks and lead to the development of the various types of alterations such as silicification, carbonatization, tourmaliniazation, and chloritization. Trench data results and field observation also indicated that gold occurs both as a “free gold" and hosted in quartz veins predominantly in the lower grade meta-sediments. The gold mineralization is particularly associated with pyrite as evidenced from trench analytical results and lithological descriptions, where the presence of pyrite crystals often resulted in relatively higher gold values (Table 5.1). Even though it is not as such significant with respect to the gold mineralization, supergene processes also produced secondary minerals such as covellite and limonite. Although the ore minerals are associated with quartz and/or calcite veins, magnetite is observed to occur as a disseminated primary mineral, particularly in the amphibolite rock (Fig. 5.15 a).

6.2 Possible sources of fluids and gold

Field observations, trench data results, petrographic studies of ore minerals, and the extensive engagement of the local people by small scale artisanal gold mining in the study area suggests the association of gold with lower grade meta-sediments that are sheared, hydrothermally altered, and invaded by quartz and/or calcite veins and stringers. On the other hand, at present the higher grade rocks are not as such gold mineralized.

Field geological mapping and rock petrography further indicated that the lower stratigraphy of the study area is occupied by relatively higher grade amphibolite rocks that are well exposed and ridge forming in the central and south-western parts of the study area even though it is not revealed in the northern and eastern parts. Pegg (1999); as cited in Basson (2000) studied the orientations of fold hinge zones of folded quartz veins hosted by the amphibolite and suggested that the northern part of the amphibolite is actually a fold hinge zone possibly plunging to N or NNE and his further examination of the Burikaro area (north-eastern part of the present study area) proved this with the amphibolite disappearing there and the shearing being consequently expressed in the meta-sandstone and meta-conglomerates. Therefore; the amphibolite rock is still present in the rest parts of the study area underlying the gold mineralized lower grade meta-sediments.

Even though generally mafics rocks are observed to be sources for gold and associated base metals like cobalt and nickel, the negative relationship between these elements observed in the surface rock sample analytical results indicate that differential mobilization of components have occurred in the history of ore formation in the study area. Gold has been leached from such mafic rock of the area whereas the cobalt and nickel probably remained there due to their relatively immobile character. This is also indicates from the occurrence of gold together with the chalcophile groups (sulfides) in the quartz veins and its higher concentration in the lower grade meta-sediments of the study area.

Review of regional geodynamics and geologic setting of the Adola area indicated that the present architecture of the region is associated with orogeny, notably with the evolution of the East African Orogeny, which is characterized by rifting, associated sedimentation and ocean basin formation, subduction and island arc formation, and continent-continent/continent-island/island-island collisions, respectively leading to crustal shortening, orogenic collapse and extension, which intern resulted in the break-up of Gondwana. All the above discussions suggest that possibly the prominent source of the hydrothermal fluids was metamorphic dehydration. Even though all of the above-mentioned discussions point to metamorphic dehydration, the role of magmatic fluids cannot be totally neglected.

In the evolution of the East African Orogen, there was disappearance of oceanic crust prior to continent-continent collision. Such subduction event probably resulted in the introduction of huge amount of water beneath the overlying block. The introduced water then probably became part of the subducted ocean sediments. When the subducted sediments later exposed to deformation and metamorphism, probably heated and dehydrated losing their water which is perhaps moved upward in to overlying rocks through the deep seated N-S shear zone. As discussed in Debele (2000) such N-S shear deformation is part of the final stage of the evolution of the Adola belt. Subsequent deformation and metamorphism events probably further expelled out the hydrothermal fluids incorporated in the rocks and leading to the leaching of gold from the higher grade metamorphic rocks of the study area and their transportation to the site of deposition. However; it is beyond the scope of this study to determine the exact sources of the fluids and gold which needs further study of isotopic composition of the hydrothermal fluids and will be a question for future work.

6.3 Means of transportation of fluids and gold

Among sulfur species, HS^- or H_2S is the dominant complexing ligand for the temperature-pH range appropriate for ore-forming fluids (Misra, 2000). Trench data results and ore petrography indicated that the gold occurrence in the study area is generally associated with sulfides (particularly with pyrite) implying that probably HS^--or H_2S-complexes were the responsible agents for gold transport in the area. As discussed in Robb (2005) gold typically occurs in monovalent state (Au+) in aqueous solutions and will form the complex AuHS at low pH and $Au(HS)^{2-}$ under weakly acidic to basic solutions and the bisulfide complexes predominate in most hydrothermal fluids and are stable over a wide range of temperature. The sources of sulfur for hydrothermal fluids are either magmas from which the fluids are derived, or rocks with which the fluids interact, or both (Misra, 2000). However, the exact determination of these sources needs sulfur isotope studies. The transportation mechanisms of fluids and gold in the study area also seem directly linked with the evolution of the region. The continent-continent collision that occurred at the waning stages of the East African orogeny have probably resulted in deep seated faults and shear zones. Such discontinuities possibly served as pathways for the heated water within the suggested source rocks. The moving hydrothermal water then further leached its ore constituents due to the interaction with the country rocks and come upward due to the decrease in density of the heated water. The various types of quartz veins crowding the shear zone are, therefore, possibly precipitated from such solutions and formed as channel ways for the subsequent gold mineralization.

6.2 Methods of gold deposition

God deposition in the study area can be generally associated with the changes in the physicochemical characteristics of the overall ore-forming system that may arise from a variety of sources including, but not limited to, fall in temperature, interaction of fluids with wall rocks, and changes in the pH of the solutions. This is mainly because the changes brought to the ore-forming system possibly bring changes in the composition of the gold complexes discussed in section 6.3. The decrease in temperature probably induced gold deposition in that when high temperature hydrothermal fluids carrying ore constituents and channeled upward through shear zones interact with cooler surface rocks and meteoric water, they are forced to decrease in temperature. Such a decrease in temperature may eventually led to the localized deposition of ore constituents because cold water has less capacity of transporting suspended load. The depositions of ore constituents can be open space filling and replacement type since both types of mineralization are observed in the ore petrography. Though not clearly observed in any of the polished sections, the occurrence of gold both as a free gold and associated with sulfides (particularly of pyrite) in the quartz veins is observed from local gold panning activities and trench data results, respectively.

The role of the interaction of fluids with wall rocks in ore deposition, on the other hand, is generally associated with the pathways the fluids traveled. Field observations, ore petrography, and descriptions of trench cross-sections indicated that the major quartz veins that act as main channels for the circulating metal rich fluids are interlinked by many smaller veinlets. Such major quartz veins probably act as "feeders" of ore constituents for the smaller veinlets that are dispersed within the brittle fractures of the surface environment, in an analogy similar to a main irrigation canal feeding smaller sub-canals. During their movement in the major quartz veins, the metal rich hydrothermal fluids might interact with the country rocks. The same history will happen after the fluids have been channeled to the small veinlets and continue their journey until they become cooled and supersaturated, a situation leading to the abrupt dropping of their loads. During such interaction there will be exchange of components between the fluids and the country rocks which may bring changes in the physicochemical behavior of the fluids that may led to the precipitation of gold and associated sulfides. Skinner (1979); as cited in Misra (2000) identified three types of fluid-wall rock interactions that may cause sulfide precipitation from hydrothermal fluids: (i) hydrogen exchange reactions that modify the pH of the solution, especially the H^+ consuming reactions; (ii) addition of components from the wall rock, especially of reduced sulfur species (H_2S or S^{2-}) from pyrite; and (iii) reactions such as sulfate reduction that change the oxygen fugacity of the fluid.

In addition to the above-mentioned physicochemical parameters, the favorable geologic setting of the study area, presence of sulphide and oxide ore minerals, and the observed fractures that are more intense in shear zones also have created conducive situations for gold deposition. As discussed in Nekrasov (2009) iron oxides (magnetite and hematite), sulfides and sulfosalts (pyrite, pyrrhotite, and asrsenopyrite), and carbonaceous matter (graphite and kerite) are among agents precipitating minerals and sorbants that serve as an important geochemical barrier for gold deposition and significantly influenced the distribution of gold in the ore bodies along with the main factor-supersaturation of solutions. The presence of such agents precipitating minerals and sorbants in the study area probably influenced the gold mineralization, too. The important lithology with respect to gold mineralization in the Ejersa sub-area is the graphite-quartz-mica schist, dominating the mineralized contact zone. The presence of carbonaceous matter (graphite) in this rock probably served as an important geochemical barrier by trapping/sorbing gold from moving hydrothermal fluids. In addition to the occurrence of carbonaceous matter, this rock is predominantly britley deformed characterized by the presence of fault breccias and brittle shear zone materials that are intersected by quartz veins. The presence of such discontinuities probably increased the porosity of the rock, an important factor in ore deposition. As observed from ore petrography, pyrite is the most abundant ore mineral in the study area occurring both as an open-space filling and replacement type mineralization and it is evidenced from the trench data results that gold mineralization is directly linked with pyrite. From such observations it can be deduced that probably pyrite has a strong control on the gold mineralization of the study area although the occurrence of free gold is noted.

Gold mineralization in the Burikaro sub-area is associated predominantly with the meta-conglomerate and meta-sandstone rocks that are forming the bedrock and covered by thick soil. These rocks are highly weathered, slightly sheared, and intersected by quartz veins having variable orientations and dimensions. Lithological descriptions made along trenching indicated that these bedrocks are intersected by a number of small scale faults. Rock petrography indicated that there are considerable amounts of voids between grains that are probably produced due to deformation and typically observed under thin sections. All of the above discussed features led to the development of secondary porosity within these rocks besides the already available primary porosity. These and the presence of more phenocrysts compared to the groundmass probably made the rock more permeable. The mechanism of gold deposition is also directly associated with such properties of the meta-conglomerate and meta-sandstone. These rocks probably act as a porous medium within which gold and associated sulfides were deposited from gold bearing hydrothermal solutions that are derived predominantly from dehydration of the underlying amphibolite rock and invaded the country rocks through quartz veins.

CHAPTER SEVEN

7 CONCLUSION AND RECOMMENDATIONS

7.1 Conclusion

The study area forms part of the greenstone belt of Adola region. The mappable rock units of the study area from those forming the upper stratigraphy to the lower stratigraphy are meta-gabbro, meta-conglomerate, quartz-biotite schist, graphite-quartz-mica schist, talc-tremolite-actinolte schist, and amphibolite. Meta-sandstone and phyllite are minor unmappable units often occurring as intercalations. The metamorphosed mafic rocks are separated from the overlying meta-sediments by ductile-brittle shear contact which is highly weathered and characterized by the mixing of materials from both rock types, making the determination of its nature difficult. Based on characteristic mineral assemblages and field work observations, it is interpreted that the rocks underwent upper greenschist to epidote-amphibolite facies metamorphism. The mafic rocks (amphibolites) are generally deformed in a ductile manner which is observed from several mesoscale folded quartz veins hosted in the rocks. The meta-sediments, on the other hand, are mainly exposed to brittle deformation characterized by fault breccias, joints, and further intense fracturing leading to fragmentation of the rocks.

The most important structure with respect to gold mineralization in the study area is the N-S trending shear zone which is generally ductile in the amphibolite and brittle in the overlying meta-sediments. Field observations, ore petrography, and chemical analysis results indicated that the gold mineralization in the Ejersa sub-area is prominently hosted in the graphite-quartz-mica schist rocks that are located in the contact between the amphibolite and the meta-sediments and have relatively well-developed schistosity which is parallel to the above-mentioned shear zone. On the other hand, the gold mineralization in the Burikaro sub-area is associated with the intercalation of meta-conglomerate and meta-sandstone rocks that are covered by thick soil. The shearing and resulted fracturing in this area is only observed through trench cross-section descriptions since it is hardly possible to get exposures of these bedrocks. Chemical analysis further indicated that the gold mineralization in the study area is associated with quartz (± calcite) veins that are hydrothermally altered, undeformed (or late tectonic), generally randomly oriented in the shear zones and other available fractures, and that have variable dimensions. The dominant types of alterations observed are silicification, carbonatiztion, and tourmalinization.

The extensive small scale gold panning by the local people suggests the occurrence of free gold. However, chemical analysis results showed the occurrence of gold associated with sulfides (notably with pyrite) in quartz veins. The ore minerals of the study area are very fine grained and highly weathered and it is observed from polished section study that the approximated percentages of these ore minerals are mostly below 20%. Nevertheless, the observed ore minerals are predominantly pyrite, magnetite, ilmenite; minor amounts of hematite, chalcopyrite; accessory amounts of covellite, limonite, and gold. The majority of the mineralization in the area is characterized by three major types of textural features suggesting the mineralization is associated with hydrothermal fluids: open-space filling, replacement, and exsolution textures.

Paragenetic sequence study indicated that the mineralization in the study are can be categorized in to three types. The first of these is the disseminated type in which magnetite is the only ore mineral observed to occur in this form and probably it suggests the possible occurrence of magnetite from magmatic process. The second and the most important category with respect to gold mineralization is the hydrothermal quartz/calcite vein mineralization. Most of the ore minerals listed above including magnetite itself are precipitated in this phase. The last phase of the paragenetic sequence is mineralization related with supergene processes and characterized by the formation of the secondary minerals such as covellite and limonite.

Based on field observations, chemical analysis results, ore petrography, and review of regional geodynamics and geologic setting, it can be said that metamorphic dehydration is the most important source of hydrothermal fluids, probably with minor role from magmatic processes. Such dehydration processes probably occurred in the amphibolite facies environment expelling out the water contained within the hydrous minerals and also might leached the gold from the higher grade mafic rocks. The presence of shear zones and other fractures probably served as transportation pathways to the site of deposition.

The presence of sulfides and carbonaceous matter (graphite) in the graphite-quartz-mica schist of the contact zone between the amphibolite and the meta-sediments of Ejersa sub-area served as important agents of precipitating minerals and sorbants. The schistose nature of this rock, the presence of shear zones and other fractures probably served as transportation pathways for the hydrothermal fluids.

Similarly, the presence of sulfides and the slight graphitic nature of the meta-conglomerate/meta-sandstone rocks of Burikaro sub-area used as suitable agents for ore precipitation. The meta-conglomerate/meta-sandstone rocks, on the other hand, act as a porous medium for migration of hydrothermal fluids. Moreover, as observed from trench descriptions these rocks are also sheared and contain small scale faults. The circulating metal bearing hydrothermal fluids then probably deposited the gold and associated sulfides perhaps because of changes in the physicochemical characteristics of the overall ore-forming system that may arise from, but not limited to, fall in temperature and interaction of fluids with the wall rocks. Based on the discussions so far done, it can be concluded that the deposit in the study area generally fits with the orogenic model provided by Robert et al.(2007).

7.2 Recommendations

Based on the results obtained in this research work, it can be said that the graphite-quartz-mica schist and the meta-conglomerate/meta-sandstone rocks have good potential for gold mineralization. Review of previous exploration works in the study area indicated that the study are has, to date, undergone only trenching. However; most of fresh materials from the brecciated contact zone and the bedrock of Burikaro sub-area, to which the mineralization associated with, are covered by weather regolith making their recovery difficult by such trenching. It is, therefore, recommended to undertake further exploration works, such as test drillings.

The second recommendation is related with the scientific aspect. Due to financial and time limitations, important analytical methods in ore genesis such as fluid inclusion and isotope studies are not incorporated in the present work. It is, therefore, recommended to undertake further studies incorporating the afore-mentioned methodologies so that to determine the exact source(s) of the hydrothermal fluids and gold, which really needs the study of isotopic compositions of the hydrothermal fluids.

References

Abdelsalam, M.G. and Stern, R.J. (1996). Sutures and shear zones in the Arabian-Nubian Shield. Journal of African Earth Sciences, **23**(3): 289-310.

Adugna Debele, Girma Mekonin, and Ksahun Areaya .(2010). Preliminary compilation of report on placer gold prospecting in Bersisa Kochore locality, Guji zone of Oromia National Regional State, southern Ethiopia. Geological Survey of Ethiopia, mineral exploration and evaluation core process, Addis Ababa, Ethiopia, pp102.

Ayalew, T., Bell, K., Moore, J.M., and Parrish, R.R. (1990). U-Pb and Rb-Sr geochronology of the western Ethiopian shield. Geological Society of America , Bulletin102 :1309-1316.

Ayalew, T. and Gichel, S. (1990). Preliminary U-Pb ages from southern Ethiopia. Extended abstracts, 15th colloquium, African Geology:127-130.

Barnes, H.L.(1997). Geochemistry of hydrothermal ore deposits . 3rd edition, John Willey and Sons, New York, pp972.

Basson, I . J. (2006). Structural analysis of selected areas in the Dawa Digati prospect area, Adola Gold belt, Ethiopia and recommendations on data formats for their evaluation. Unbpubl. technical report, NMiC, Addis Ababa, Ethiopia, pp62.

Berhe, S.M. (1990). Ophiolites in Northeast and East Africa: implication for Proterozoic crustal growth. Journal Geological Society of London,**147**:41–57.

Beraki, W.H. , Bonavia, F.F. Getachew, T., Schmerold, R., and Tarekegn, T. (1989). The Adola fold and thrust belt, southern Ethiopia: a re-examinations with implications for Pan- African Evolution. Geol.Mag, **126**:647-657.

Billay, A.Y., Kisters, A.F.M., Meyer, F.M. and Schneider, J.(1997). The geology of the Lega Dembi gold deposit, southern Ethiopia: Implications for Pan-African gold exploration. Mineralium Deposita,**32**: 491-504.

Bonavia, F.F. and Chorowicz, J. (1993). Neoproterozoic structures in the Mozambique belt of southern Ethiopia. Precambrian Research, **68**: 307-322.

Boyle, R.W. (1987). Gold: history and genesis of deposits. Van Nostrand Reinhold, London, England, pp676.

Chater, A.M. (1971). The geology of the Megado area of southern Ethiopia. Unpubl. Ph.D. thesis, University of Leeds, Leeds, England.

Clifford, T. N. (1970). The structural framework of Africa. In: Clifford & Gass: African magmatism and tectonics, Oliver & Boyd, Edinburgh, pp1-26.

Cline, J.S., Hofstra, A.H., Muntean J.L., Tosdal R.M., and Hickey K.A. (2005). Carlin-type gold deposits in Nevada: Critical geological characteristics and viable models. In Economic Geology 100th Anniversary: 451-484.

Collins, A.S. and Pisarevsky, S.A. (2005). Amalgamating eastern Gondwana: the evolution of the Circum-Indian Orogens. Earth-Science Reviews, **71**: 229–270.

Cox, D.P. and Singer, D.A. (1987). Mineral deposit models. U.S. Geological Survey bulletin 1693, United States government printing office, Washington, pp379.

Craig, J. R., and Vaughan, D. J. (1994). Ore microscopy and ore petrography. 2nd edition, John Willey and Sons, USA, pp434.

Debele, D.J. (2000). Geology, geochemistry , and genesis of gold mineralization of the Okote area, southern Ethiopia. Ph.D. dissertation, Institute for Geochemistry, University of Wein, Austria, pp262.

Debele, D.J. and Koeberl, C. (2004). Geology, alteration , and genesis of gold mineralization in the Okote area, southern Ethiopia. Geochemical journal, **38**: 307-331

De Wit, M.J. and Chewaka, S. (1981). Plate tectonic evolution of Ethiopia and origin of its mineral deposits: an overview. In: Chewaka, S., de Wit, M.J. (Eds.), Plate

Tectonics and Metallogenesis: Some Guidelines to Ethiopian Mineral Deposits, Ethiopian Institute of Geological Surveys, Bulletin 2, pp115–129.

Dubé, B. and Gosselin, P. (2007). Greenstone-hosted quartz-carbonate vein deposits. Geological Association of Canada, special publication no.5, pp49-73.

Evans, A.M .(1980). An introduction to ore geology. 1st edition, Blackwell Scientific Publications, Oxford, England, pp231.

Evans, A.M. (1993). Ore geology and industrial minerals: an introduction . 3rd edition, Blackwell Publishing Company, Oxford, England, 389.

Frimmel, H.E., Groves, D.I., Kirk, J., Ruiz, J., Chelsey, J., and Minter, W.E.L. (2005). The Formation and Preservation of the Witwatersrand Goldfields, the World's Largest Gold Province, in Economic Geology 100th Anniversary: 769-798.

Fritz, H., Abdelsalam, M., Ali, K.A., Bingen, B., Collins, A.S., Fowler, A.R., Ghebreab, W. Hauzenberger, C.A., Johnson, P.R., Macey, P., Muhongo, S., Stern, R.J. and Viola, G. (2013). Orogen styles in the East African Orogen: A review of the Neoproterozoic to Cambrian tectonic evolution. Journal of African Earth Sciences, **86** : 65–106.

Gebremichael, M. **(**2006). Mineral potential of SEAMIC member countries. News Article inSouthern and Eastern African Mineral Centre (SEAMIC), Editors: Nkini, G. R., Kimaro, E.C. and Moshi, L. SEAMIC Newsletter. **9**(1): 28 .

Ghebreab, W. (1989). Geological evolution of the Adola Precambrian greenstone belt, Southern Ethiopia. Report, EIGS, Addis Ababa, Ethiopia.

Ghebreab, W., Yohannes, E. and Giorgis, L.W. (1992). The Lege Dembi gold mine: an example of shear zone hosted mineralization in the Adola green stone belt, Southern Ethiopia. African Journal of Earth Sciences, **15**:489-500.

Geological Survey of Ethiopia (GSE). (2008). Annual report of the years 2006-2007. GSE, Addis Ababa, Ethiopia, pp60.

Gichile, S. (1991). Structure, metamorphism and tectonic setting of a gneissic terrane, the Segen Afelata area, southern Ethiopia. M.Sc. thesis, University of Ottawa, Canada, pp1–225.

Gilboy, C.F. (1970). The geology of the Gariboro region southern Ethiopia. Unpubl. PhD thesis, University of Leeds, Leeds, England.

Girma Woletisae, Masresha Nigussie, and Tesfaye Kassaye .(2007). Magnetic and spectral induced polarization (SIP)/resistivity signatures of Burikaro prospect, Adola belt. Geological Survey of Ethiopia, Addis Ababa, Ethiopia,pp59.

Goldfarb, R. J., Baker, T., Dubé, B., Groves, D. I., Hart, C. J. R., and Gosselin, P. (2005). Distribution, character, and genesis of gold deposits in metamorphic terrains. Society of Economic Geologists, Inc. Economic Geology 100th Anniversary Volume, pp407–450.

Groves, D.I., Goldfarb, R.J., Gebre-Mariam, M., Hagemann, S.G and Robert, F. (1998). Orogenic gold deposits: a proposed classification on the context of their crustal distribution and relationship to other gold deposit types. Ore Geology Reviews, **13**: 7-27.

Groves, D.I., Goldfarb, R.J., Robert, F. and Hart, C.J.R.(2003). Gold deposits in metamorphic belts: Overview of current understanding, outstanding problems, future research, and exploration significance. Economic Geology, **98**: 1-29.

Guilbert, J. M. and Park, C. F. (2007). The geology of ore deposits. Waveland Press, Inc., USA, pp985.

Hailu Worku and Kinetbeb Yifa. (1989). The tectonic evolution of the Precambrian metamorphic rocks of the Adola belt (southern Ethiopia) and its implication on gold mineralization. EIGS, Addis Ababa, Ethiopia, pp56.

Hannington, M.D. (2004). Spectrum of gold-rich volcanic massive sulfide deposits from the Archean to the Present. In 24ct gold workshop, CODES special publication, **5**: 79-85.

Hart, C. J. R. (2005). Classifying, distinguishing, and exploring for intrusion related gold systems. Gangue Publications, Yukon, Canada, **87**:18.

Hart, C.J.R and Goldfarb, R.J.(2007). Distinguishing intrusion-related from orogenic gold systems. From www.nzpam.govt.nz/cms/pdf-library/minerals, on 12/11/2013.

Heinrich, C.A., Driesner, T., Stefansson, A. and Seward, T.M.. (2004). Magmatic vapor contraction and the transport of gold from the porphyry environment to epithermal ore deposits. Geology, **32**:761-764.

Holmes, A. (1951). The sequence of Precambrian orogenic belts in south and central Africa. 18thInternational Geological Congress, **18** (14): 254-269.

Hundie Melka (2010).'The extractive industry in Ethiopia and efforts made to join and implement the extractive industries transparency initiative in Ethiopia', a paper presented to the public dialogue on government and transparency in extractive industries and natural recourse management, Addis Ababa.

Huston, D.L. (2000). Gold in volcanic-hosted massive sulfide deposits: Distribution, genesis and exploration. In Society of economic Geologists, Reviews in Economic Geology, **13**: 401-426.

Hyndman, D.W. (1972). Petrology of igneous and metamorphic rocks. McGraw Hill, USA, PP533.

Jacobs, J., Fanning, C.M., Henjes-Kunst, F., Olesch, M., and Paech, H. J. (1998). Continuation of the Mozambique into East Antarctica: Grenville-age metamorphism and polyphase Pan-African high-grade events in central Dronning Maud Land. Journal Geology, **106**: 385–406.

Jensen, M.L. and Bateman, A.M. (1981). Economic mineral deposits. 3rd edition, John Wiley and Sons, New York, pp593.

Kazmin, V. (1972). Geology of Ethiopia. Unpub. report, Ministry of Mines and Energy, Addis Ababa, Ethiopia.

Kazmin, V. (1975). Explanatory Note to the Geology of Ethiopia. Ethiopian Institute of Geological Surveys, Bulletin no. 2, Addis Ababa, Ethiopia.

Kazmin, V. (1976). Ophiolites in the Ethiopia basement. Ethiopian Institute of Geological Surveys, note no. 35, Addis Ababa, pp1–15.

Kazmin, V., Shiferaw, A. and Balcha, T. (1978). The Ethiopian basement: stratigraphy and possible manner of evolution. Geol. Rdsch, **67**(2): 531-546.

Koeberl, C. (2000). Geology, geochemistry, and genesis of gold mineralization of the Okote area, southern Ethiopia. Unpub.report, Ethiopian Institute of Geological Survey, Addis Ababa, Ethiopia, pp321.

Kozyrev, V., Girma, K., Safonov, J., Bekele, W.M., Tuliankin, V., Bestujev, A., Baijapov, A., Teweldemedhin, T., Gurbanivich, G., Kaitukov, M., and Arijapov, A. (1985). Regional geological and exploration work for gold and other minerals in the Adola goldfields. Report, EMRDC, Addis Ababa, Ethiopia.

Krauskopf, K. B and Bird, D. K . (1995). Introduction to geochemistry. 3rd edition, McGraw-Hill, New York, pp647.

Kroner, A. (1977). Precambrian mobile belts of southern and eastern Africa - Ancient sutures or sites of ensialic mobility? A case for crustal evolution towards plate tectonics. Tectonophysics 40, Amsterdam, pp101-135.

Kroner, A., Hegner, E., Collins, A.S., Windley, B.F., Brewer, T.S., Razakamanana, T., and Pidgeon, R.T. (2000a). Age and magmatic history of the Antananarivo block, central Madagascar, as derived from zircon geochronology and Nd isotopic systematics. American Journal Science, **300**: 251–288.

Kroner, A., Willner, A.P., Collins, A.S., Hegner, E., and Muhongo, S., (2000b).The Mozambique Belt of East Africa and Madagascar: New zircon and Nd ages–implications for Rodinia and Gondwana Supercontinent formation and dispersal. Journal African Earth Sciences, **30** (4A): 49–50.

Law, J.D.M. and Phillips G.N. (2005). Hydrothermal replacement model for Witwatersrand gold: In Economic Geology 100th Anniversary : 799-812.

Lingeswara**,** B. K, Solomon Gebresillassie and Kassa Amare.(2012). Shear zone hosted base metal mineralization near Abreha Weatsbeha-Adidesta and Howzein, Tigray Region, northern Ethiopia. Momona Ethioipian Journal of Science,**4**: 3- 28.

Mengesha Tefera, Tadiwos Cherinet and Workineh Haro. (1996) . Explanation of the geological map of Ethiopia at 1: 2,000,000 scale. 2nd edition, Ethiopian Institute of Geological Surveys, Technical publication team, Addis Ababa, Ethiopia, pp79.

Ministry of Mines and Energy (MoME). (1992). Geological map of Adola area, a 1:100, 000 scale. EIGS, Addis Ababa, Ethiopia.

Ministry of Mines and Energy (MoME). (1993).Final report onmineral explorationin Adola area (sidamo). EIGS/UNDP PROJECT ETH/86/034, pp 202.

Ministry of Mines and Energy (MoME). (1994). Megado-Serdo primary gold exploration and development project: exploration information on the Megado-Serdo prospects. Ethiopian Institute of Geological Surveys, Addis Ababa, pp23.

Ministry of Mines and Energy (MoME). (1995). A report on mineral exploration work in Dawa Digati area, Adola ore district, southern Ethiopia. EIGS, Addis Ababa , Ethiopia, pp242.

Ministry of Mines and Energy (MoME) .(2007). The potential for gold in Ethiopia. Retrieved from: www.gse.gov.et/phocadownload/.../**Gold**%20In%20**Ethiopia**.pdf viewed on 29/11/2013.

Ministry of Mines Mineral Licensing and Administration Department .(2010). Gold in Ethiopia. From http://extra.geus.info/cet/ethiopia/EthiopiaBroch_Gold_Web.pdf viewed on 24/02/2013.

Misra, K.C.(2000) . Understanding Mineral Deposits. Kluwer Academics, pp885.

Mogessie, A., Krenn, k., Schaflechner, J., Koch, U., Egger, T., Goritchnig , B., Kosednar, B., Pichler, H., Ofner, L., Bauernfiend, D., Tadesse, S., Hailu, K. and Demessie, M . (2002). A geological excursion to the Mesozoic sediments of the Abay basin (Blue Nile), recent volcanics of the Ethiopia Main Rift and basement rocks of the Adola area, Ethiopia. Mitt Osterr Miner, **147**: 43-74.

Moon, C.J., Whateley, M. k and Evans, A.M. (2006). Introduction to mineral exploration. 2nd edition, Blackwell Publishing, USA, PP41.

Morton (2009). A brief guide to the geology of ore deposits. Retrieved from:

www.d.umn.edu/~p**morton**/geol5350/2009/econclass**notes**2009.pdf, viewed on 15/11/2013.

National Mining Corporation (NMiC) .(1998). Dawadigati gold exploration project final report for the second year of the initial gold exploration period (1997/98), vol. IV, Addis Ababa.

National Mining Corporation (NMiC) .(2004). Summary of exploration work on Dawa Digati gold exploration project, southern Ethiopia. Unpubl. technical report, NMiC, Addis Ababa, Ethiopia, pp58.

Nekrasov, I. Ya. (2009) . Geochemistry , Mineralogy and Genesis of gold deposits . CRC press, New York, pp329.

Park, C.F and MacDiarmid, R.A. (1975). Ore deposits. 3rd edition, W.H. Freeman and Company, San Francisco, USA, pp530.

Robb, L. J. (2005). Introduction to Ore forming Processes.1st edition, Blackwell publishing, UK, pp386.

Robert, F., Brommecker, R., Bourne, B.T., Dobak, P.J., McEwan, C.J, Rowe, R.R., and Zhou, X. (2007). Models and exploration methods for major gold deposit types. **In**: Proceedings of Exploration 07: Fifth Decennial International Conference on MineralExploration,pp691-711. From: www.southernarcminerals.com/.../viewed on 12/11/2013.

Robert, F., Poulsen, K.H., Cassidy, K.F. and Hodgson, C.J. (2005). Gold metallogeny of the superior and Yilgarn cratons, in Economic Geology 100th Anniversary.

Robert, F, Poulsen, K.H., and Dubé, B. (1997). Gold deposits and their geological classification. **In**: Proceedings of Exploration 97: Fourth Decennial International Conference on Mineral Exploration, 209-220.

Rogers, J.J.W., Unrug, R., and Sultan, M., (1995). Tectonic Assembly of Gondwana. Journal of Geodynamics, **19**:1–34.

Schmerold, R. (1988). Report on quartz c-axis fabrics and microstructural features of selected localities in the Adola Goldfield (Sidamo, Ethiopia). EIGS/UNDP Training for Mineral Exploration Project ETH/86/034, Addis Ababa, Ethiopia.

Sillitoe, R.H., Hannington, M.D., and Thompson, J.F. (1996). High sulfidation deposits in the volcanogenic massive sulfide environment. Economic Geology, **91**: 204-212.

Sillitoe, R.H. and Hedenquist, J.W. (2003). Linkages between volcanotectonic settings, ore-fluid compositions, and epithermal precious metal deposits. In Society of Economic Geologists Special Publication, **10**: 315-343.

Sillitoe, R. H.and Thompson, J. F. H. (1998). Intrusion–related vein gold deposits: types, tectono-magmatic settings and difficulties of distinction from orogenic gold deposits. Society of Resource Geology, **48**(4): 237–250.

Solomon Tadesse .(2009). Mineral Resources Potential of Ethiopia, Addis Ababa University press, Addis Ababa , Ethiopia, pp293.

Stern, R. J. (1994). Arc assembly and continental collision in the Neoproterozoic East African Orogen: implication for the consolidation of Gondwana. Annual Review Earth Planetary Sciences, **22**:319–351.

Stern, R. J. (2002) .Crustal evolution in the East African Orogen: a neodymium isotopic perspective. Journal of African Earth Sciences, **34**: 109–117.

Stern, R. J. and Johnson, P.(2010).Continental lithosphere of the Arabian Plate: A geologic, petrologic, andgeophysical synthesis. Earth-Science Reviews, **101**:29–67.

Stuwe, K. (1998). Tectonic constraints on the timing relationships of metamorphism, fluid production and gold-bearing quartz vein emplacement. Ore Geology Reviews, **13:**219-228.

Tatsch, J. H. (1975). Gold deposits: origin, evolution and present characteristics. Tatsch Association, USA, pp275.

Tedbabu Worku, Mustefa Sultan and Gebremeskel Gebreselassie. (2003). Report on geological and geochemical exploration work for gold and basemetals in Genale Korcha area, Oromia National Regional state (southern Ethiopia). Geological Survey of Ethiopia, Addis Ababa , Ethiopia, pp75.

Teklay, M., Kroner, A. and Oberhansli, R. (1993). Reconnaissance Pb–Pb zircon ages from Precambrian rocks in eastern and southern Ethiopia and an attempt to define crustal provinces. In: Thorweihe, U., Schandelmeier, H. (eds.) Geoscientific research in northeast Africa. Balkema, Rotterdam, pp 133–138.

Thompson, J.F.H., and Newberry, R.J. (2000). Gold deposits related to reduced granitic intrusions. In Society of Economic Geologists Reviews, **13**: 377-400.

Tsige, L. (2006). Metamorphism and gold mineralization of the Kenticha–Katawicha area: Adola belt, southern Ethiopia. Journal of African Earth Sciences, **45**:16–32.

United States Geological Survey Mineral Commodity Summaries. (USGS, 1900 - 2010). World gold production in tons from 1900 up to 2010. Retrieved from *www*.minerals.usgs.gov/minerals/pubs/commodity/gold/mcs,viewed 13/05/2014.

Warden, A.J. and Horkel, A.D. (1984). The geological evolution of the northeast branch of the Mozambique Belt (Kenya, Somalia, Ethiopia). Mitteilungen Osterr,**77**:161-184.

Winkler, H.G. (1976). Petronesis of metamorphic rocks. fourth edition, Springer Verlag, New York, USA, pp334.

Worku, H. (1996a). Geodynamic development of the Adola belt (southern Ethiopia) in the Neoproterozoic and its control on gold mineralization. Ph.D. Thesis, Technical University of Berlin, Berlin, pp1–156.

Worku, H. (1996b). Structural control and metamorphic setting of the shear zone related Au mineralization o the Adola belt southern Ethiopia and its tectonogenetic development. Journal of African Earth Sciences, **23**(3): 383-409.

Worku, H. and Schandelmeier, H. (1996). Tectonic evolution of the Neoproterozoic Adola Belt of southern Ethiopia: evidence for a Wilson Cycle process and implication for oblique plate collision. Precambrian Research, **77**:179–210.

Worku, H. and Yifa, K . (1992). The tectonic evolutions of the Precambrian rocks of the Adola belt (southern Ethiopia). Journal of African Earth Sciences, **14**(1): 37-55.

Yibas, B. (2000). The Precambrian geology, tectonic evolution, and controls of gold mineralization in southern Ethiopia. Unpubl. Ph.D. thesis, University of the Witwatersrand, Johannesburg, South Africa, pp448.

Yibas, B., Reimold, W.U., Anhaeusser, C.R., Koeberl, C. (2000). Geochemistry of the mafic rocks of the ophiolitic fold and thrust belts of southern Ethiopia: constraints on the tectonic regime during the Neoproterozoic (900–700 Ma). Economic Geology Research Institute, University of the Witwatersrand, Johannesburg, pp46.

Yibas, B., Reimold, W.U., Armstrong, R., Koeberl, C., Anhaeusser, C.R. and Phillips, D. (2002). The tectonostratigraphy, granitoid geochronology and geological evolution of the Precambrian of southern Ethiopia. Journal of African Earth Sciences, **34**:57–84.

Yihunie, T. and Tesfaye, M. (2002). Structural evidence for the allochthonous nature of the Bulbul terrane in southern Ethiopia: A west-verging thrust nappe. Journal of African Earth Sciences **34**:85–93.

Appendix 1: Analytical results of some of the trenches dug in the study area (NMiC, 1997/1998)

Trench 6FTR-550

Sample No.550	01	02	03	04	05	06	07	08	09	10	11	12
Sample Length (m)	1.0	1.0	1.0	-	-	0.8	1.0	-	1.0	1.0	2.0	-
Assay result Au (ppm)	0.13	0.16	0.13	0.07	0.08	0.26	0.27	0.05	0.19	0.60	0.27	0.05

Trench 6FTR-585

Sample No.585	01	02	03	04	05	06	07	08	09	10	11
Sample Length (m)	1.0	1.0	1.0	1.0	1.0	1.0	1.0	1.0	1.0	1.0	0.9
Assay result Au (ppm)	<0.01	0.01	0.02	0.06	0.01	<0.01	<0.01	<0.01	0.03	0.02	0.01

Sample No.585	12	13	14	15	16	17	18	19	20	21	22	23
Sample Length (m)	0.5	1.0	1.0	1.0	1.0	1.0	1.0	1.0	1.0	1.0	1.0	1.0
Assay result Au (ppm)	0.01	0.08	2.4	0.36	0.6	0.52	1.3	0.65	0.15	0.06	0.03	0.03

Sample No.585	24	25	26	27	28	29	30	31	32	33	34	35
Sample Length (m)	1.0	1.0	1.0	1.0	1.0	1.0	1.0	1.0	1.0	1.0	1.0	1.0
Assay result Au (ppm)	0.04	0.01	0.04	0.18	0.03	0.03	0.04	0.05	-	-	-	-

Trench 6FTR-584

Sample No.584	01	02	03	04	05	06	07	08	09	10	11
Sample	1.0	1.0	1.0	1.0	1.0	1.0	1.0	1.0	0.7	0.7	0.5

Length (m)											
Assay result Au (ppm)	<0.01	<0.01	<0.01	<0.01	0.02	0.02	0.04	0.66	0.30	0.75	1.30

Sample No.584	12	13	14	15	16	17	18	19	20	21	22
Sample Length (m)	0.5	0.5	0.5	0.5	0.5	0.5	0.5	0.5	1.0	1.0	1.1
Assay result Au (ppm)	3.6	0.90	0.80	0.4	0.4	0.21	0.52	0.71	0.44	0.08	0.15

Sample No.584	23	24	25	26	27	28	29	30	31
Sample Length (m)	0.5	1.0	1.0	1.0	1.0	1.0	1.0	1.0	1.0
Assayed Au (ppm)	0.03	0.02	0.01	<0.01	<0.01	<0.01	0.01	0.01	0.03

Trench 6FTR-564

Sample No.564	01	02	03	04	05	06	07	08	09	10	11	12
Sample Length(m)	2.0	2.0	1.0	1.0	1.0	1.0	1.0	1.0	1.0	1.0	1.0	1.0
Assayed Au (ppm)	<0.01	<0.01	<0.01	<0.01	<0.01	0.71	0.14	0.3	0.31	0.12	0.24	1.1

Sample No.564	13	14	15	16	17	18	19	20	21	22	23	24
Sample Length(m)	1.2	0.7	1.0	1.0	1.0	1.0	1.0	1.0	1.0	1.0	1.0	1.6
Assayed Au (ppm)	0.28	1.2	0.54	0.76	0.2	0.4	0.12	0.14	0.06	0.16	0.07	0.11

Sample No.564	25	26	27	28	29	30	31	32	33	34	35	36
Sample	1.0	1.0	1.0	1.0	1.0	1.0	1.0	1.0	1.0	1.0	1.0	1.0

Length(m)												
Assayed Au (ppm)	0.11	0.04	0.06	0.04	0.03	0.02	0.09	0.11	0.21	0.04	0.03	0.11

Trench 6FTR-547

Sample No. 547	01	02	03	04	05	06	07	08	09	10	11
Sample Length (m)	1.0	2.0	2.0	2.0	2.0	1.0	1.0	1.0	1.0	1.0	1.0
Assayed Au (ppm)	<0.01	0.03	0.03	0.02	0.02	0.01	<0.01	0.05	0.70	<0.01	0.04

Sample No. 547	12	13	14	15	16	17	18	19	20	21	22
Sample Length (m)	1.0	1.0	1.0	1.0	1.0	1.0	1.0	1.0	1.0	0.65	0.75
Assayed Au (ppm)	0.02	1.00	0.24	0.01	0.25	0.32	0.45	0.19	0.02	0.02	<0.01

Trench 6FTR-545

Sample No.545	01	02	03	04	05	06	07	08	09	10	11
Assayed Au (ppm)	0.02	0.05	0.24	0.03	0.04	0.52	0.03	0.08	0.05	0.25	<0.01

Trench 6FTR-591

Sample No.591	01	02	03	04	05	06	07	08
Sample Length (m)	1.0	1.0	1.0	1.0	1.0	1.0	1.0	1.0
Assayed Au (ppm)	0.25	0.15	0.21	0.31	0.68	0.40	0.37	0.64

Trench 6FTR-551

Sample No. 551	01	02	03	04	05	06	07	08	09	10

Sample Length (m)	1.0	1.0	1.0	1.0	1.0	1.0	1.0	1.0	1.0	1.0
Assayed Au (ppm)	<0.01	<0.01	<0.01	<0.01	<0.01	<0.01	<0.01	<0.01	<0.01	<0.01

Sample No. 551	11	12	13	14	15	16	17	18	19	20	21
Sample Length (m)	1.0	1.0	1.0	1.0	1.0	1.0	1.0	1.0	2.0	2.0	2.0
Assayed Au (ppm)	0.03	0.03	0.13	0.10	0.61	0.01	0.0.37	0.04	0.07	0.08	0.14

Trench 6FTR-580

Sample No. 580	01	02	03	04	05	06	07	08	09	10	11	12
Sample Length (m)	1.7	1.0	1.0	1.0	1.0	7	1.0	1.0	1.0	0.8	1.0	1.0
Assayed Au (ppm)	0.03	0.05	0.04	0.01	0.03	0.12	0.20	0.08	0.08	0.08	0.14	0.16

Sample No. 580	13	14	15	16	17	18	19	20	21	22	23	24	25
Sample Length(m)	0.5	0.5	0.5	1.0	1.0	1.0	1.0	1.0	1.0	1.0	1.0	0.5	0.5
Assayed Au (ppm)	0.33	0.19	0.30	0.31	0.20	0.17	0.06	0.09	0.27	0.41	0.15	0.06	0.12

Sample No. 580	26	27	28	29	30	31	32	33	34	35	36	37	38
Sample Length (m)	0.5	1.0	1.0	1.0	1.0	0.5	0.5	0.5	0.5	0.5	0.5	0.5	0.5
Assayed Au (ppm)	0.07	0.42	0.04	0.05	0.08	0.18	0.22	0.31	0.43	0.16	0.78	0.58	0.3

Trench 6FTR-573

Sample No. 573	35	34	33	32	31	30	29	28	27	26	25	24	23
Assayed Au(ppm)	0.02	0.01	0.03	0.02	0.06	0.48	0.08	0.28	2.0	5.7	0.16	0.34	0.27

Sample No. 573	22	21	20	19	18	17	16	15	14	13	12	11	10
Assayed Au(ppm)	0.13	0.08	0.13	0.06	0.04	0.02	0.03	0.02	5.0	5.9	-	0.04	0.10

Sample No. 573	09	08	07	06	05	04	03	02	01
Assayed Au (ppm)	0.08	0.02	2.1	0.02	0.29	0.15	0.09	4.2	0.06

Trench 6FTR-575

Sample No. 575	01	02	03	04	05	06	07	08	09	10	11	12	13	14
Assayed Au(ppm)	0.24	0.06	-	0.02	-	0.03	0.03	0.02	0.02	0.02	-	-	0.01	0.02

Sample No. 573	15	16	17	18	19	20	21	22	23	24	25	26	27
Assayed Au(ppm)	0.13	0.03	0.10	0.35	0.09	0.10	0.80	1.40	0.15	0.15	0.5	0.05	0.1